NASA TECHNICAL TRANSLATION NASA TT F-12,786

NASA TT F-12,786

STUDY ON THE STABILITY OF BOUNDARY LAYERS AND COMPRESSIBLE FLUIDS

Hans Gropengiesser

Translation of "Beitrag zur Stabilitat freier Grenzschichten in kompressiblen Medien", Deutsche Luft- und Raumfahrt, Report 69-25, 1969, 123 p. 42 figures.

DLR FB-

NATIONAL AERONAUTICS AND SPACE ADMINISTRATION
WASHINGTON, D. C. 20546 FEBRUARY 1970

NOTATIONS

Dimensional Quantities	Dimensionless Quantities	Reference Quantities	
x^*, y^*, z^*	x, y, z	$l = \sqrt{\nu_1^* x^* / u_1^*}$	Cartesian Coordinates
t^*	t	l^*/u_1^*	Time
u^*, v^*, w^*	u, v, w	u_1^*	Velocity Components
p^*	p	p_1^*	Pressure
T^*	T	T_1^*	Temperature
ρ^*	ρ	ρ_1^*	Density
a^*	a	a_1^*	Sonic Velocity
μ^*	μ	μ_1^*	Dynamic Viscosity
ν^*	ν	ν_1^*	Kinematic Viscosity
λ^*	λ	λ_1^*	Thermal Conductivity
c_p^*	c_p	c_{p1}^*	Specific Heat at p = const.
R^*			Gas Constant
δ^*	δ	l^*	Boundary-Layer Thickness
ϑ^*	ϑ	l^*	Momentum Thickness

$$Re = \frac{u_1^* l^*}{\nu^*}$$ Reynolds Number

$$M = \frac{u_1^*}{a_1^*}$$ Mach Number

$$Pr = \frac{\mu^* c_p^*}{\lambda^*}$$ Prandtl Number

Dimensional Quantities	Dimensionless Quantities	Reference Quantities	
	$\varkappa = \frac{c_p^*}{c_p^* - R^*}$		Isentropic Exponent
$\alpha^* = \alpha_r^* + i\alpha_i^*$	$\alpha = \alpha_r + i\alpha_i$	$1/l^*$	Disturbance Wave number in x direction
γ^*	γ	$1/l^*$	Disturbance Wave number in z direction
β^*	β	u_1^*/l^*	Disturbance Frequency /81
$c_r^* = \frac{\beta^*}{\alpha_r^*}$	$c_r = \frac{\beta}{\alpha_r}$	u_1^*	Phase Velocity of Disturbance in x direction

$$(u', v', w') = \left(f(y), \alpha\varphi(y), h(y)\right)\exp\left[i(\alpha x + \gamma z - \beta t)\right]$$ Velocity Fluctuation

$$p' = \pi(y)\exp\left[i(\alpha x + \gamma z - \beta t)\right]$$ Pressure Fluctuation

$$T' = \Theta(y)\exp\left[i(\alpha x + \gamma z - \beta t)\right]$$ Temperature Fluctuation

$$\rho' = r(y)\exp\left[i(\alpha x + \gamma z - \beta t)\right]$$ Density Fluctuation

Explanations:

1. Flow parameters with bars over them designate principal-flow quantities.
2. The symbol k = 1;2 indicates the flow ranges $y = +\infty$ (k = 1) or $y = -\infty$ (k = 2) for the Lock profile and the ranges $y > 0$ (k = 1) or $y < 0$ (k = 2) for the Vortex layer.
3. The symbol N indicates quantities describing neutral disturbances as limiting cases for amplified disturbances.
4. The symbol c indicates quantities in the critical layer of the flow field (only for neutral disturbances).
5. The symbol r or the expression Re <-> indicates the real component of a complex quantity.

6. The index i or the expression Im <-> indicates the imaginary component of a complex quantity.

All quantities not explained in this section are defined within the text.

TABLE OF CONTENTS

STUDY ON THE STABILITY OF BOUNDARY LAYERS AND COMPRESSIBLE FLUIDS[1]

H. Gropengiesser, Diploma Engineer, Turbulence Research Institute of the DVL

ABSTRACT. This paper is concerned with the stability of free boundary or shear layers observed in jet flows and in the wakes of blunt bodies. The investigation of inviscid stability properties involved a laminar velocity profile which develops from a compressible vortex layer under the influence of fluid friction. The amplification and propagation of phase velocity of small-amplitude disturbances were studied as a function of disturbance frequency and angle of wave propagation at various Mach numbers and temperature ratios. The phase velocities of disturbances relative to flow can be less than or greater than the speed of sound. Accordingly, the disturbance is classified as subsonic or supersonic. It is found that a change in the character of the disturbance may involve the amplification of a second mode.

1. Introduction /7*

In past years, a large number of papers on boundary-layer stability studies have appeared which involved the formation of turbulence in laminar flows. Stability theory has reached this goal only to the extent that it permits the determination of an upper boundary for the Reynolds number range (the so-called upper critical Reynolds number) for a particular flow, within which the laminar configuration exhibits stable behavior with respect to all disturbance. If one does not consider special types of flow in which one laminar flow configuration develops into another, exceeding the critical Reynolds number Re_{crit} always initiates the first step of the transition process, since disturbances carried into the flow are now amplified in the direction of flow and form "nucleus cells" for turbulence downstream. Until now, however, stability theory has not been able to provide any information regarding this mechanism.

This paper is concerned with the stability of free boundary layers or shear layers which are formed from each wall, under the influence of a high velocity gradient and fluid friction. They are observed with free jets and in the wakes of blunt bodies (see Figure 1). An important characteristic of these boundary layers is the inflection point which occurs in the velocity

[1] Dissertation accepted by the Mechanical Engineering Faculty of the Engineering University of Berlin for the Doctorate in Engineering.

*Numbers in the margin indicate pagination in the foreign text.

profile. Rayleigh [43] showed that velocity profiles with inflection points are unstable in a frictionless, incompressible fluid. According to Tollmien [54], this "inflection-point criterion" is, as a rule, not only a necessary but also a sufficient condition. This "inflection-point criterion" was physically interpreted by Lin [29] as a condition for instability of the equilibrium of the induction effects originating at various points in the flow. The instability of free boundary layers is a pure induction instability, upon which the fluid friction has only one damping effect.

Such a boundary-layer instability was first observed by Leconte [18] with gas flames. He found that a flame was shortened by the effect of sound. Tyndall [55] demonstrated the character of this instability by experimental means. He made a free air jet visible with smoke and observed /8
that the edges of the jet developed vortices and became turbulent. A year later, while studying vortical layers, which would also mark the edges of an ideal frictionless free jet, Helmholtz [13] came to the conclusion that a disturbed vortex layer must always be formed as the result of self-induction. Mathematical confirmation of this concept was provided by Rayleigh [42]. He was able to show, among other things, that a plane vortex layer in a frictionless fluid is unstable relative to small, wave-shaped disturbances of arbitrary frequency and wavelengths..

Many years later, the problem of the effect of sound upon free boundary layers was once more studied by G. B. Brown [3, 4]. Brown found that sound can only have an effect upon the formation of the vortex, but not upon its further development, and that the flow can be affected only within a particular range of sound frequencies. The preference exhibited for a particular frequency range can be explained by the fact that a free jet in a real fluid is bounded by a shear layer of finite thickness; in contrast to this, a plane vortex layer in an ideal fluid possesses no characteristic length, and all frequencies have equivalent effects.

New, extensive studies on the phenomenology of free jets have been carried out by Wille [58, 59, 60, 61] and his colleagues, Domm [7], Wehrmann [56, 57], Timme [53] and Fabian [10]. With the aid of hot-wire measurement techniques, they studied the formation of vortices with and without acoustic effects, in flat and round free jets in air at Reynolds numbers of $Re = 10^3$ to 10^5 and jet velocities of up to $\bar{u}_1 = 20$ m/s. The following concept was worked out for the formation of free-jet turbulence: The boundary layer separated from the nozzle edge in a laminar manner experiences an undulation which becomes highly amplified in the direction of flow. The boundary layer subsequently rolls into individual vortices which decay three-dimensionally downstream and initiate the turbulence.

Sato [45, 46, 47] and Michalke and Wille [37] have measured the amplification of disturbances induced artificially in free-jet boundary layers at low velocities by acoustic effects. New detailed and improved measurements have been carried out by Freymuth [11]. He found that the dis- /9
turbance amplitudes in the direction of flow increase exponentially until a

"saturation value" is reached. By correlating hot-wire signals and smoke images of free-jet boundary layers, Freymuth was able to show that the boundary layer becomes very wavy in the region of exponentially increasing disturbance amplitude, whereas the actual vortex-buildup process occurs in the "saturation amplitude" region.

It is due to historical factors that all theoretical stabilities studies until now have assumed the existence of disturbances amplified as a function of time, rather than location, as they actually occur in experiments. A comparison of theoretical and experimental results was only possible if the timewise increase in disturbances at a fixed position was interpreted as three-dimensional development in the direction of flow, using a linear transformation with the phase velocity of the disturbance (see Schubauer and Skramstad [49]). Since the velocity profiles measured in the free-jet boundary layer are described well by the hyperbolic-tangent profile, Michalke [34, 36] calculated the stability behavior of this profile with respect to small, two-dimensional, wave-shaped disturbances, assuming spacial and timewise nullification, flat flow and frictionless fluid. Michalke found that only the stability calculations for spacially amplified disturbances correlated properly with the experimental results of Freymuth; there was very good agreement with respect to magnitude of exponential amplification of the disturbances and their amplitude and phase curves at low frequencies. It is also not surprising that the theory of timewise amplification does not produce the expected results since, as Gaster [12] has shown theoretically, the transformation of the timewise amplification parameter mentioned above is permissible only for slightly amplified disturbances, whereas a high amplification of disturbance, as occurs for example in the free-jet boundary layer, also makes a stability calculation for spacially amplified disturbances necessary.

The conditions for the stability calculations on a free shear layer in air at low velocities and with spacial amplification, as carried out by Michalke, will be discussed once more in detail, since they also form part of the foundation for the author's own calculations:

1. The calculations are based on incompressible disturbance equations. /10
   It will be shown later that this is only possible if the temperature differences occurring in the boundary layer are small.

2. The principal flow was assumed to be planar, a step which is always possible if the dimensions of the core of the jet are large relative to the boundary-layer thickness.

3. The flow was assumed parallel, i.e., it possessed only a velocity component in the direction of flow. This assumption is approximately valid for all flows with boundary-layer character. In addition, a change in the velocity profile in the flow direction was not considered.

4. The stability calculation was carried out for frictionless conditions ($Re \to \infty$), i. e., it was assumed that the only effect of a fluid friction is the formation of the velocity profile and that the disturbance motion can be described with frictionless character (induced instability). This assumption is justified by Freymuth's measurements and by Lessen's [22, 26] theoretical studies on the stability of the Lock profile[1])with spacial amplification and low Reynolds numbers in a compressible fluid. Figure 2a shows the effect of fluid friction upon the disturbance-wave number for various degrees of amplification. One can see that the Lock profile for $Re < 3.7$ is completely stable and that the wave numbers for large Reynolds numbers (according to Figure 2b, for $Re > 300$) are still only a function of the amplification and can thus be determined from a frictionless stability computation. Figure 3 shows that the disturbance amplification for finite Reynolds number is always smaller than amplification in the frictionless case, and thus the fluid friction has only a damping effect (see Betchov [1]).

5. Disruption amplitudes were assumed to be small relative to the corresponding principal-flow quantities, so linearized equations can be used. Thus the disturbances are found to experience a purely exponential rate of growth. Michalke [35, 36] was able to use this simplified theory for approximately calculating the rolling of the free-jet boundary layer, although the measurements by Freymuth [11] have shown the nonlinear character of this rolling. /11

6. It was assumed that the undulating disturbances are propagated only in the direction of flow (two-dimensional disturbances). It should be noted here that, according to Squire's theorem [50], two-dimensional disturbances involve a smaller upper critical Reynolds number than three-dimensional disturbances in incompressible, plane flow; these are disturbances which are propagated at an angle Θ to the direction of flow (see Section 3). In other words, two-dimensional disturbances are more strongly amplified than three-dimensional ones in incompressible flow, a fact which is also supported by the author's calculations for the Lock profile (see Figures 32 through 34). From the good agreement between the measured and calculated amplification parameters, one can conclude that a disturbance produced artificially in the boundary layer is propagated at the angle Θ to the direction of flow which is

---

[1] In this paper, Lock profile refers to the velocity profile formed from a plane discontinuous profile under the influence of fluid friction. It was first calculated by Lock [30] for incompressible fluids, and later by Chapman [6] for compressible fluids (cf. Section 2).

associated with the greatest degree of amplification or for which it can remove a maximum level of fluctuation energy from the principal flow. However, this conclusion does not appear to be completely certain, due to the small number of available experimental results (see W. B. Brown [5] and Mack [33]).

The first theoretical stability studies which take the effect of the compressibility of the flowing medium into consideration were carried out, among others, by Lees and Lin [19], Lees [20], Dunn and Lin [9], Reshotko [44] and Lees and Reshotko [21] for wall boundary layers, and by Landau [16], Pai [41], Lin [28], Lessen, Fox and Zien [23, 24, 25] and Miles [39] for free boundary layers. The results obtained up to 1955 have been summarized by Lin [29].

The difficulties introduced into the stability studies through consideration of the compressibility of the fluid result from the interaction between the mechanical and internal energy of the flowing gas, manifest by the coupling between velocity and temperature profiles of the flow, and from the fact that the flow velocity and the phase velocity of the flow can be on the order of the velocity of sound. Compressibility produces a marked change in the velocity and temperature profiles and at the same time affects the development of disturbances. In this connection, Lees and Lin [19] pointed out the possibility that a disturbance and compressible flow can produce a turbulent transition, but can also lead to the formation of a shock. It was found desirable to characterize the distrubances as subsonic, sonic or supersonic, depending upon their behavior outside the boundary layer. This is meant to indicate that the velocity of the disturbance in the direction of flow, relative to that of the fluid, is less than, equal to, or greater than the local sonic velocity of the gas. /12

The two most interesting results obtained for compressible wall boundary layers indicate (see Lees and Lin [19]) that the upper critical Reynolds number increases with increasing Mach number and with decreasing wall temperature. In other words, increasing Mach number and cooling of the flow stabilize the wall boundary layer. These results were obtained by Lees [20] for Mach number $M \leq 1.3$ and two-dimensional subsonic disturbances. In more recent articles, Mach [31, 32, 33] points out that for $M > 2.2$, the stability behavior of wall boundary layers is changed markedly by the occurrence of supersonic disturbances. The calculations show that, in addition to the first disturbance mode covered by Lees [20], other modes with smaller and smaller disturbance-wavelengths are also possible, of which the second mode is most strongly amplified and thus determines the stability behavior of wall boundary layers for Mach numbers $M > 2.2$. The result is that the upper critical Reynolds number becomes almost independent of the temperature conditions at the wall for high Mach numbers. A stabilizing effect is produced by cooling only so far as the "integral amplification" of a disturbance decreases with decreasing wall temperature due to the increasing Reynolds number in the direction of flow. "Integral amplification" refers to the amplification which a disturbance in the boundary layer undergoes when the changing velocity profile in the direction of flow and the

local amplification parameter, which changes with it, are taken into consideration. /13

Mack also found that for Mach numbers $M > 3.8$, the stability behavior of wall boundary layers changes considerably. The maximum amplification is only reached as $Re \to \infty$, and fluid friction has only a damping effect, as was also found for imcompressible, free boundary layers; only the critical Reynolds number is very much greater for wall boundary layers than for free boundary layers. It was thus possible to carry out frictionless disturbance calculations for high Mach numbers. Mack and W. B. Brown [5] also calculated the amplification of three-dimensional disturbances of the first mode and found that they are much more highly amplified at high Mach numbers than two-dimensional disturbances.

Experimental studies on the amplification of artificially induced disturbances in wall boundary layers were carried out, among others, by Laufer and Vrebalovich [17] and Kendall [15]. Comparison with theory only showed satisfactory agreement for maximum amplification if one assumed that the disturbances were propagated at an angle $\Theta = 60°$, for which the theory gives a maximum amplification of the first mode. W. B. Brown was able to improve the agreement by taking the effect of the $\bar{v}$ component of the principal flow into consideration in his stability calculations. However, one should still exercise caution in assessing the level of agreement attained, since unfortunately all of the theoretical works cited are still based upon the concept of timewise-amplified disturbances, and in addition, there is no experimental proof of the three-dimensionality of the disturbance for the work of Laufer and Vrebalovich [17].

From the studies by Mack, which have shown the change in the instability character of wall boundary layers with increasing Mach number, one can conclude, with a certain degree of justification, that the instability behavior of free boundary layers is also satisfactorily described in compressible fluids, qualitatively and quantitatively, by a frictionless disturbance calculation.

The articles quoted above regarding free boundary layers in gases thus all study their frictionless stability behavior. While very many articles cover the compressible vortex layer (see Pai [41], Lessen, Fox and Zien [23, 24] and Miles [39]), three studies by Lin [28] and Lessen, Fox and Zien [25, 27] are concerned with the stability of the Lock profile. These works are limited to determination of the neutral disturbances as a function of Mach number and angle of incidence of the disturbances. The temperature of the tranquil surroundings was always equal to the isentropic stagnation temperature; this refers to the temperature which is achieved if the principal flow is decelerated isentropically to zero velocity. Lessen found a change in the character of neutral disturbances with increasing Mach number: While the disturbance equations for two-dimensional neutral disturbances remain regular at low Mach numbers, they become singular for larger Mach numbers. Mack found similar neutral solutions in the frictionless disturbance computations for wall boundary layers and coined the phrase "singular /14

neutral solutions" for them. A computation of the timewise or spacial amplification of disturbances has not been made for compressible free boundary layers.

This paper provides several new results regarding the spacial amplification of two-dimensional and three-dimensional disturbances in the free boundary layers, taking into consideration the effect of Mach number and temperature of the quiescent surroundings. The calculations were carried out for Mach numbers $0 \leqq M \leqq 3$ and environment temperatures $0.6 \leqq T_2 \leqq 2$ for air under the conditions discussed above. As for the wall boundary layer, the Mach number has a stabilizing effect. On the other hand, one finds that cooling of the free jet makes the boundary layer unstable. The effect of the temperature of the surroundings is reversed with the occurrence of supersonic disturbances, and cooling of the free jet now has a stabilizing effect. It is shown, moreover, under what conditions singular neutral disturbances occur as a limiting case of amplified disturbances and how they come under the regular neutral solutions. The transition is related to the occurrence of a second, though relatively weakly amplified mode. The amplification of higher modes was not found, but their existence can not be ruled out.

All numerical calculations were carried out on a Type Z 23V digital computer from the Zuse Co., Bad Hersfeld.

2. Computation of the Undisturbed Plane Principal Flow /15

The laminar velocity profile of the free boundary layer, on which the stability study is based, is produced from a plane vortex layer through the effect of fluid friction (Figure 1). A velocity profile computed in this manner is a good approximation for a free jet with a large jet core and thin wall boundary layer at the nozzle outlet. For a supersonic free jet, a Laval nozzle is required which is corrected for flow parallelism.

2.1 Initial Equations

The initial equations for computing the principal plane flow are first given for dimensional quantities (symbols with asterisks) and only later made dimensional by suitable means (symbols without asterisks). It is assumed that the principal flow has boundary-layer character so that the known boundary-layer simplifications apply. In addition, pressure $p^* = \text{const.}$ is to prevail throughout the entire flow volume. The flowing medium is to obey the thermal equation of state for ideal gases. As is well known, the specific heats of the gases can then also be a function of temperature. The velocity components u^* and v^* and the density ρ^* and temperature T^* are then calculated from the following equations:

$$\rho^*\left(u^* \frac{\partial u^*}{\partial x^*} + v^* \frac{\partial u^*}{\partial y^*}\right) = \frac{\partial}{\partial y^*}\left(\mu^* \frac{\partial u^*}{\partial y^*}\right). \qquad (2.1)$$

Continuity equation:

$$\frac{\partial(\rho^* u^*)}{\partial x^*} + \frac{\partial(\rho^* v^*)}{\partial y^*} = 0 . \tag{2.2}$$

Energy equation:

$$\rho^* c_p^* \left(u^* \frac{\partial T^*}{\partial x^*} + v^* \frac{\partial T^*}{\partial y^*}\right) = \frac{\partial}{\partial y^*}\left(\lambda^* \frac{\partial T^*}{\partial y^*}\right) + \mu^* \left(\frac{\partial u^*}{\partial y^*}\right)^2 . \tag{2.3}$$

Thermal equation of state for ideal gases:

$$p^* = R^* \rho^* T^* = \text{const.} \tag{2.4}$$

The following boundary equations apply: /16

$$\begin{aligned} y^* \to +\infty \qquad & u^*(x^*, y^*) = u_1^* \qquad & T^*(x^*, y^*) = T_1^* \\ y^* \to -\infty \qquad & u^*(x^*, y^*) = u_2^* = 0 \qquad & T^*(x^*, y^*) = T_2^* . \end{aligned} \tag{2.5}$$

2.2 Transformation of the Initial Equations

According to Busemann and Crocco (see Schlichting [48]), it is possible to satisfy the energy equation (2.3) identically under certain conditions by using a suitable equation for the temperature. If one introduces into the boundary-layer equations (2.1) to (2.3) the assumption that temperature is dependent only upon the variable u*, equation (2.3) yields:

$$\frac{dT^*}{du^*}\left[c_p^* \frac{\partial}{\partial y^*}\left(\mu^* \frac{\partial u^*}{\partial y^*}\right) - \frac{\partial}{\partial y^*}\left(\lambda^* \frac{\partial u^*}{\partial y^*}\right)\right] = \left(\lambda^* \frac{d^2 T^*}{du^{*2}} + \mu^*\right)\left(\frac{\partial u^*}{\partial y^*}\right)^2 . \tag{2.6}$$

For gases, the Prandtl number

$$Pr = \frac{\mu^* c_p^*}{\lambda^*}$$

is independent of temperature over wide ranges, so (2.6) can be written in the form:

$$c_p^* \frac{Pr-1}{Pr} \cdot \frac{dT^*}{du^*} \cdot \frac{\partial}{\partial y^*}\left(\mu^* \frac{\partial u^*}{\partial y^*}\right) = \lambda^* \left(\frac{d^2T^*}{du^{*2}} + \frac{Pr}{c_p^*}\right)\left(\frac{\partial u^*}{\partial y^*}\right)^2. \quad (2.7)$$

The statement $T^* = T^*(u^*)$ is thus a solution to the system of equations for Pr = 1 and

$$\frac{d^2T^*}{du^{*2}} = -\frac{1}{c_p^*}. \quad (2.8)$$

The following studies are to be limited to gases whose Prandtl numbers are approximately equal to 1 and for which the change in specific heat is negligible for temperature range occurring in the boundary layer, i.e., we make the overall assumptions, for the flowing gas, that Pr = 1 and c_p^* = const. In this case, however, (2.8) can be integrated twice, taking the boundary conditions (2.5) into consideration, and one obtains:

$$\frac{T^*-T_2^*}{T_1^*} = \frac{u_1^{*2}}{2c_p^* T_1^*} \cdot \frac{u^*}{u_1^*}\left(1 - \frac{u^*}{u_1^*}\right) + \left(1 - \frac{T_2^*}{T_1^*}\right)\frac{u^*}{u_1^*}. \quad (2.9) \quad /17$$

Equation (2.9) shows the coupling between velocity profile and temperature profile. This identically satisfies the energy equation (2.3). Dimensionless quantities are introduced for further treatment of the system of equations (2.1), (2.2) and (2.4) for determining the velocity components u* and v* and the density ρ^*. The flow parameters in the undisturbed free jet for $y^* = +\infty$ (subscript 1) are used as reference quantities. The reference length l^* which is introduced only becomes available at the end of this Section. The laminar principal flow is then described by the following dimensionless characteristics:

Reynolds number	$Re = \frac{u_1^* l^*}{\nu_1^*}$	(2.10)
Mach number	$M = \frac{u_1^*}{a_1^*}$	
Isentropic exponent	$\varkappa = \frac{c_p^*}{c_p^* - R^*}$.	

Equations (2.1), (2.2) and (2.4) then have the following dimensionless form:

$$\rho\left(u\frac{\partial u}{\partial x}+v\frac{\partial u}{\partial y}\right)=\frac{1}{Re}\frac{\partial}{\partial y}\left(\mu\frac{\partial u}{\partial y}\right) \tag{2.11}$$

$$\frac{\partial(\rho u)}{\partial x}+\frac{\partial(\rho v)}{\partial y}=0 \tag{2.12}$$

$$T:\rho=1. \tag{2.13}$$

For the coupling condition, equation (2.9), in dimensionless form,

$$T=\left(\frac{\varkappa-1}{2}M^2u+T_2\right)(1-u)+u. \tag{2.14}$$

By introducing a stream function, one can first satisfy the continuity equation (2.12) identically: /18

$$\rho u=\frac{\partial\psi}{\partial y}\;;\qquad \rho v=-\frac{\partial\psi}{\partial x}. \tag{2.15}$$

Employment of a transformation given by L. Howarth (see Schlichting [48]) makes it possible to give the equation almost the same form as for incompressible flow. In L. Howarth's work, a new, independent variable Y is defined in accordance with the equation

$$Y=\int_0^y\frac{dy}{T}. \tag{2.16}$$

If the stream function Ψ and the new coordinate Y are introduced into the boundary-layer equation (2.11) and the gas equation (2.13) is taken into consideration, the result is

$$\frac{\partial\psi}{\partial Y}\cdot\frac{\partial^2\psi}{\partial x\partial Y}-\frac{\partial\psi}{\partial x}\cdot\frac{\partial^2\psi}{\partial Y^2}=\frac{1}{Re}\cdot\frac{\partial}{\partial Y}\left(\frac{\mu}{T}\cdot\frac{\partial^2\psi}{\partial Y^2}\right). \tag{2.17}$$

The transformation

$$\psi = F(\eta)\cdot\sqrt{\frac{x}{Re}} \quad \text{with} \quad \eta = Y\sqrt{\frac{Re}{x}} \tag{2.18}$$

can be used to reduce the partial differential equation (2.17) to the following ordinary third-order differential equation F:

$$2\left(\frac{\mu}{T}F''\right)' + F\cdot F'' = 0 \quad \text{with} \quad (\,)' = \frac{d}{d\eta}. \tag{2.19}$$

Assuming that the dynamic viscosity μ of the gas can be approximated linearly in the temperature range under consideration, expressed in dimensionless notation by $\mu = T$, (2.19) is converted into the corresponding equation for incompressible flow:

$$2F''' + F\,F'' = 0. \tag{2.20}$$

Chapman [6] solved (2.19) numerically for air with the approximation $\mu = T$ and the more exact Sutherland equation $\mu = T^{0.76}$ for dynamic viscosity. The two results deviate from each other by only a small amount, so the velocity profile can be calculated by numerical integration of the differential equation (2.20). For special values of Mach number M and environment temperature T_2, the profiles are obtained by converting the results to the (x, y)-coordinate system using (2.16) and (2.18): /19

$$y\sqrt{\frac{Re}{x}} = \int_0^\eta T\,d\eta. \tag{2.21}$$

In particular, $y\sqrt{Re/x} = \eta$ is obtained for $M = 0$ and $T(y) = T_2 = 1$, which shows its relationship to the incompressible problem. Numerical integration of (2.20) was carried out by Lock [30] with the boundary conditions

$$\begin{aligned} \eta &\to +\infty \qquad F' = u_1 = 1, \\ \eta &\to -\infty \qquad F' = u_2 = 0 \end{aligned} \tag{2.22}$$

and the requirement that the flow-division line coincide with the x-axis. The flow-division line, originating at the nozzle edge, is so defined that the momentum loss of the principal flow above the division line is recovered in the flow below the division line. From the solution curve $F = F(\eta)$,

equations (2.15), (2.18) and (2.21) yield, following several intermediate calculations, the velocity components

$$u = F', \quad v\sqrt{x \cdot Re} = \frac{1}{2}\left(F'\int_0^{\eta} T\,d\eta - T \cdot F\right), \tag{2.23}$$

where $T = T(F'(\eta))$. For momentum thickness ϑ, Lock finds

$$\vartheta\sqrt{\frac{Re}{x}} = -F(\eta = -\infty) = 1{,}2386. \tag{2.24}$$

Momentum thickness is thus independent of Mach number and environment temperature. If (2.24) is again written with dimensional quantities, one obtains /20

$$\frac{\vartheta^*(x^*)}{\sqrt{v_1^* x^*/u_1^*}} = 1{,}2386.$$

It can be seen that the momentum thickness is a characteristic length in the problem; for this reason the reference length l^* is chosen proportional to the momentum thickness:

$$l^*(x^*) = \sqrt{v_1^* x^*/u_1^*}. \tag{2.25}$$

In the following, therefore, we use

$$\eta = Y\sqrt{\frac{Re}{x}} \Rightarrow Y \qquad \text{and} \qquad y\sqrt{\frac{Re}{x}} \Rightarrow y.$$

2.3. Solution to Differential Equation (2.20)

The profiles calculated for the u and v components of velocity and the temperature are shown in Figures 4, 5 and 6 for various Mach numbers M and environment temperatures T_2. One can see that the temperature profiles are effected much more by the Mach number than the velocity profiles of the u component. For the boundary-layer thickness δ ($u_1 = 0.999$; $u_2 = 0.001$), the numerical results yield

$$\delta = 5{,}608 + 0{,}249\, M^2 + 10{,}492\, T_2, \tag{2.26}$$

which clearly shows the great effect of environment temperature upon the boundary-layer thickness.

It was found that the velocity profile $u = u(Y)$ can be approximated well by the generalized hyperbolic-tangent profile, in accordance with Michalke [38]:

$$u = 1 - \left[\frac{1}{2}\left(1 - \tanh a\,(Y - Y_0)\right)\right]^b, \tag{2.27}$$

with $a = 0.307257$, $b = 3.695640$, $Y_0 = 2.127137$. Lock's results are given very well by this function up to the third derivative. The coordinates of the inflection point are independent of Mach number and environment temperature, $Y = y = 0$ and $u = 0.5873$. /21

For the v-component at the boundary-layer edges, the computation (cf. Figure 5) yields

$$v(+\infty)\sqrt{x \cdot Re} = 0{,}040\, M^2 + 0{,}266\, T_2, \tag{2.28}$$

$$v(-\infty)\sqrt{x \cdot Re} = 0{,}620\, T_2.$$

At constant environment temperature T_2,

$$\frac{v}{u} \sim \frac{M^2}{\sqrt{x \cdot Re}}$$

applies for the ratio of transverse velocity to principal-flow velocity within the jet. Both components can thus be of the same order of magnitude near the forward nozzle edge ($x = 0$), for very small Reynolds numbers and in the hypersonic region. In this work, it was assumed that $Re = \infty$, so $v \ll u$ for $x \neq 0$. The boundary-layer flow can therefore be treated as plane parallel flow for a good approximation.

Due to the reference length $l^* = l^*(x^*)$ which was chosen, the velocity profile u given by (2.27), on which the stability computation is based, and the temperature profile T given by (2.14) are only functions of the Y-coordinate or y-coordinate (similar profiles). Thus the stability study also yields "similar" Eigenfunctions, though which the secondary effect of fluid friction upon the "integral amplification" of a disturbance in the

direction of flow is expressed. Again, "integral amplification" refers to the amplification which a disturbance in the boundary layer experiences, taking into consideration the boundary-layer profile of the principal flow, which changes in the direction of flow.

3. Derivation of the Linearized Frictionless Disturbance Equation and Formulation of the Eigenvalue problem /22

3.1 Initial Equations

In order to derive the linearized frictionless disturbance equations, one starts with the motion equations, the continuity equation and the energy statement and Cartesian coordinates for a frictionless fluid, and with the equation of state for ideal gases, which in dimensionless form are

$$\rho\left(\frac{\partial u}{\partial t}+u\cdot\frac{\partial u}{\partial x}+v\cdot\frac{\partial u}{\partial y}+w\cdot\frac{\partial u}{\partial z}\right)=-\frac{1}{\varkappa M^2}\cdot\frac{\partial p}{\partial x},$$

$$\rho\left(\frac{\partial v}{\partial t}+u\cdot\frac{\partial v}{\partial x}+v\cdot\frac{\partial v}{\partial y}+w\cdot\frac{\partial v}{\partial z}\right)=-\frac{1}{\varkappa M^2}\cdot\frac{\partial p}{\partial y},$$

$$\rho\left(\frac{\partial w}{\partial t}+u\cdot\frac{\partial w}{\partial x}+v\cdot\frac{\partial w}{\partial y}+w\cdot\frac{\partial w}{\partial z}\right)=-\frac{1}{\varkappa M^2}\cdot\frac{\partial p}{\partial z},$$

$$\frac{\partial \rho}{\partial t}+u\cdot\frac{\partial \rho}{\partial x}+v\cdot\frac{\partial \rho}{\partial y}+w\cdot\frac{\partial \rho}{\partial z}=-\rho\left(\frac{\partial u}{\partial x}+\frac{\partial v}{\partial y}+\frac{\partial w}{\partial z}\right), \tag{3.1}$$

$$\rho\left(\frac{\partial T}{\partial t}+u\cdot\frac{\partial T}{\partial x}+v\cdot\frac{\partial T}{\partial y}+w\cdot\frac{\partial T}{\partial z}\right)=-p\left(\frac{\partial u}{\partial x}+\frac{\partial v}{\partial y}+\frac{\partial w}{\partial z}\right)(\varkappa-1),$$

$$p=T\cdot\rho.$$

3.2 Linearized Disturbance Equations

Equation (3.1) is valid for the disturbed flow, as well as for the undisturbed principal flow. The principal flow is assumed frictionless here; i.e., the vortex strength existing in the velocity profile at one point in time is not subject to a change caused by dissipation. The disturbed flow is now resolved into the stationary principal flow, the stability of which

is to be studied, and a superimposed disturbance motion, which changes with time. In a plane parallel flow, one can state the following for individual parameters of the flow:

$$u = \bar{u} + u';\ v = v';\ w = w';\ T = \bar{T} + T';\ \rho = \bar{\rho} + \rho';\ p = \bar{p} + p' \qquad (3.2)$$ /23

or, in general, $Q = \bar{Q}(y) + Q'(x, y, z, t)$, where $\bar{Q}$ is a parameter of the principal flow and Q' is the corresponding turbulence value. If (3.2) is substituted into (3.1), all terms which contain only principal-flow quantities cancel out, since the undisturbed flow satisfies (3.1). If one assumes that $Q' \ll \bar{Q}$ for all disturbance values, the equations in the turbulence values can be linearized, and one obtains:

$$\begin{aligned}
\bar{\rho}\left(\frac{\partial u'}{\partial t} + \bar{u}\cdot\frac{\partial u'}{\partial x} + v'\cdot\frac{d\bar{u}}{dy}\right) &= -\frac{1}{\varkappa M^2}\cdot\frac{\partial p'}{\partial x},\\
\bar{\rho}\left(\frac{\partial v'}{\partial t} + \bar{u}\,\frac{\partial v'}{\partial x}\right) &= -\frac{1}{\varkappa M^2}\cdot\frac{\partial p'}{\partial y},\\
\bar{\rho}\left(\frac{\partial w'}{\partial t} + \bar{u}\,\frac{\partial w'}{\partial x}\right) &= -\frac{1}{\varkappa M^2}\cdot\frac{\partial p'}{\partial z},\\
\frac{\partial \rho'}{\partial t} + \bar{u}\,\frac{\partial \rho'}{\partial x} + v'\cdot\frac{d\bar{\rho}}{dy} &= -\bar{\rho}\left(\frac{\partial u'}{\partial x} + \frac{\partial v'}{\partial y} + \frac{\partial w'}{\partial z}\right),\\
\bar{\rho}\left(\frac{\partial T'}{\partial t} + \bar{u}\,\frac{\partial T'}{\partial x} + v'\,\frac{d\bar{T}}{dy}\right) &= -\left(\frac{\partial u'}{\partial x} + \frac{\partial v'}{\partial y} + \frac{\partial w'}{\partial z}\right)(\varkappa - 1),\\
p' &= \bar{\rho}\,T' + \bar{T}\,\rho'.
\end{aligned} \qquad (3.3)$$

3.3 Wave-Form Disturbance Equation

Since the coefficients are functions only of the independent variable y, the following wave-form equation for the disturbance is possible:

$$Q' = q(y)\exp\left[i(\alpha x + \gamma z - \beta t)\right]. \qquad (3.4)$$

In this way the system of partial differential equations is reduced to ordinary differential equations. The amplitude function q(y), the wave numbers α and γ and the frequency β can be complex. Only the real component of Q' has physical meaning, of course. The wave-form equation for the disturbance value does not mean a limitation upon generality, since any arbitrary disturbance can be represented by a suitable Fourier series or a Fourier integral. /24

The following equation thus holds for the various disturbance parameters:

$$(u', v', w', T', \rho', p') = (f, \alpha\varphi, h, \Theta, r, \pi) \exp[i(\alpha x + \gamma z - \beta t)]. \tag{3.5}$$

If (3.5) is substituted into (3.3), one obtains a system of fixed equations for determining the amplitude functions q(y):

$$\bar{\rho}\left[i\left(\bar{u} - \frac{\beta}{\alpha}\right)f + \varphi \cdot \bar{u}'\right] = -i\,\frac{\pi}{\varkappa M^2}, \tag{3.6}$$

$$\bar{\rho}\,\alpha^2\left(\bar{u} - \frac{\beta}{\alpha}\right)\varphi = i\,\frac{\pi'}{\varkappa M^2}, \tag{3.7}$$

$$\bar{\rho}\,\alpha i\left(\bar{u} - \frac{\beta}{\alpha}\right)h = -i\gamma\,\frac{\pi}{\varkappa M^2}, \tag{3.8}$$

$$\alpha i\left(\bar{u} - \frac{\beta}{\alpha}\right)r + \alpha\varphi\bar{\rho}' = -\bar{\rho}\left[i(\alpha f + \gamma h) + \alpha\varphi'\right], \tag{3.9}$$

$$\bar{\rho}\left[\alpha i\left(\bar{u} - \frac{\beta}{\alpha}\right)\Theta + \alpha\varphi\bar{T}'\right] = -\left[i(\alpha f + \gamma h) + \alpha\varphi'\right](\varkappa - 1), \tag{3.10}$$

$$\pi = \bar{\rho}\,\Theta + \bar{T}r, \tag{3.11}$$

where now $(\,)' = \frac{d}{dy}$.

3.4 Differential Equation for the Amplitude Function

It is found desirable to first reduce the system of equations to two equations for π and ϕ. If one multiplies equation (3.9) by $\bar{T}$ and adds it to (3.10), one obtains, using (3.11) and the relationship $\bar{\rho}\bar{T}' + \bar{T}\bar{\rho}' = 0$, the expression /25

$$\alpha i\left(\bar{u} - \frac{\beta}{\alpha}\right)\pi = -\varkappa\left[i(\alpha f + \gamma h) + \alpha\varphi'\right]. \tag{3.12}$$

One eliminates h from equations (3.8) and (3.12),

$$\bar{\rho}\alpha^2(\bar{u}-\frac{\beta}{\alpha})(if+\varphi')=i\frac{\pi}{\varkappa M^2}[\gamma^2-M^2\bar{\rho}\alpha^2(\bar{u}-\frac{\beta}{\alpha})^2], \tag{3.13}$$

and then the unknown f from equations (3.6) and (3.13), producing the system of equations

$$\begin{aligned}(\bar{u}-\frac{\beta}{\alpha})\varphi'-\bar{u}'\varphi&=i\frac{\pi}{\varkappa M^2}[\bar{T}\frac{\alpha^2+\gamma^2}{\alpha^2}-M^2(\bar{u}-\frac{\beta}{\alpha})^2],\\ \bar{\rho}\alpha^2(\bar{u}-\frac{\beta}{\alpha})\varphi&=i\frac{\pi'}{\varkappa M^2}.\end{aligned} \tag{3.14}$$

For very low jet velocities, the compressibility of the gas has no effect, and the Mach number approaches zero, while the quantity $\pi/\varkappa M^2$ remains finite (see list of symbols used), so it appears desirable to introduce a new symbol $\tilde{\pi}$ for this quantity:

$$\frac{\pi}{\varkappa M^2}=\tilde{\pi}. \tag{3.15}$$

Moreover, a quantity G is defined which, as will be seen later, determines the character of the flow:

$$G=\bar{T}\frac{\alpha^2+\gamma^2}{\alpha^2}-M^2(\bar{u}-\frac{\beta}{\alpha})^2. \tag{3.16}$$

Thus equation (3.14) takes on the form

$$\begin{aligned}(\bar{u}-\frac{\beta}{\alpha})\varphi'-\bar{u}'\varphi&=iG\tilde{\pi},\\ \bar{\rho}\alpha^2(\bar{u}-\frac{\beta}{\alpha})\varphi&=i\tilde{\pi}'.\end{aligned} \tag{3.17}$$

The system of equations (3.17) can easily be solved for $\tilde{\pi}$ or ϕ; a linear second-order differential equation is always obtained, e. g., for ϕ it is: /26

$$\left[\frac{(\bar{u}-\frac{\beta}{\alpha})\varphi'-\bar{u}'\varphi}{G}\right]'-\alpha^2\frac{\bar{u}-\frac{\beta}{\alpha}}{\bar{T}}\varphi=0 \tag{3.18}$$

or, when written out,

$$\varphi'' - \frac{G'}{G}\varphi' - G\left[\frac{\left(\frac{\bar{u}'}{G}\right)'}{\bar{u}-\frac{\beta}{\alpha}} + \frac{\alpha^2}{\bar{T}}\right]\varphi = 0. \tag{3.19}$$

If the solution $\phi(y)$ to the differential equation (3.18) or (3.19) has been determined, the remaining amplitude functions are calculated from the following equations:

$$f = \frac{i}{G}\left[\bar{T}\varphi' - M^2\,\bar{u}'\left(\bar{u} - \frac{\beta}{\alpha}\right)\varphi + \bar{u}'\frac{\left(\frac{\gamma}{\alpha}\right)^2\cdot\bar{T}}{\bar{u}-\frac{\beta}{\alpha}}\right]\varphi\,, \tag{3.20}$$

$$h = i\cdot\frac{\gamma}{\alpha}\cdot\frac{\bar{T}}{G}\left[\varphi' - \frac{\bar{u}'}{\bar{u}-\frac{\beta}{\alpha}}\varphi\right], \tag{3.21}$$

$$\tilde{\pi} = \frac{i}{G}\left[\bar{u}'\varphi - \left(\bar{u} - \frac{\beta}{\alpha}\right)\varphi'\right], \tag{3.22}$$

$$\Theta = i\left[(\varkappa-1)M^2\,\bar{T}\cdot\frac{\bar{u}'\varphi - \left(\bar{u}-\frac{\beta}{\alpha}\right)\varphi'}{G} + \frac{\bar{T}'}{\bar{u}-\frac{\beta}{\alpha}}\cdot\varphi\right], \tag{3.23}$$

$$r = i\left[\frac{M^2}{\bar{T}}\cdot\frac{\bar{u}'\varphi - \left(\bar{u}-\frac{\beta}{\alpha}\right)\varphi'}{G} + \frac{\bar{\rho}'}{\bar{u}-\frac{\beta}{\alpha}}\cdot\varphi\right]. \tag{3.24}$$

3.5 Boundary Conditions

The disturbance equation (3.4) represents a three-dimensional, wave-form disturbance. The amplitude $q(y)$, the wave numbers α and γ in the x and z directions and the frequency β can be complex in the general case. If β is assumed to be complex, this implies a timewise amplification or damping of the disturbance Q' at a fixed point in the flow. Such is not observed in boundary-layer flow, however; β must therefore be real. A /27
non-zero imaginary component of wave numbers α and γ means that the disturbance Q' in the x or z direction undergoes a spacial amplification or damping. Only those disturbances are physically meaningful, however, those amplitudes become zero at the infinite extremes of every plane perpendicular to the direction of flow (y, z plane). This is satisfied in the y direction by the requirement $q(y = \pm\infty) = 0$, whereas the boundary condition for the z direction is not satisfied; thus γ must also be taken as real. Only a complex α suits the experimental results, which yields an exponential amplification or damping of the disturbance Q' in the direction of flow for $\alpha_i \neq 0$.

Thus in equation (3.4), one assumes

$$q = q_r + iq_i\ ;\quad \alpha = \alpha_r + i\alpha_i\ ;\quad \beta, \gamma \quad \text{real} \tag{3.25}$$

and for the real component of Q', the only one of physical importance, one obtains

$$\mathrm{Re}\langle Q' \rangle = e^{-\alpha_i x}\, |q(y)| \cos(\alpha_r x + \gamma z - \beta t + \iota) \tag{3.26}$$

with $$\iota(y) = \arctan \frac{q_i}{q_r},$$

where $\iota(y)$ gives the phase angle of the disturbance. The boundary condition is

$$y \to \pm\infty \qquad |q| = 0 \quad \text{or} \quad q_r = 0;\ q_i = 0. \tag{3.27}$$

3.6 Formulation of the Eigenvalue Problem

The following Eigenvalue problem is defined with these homogeneous boundary values: For a given disturbance frequency β and a given wave number γ in the z direction, the Eigenvalues α_r and α_i are to be determined in such a manner that the Eigenfunctions $q_r(y)$ and $q_i(y)$ satisfy the boundary conditions (3.27).

It follows from (3.26) that the disturbance is amplified in the direction of flow for $\alpha_i < 0$ and dampened for $\alpha_i > 0$. For $\alpha_i = 0$, one obtains neutral disturbance, the amplitude of which does not change in the direction of flow. It should be noted here that damped disturbances cannot be determined at all by means of a frictionless disturbance computation, however, /28 since it is the damping friction terms that are neglected. If, for example, a solution $\phi = \phi_r + i\phi_i$ and $\alpha = \alpha_r + i\alpha_i$ to the differential equation (3.19) has been found, the conjugate-complex quantities $\bar{\phi}$ and $\bar{\alpha}$ likewise represent a solution to the equation, and it can be concluded that there must be an amplified disturbance for every Eigenvalue with $\alpha_i \neq 0$. It is still stipulated, however, that α_i always be considered a negative quantity, since the physical character of the disturbance cannot be altered by the boundary transition $\mathrm{Re} \to \infty$.

According to (3.26), the curves of constant disturbance phase are straight lines in the x, z plane:

$$\alpha_r x + \gamma z - \beta t + \iota(y) = \text{const.} \qquad \alpha_r, \gamma, \beta > 0. \tag{3.28}$$

The phase velocity of the disturbance is $c_r = \beta/\alpha_r$ in the x direction and β/γ in the z direction. Rotation of the coordinate system about the y axis shows that a two-dimensional disturbance is involved, the propagation direction of which (ξ-axis) forms the angle Θ with the x-axis (see Figure 1). For the wave-propagation velocity c_{Ph} in the ξ direction and the propagation angle Θ, one obtains

$$\bar{c}_{Ph} = \frac{\beta}{\bar{\alpha}_r} = c_r \cdot \cos\Theta; \qquad \cos\Theta = \frac{\alpha_r}{\bar{\alpha}_r} \tag{3.29}$$

with $$\bar{\alpha}_r = \sqrt{\alpha_r^2 + \gamma^2}.$$

For the study of stability behavior of the flow relative to three-dimensional disturbances, the propagation angle Θ of the disturbance is given in place of the wave number γ.

4. Behavior of Disturbances at Infinite Distance

4.1 Asymptotic Behavior of the Eigenfunctions

The asymptotic behavior of the Eigenfunctions $\tilde{\pi}$ (y) and ϕ (y) for $y \to \pm\infty$ is found from the system of equations (3.17):

$$(\bar{u}_k - \frac{\beta}{\alpha})\,\varphi' = iG_k\tilde{\pi},$$

/29

$$\frac{\alpha^2}{\bar{T}_k}(\bar{u}_k - \frac{\beta}{\alpha})\,\varphi = i\tilde{\pi}', \quad G_k = \bar{T}_k\,\frac{\alpha^2+\gamma^2}{\alpha^2} - M^2(\bar{u}_k - \frac{\beta}{\alpha})^2, \tag{4.1}$$

with

$$\left.\begin{aligned} &y \to +\infty, \quad \bar{u} = \bar{u}_1 = 1; \quad \bar{T} = \bar{T}_1 = 1 \\ &y \to -\infty \quad \bar{u} = \bar{u}_2 = 0; \quad \bar{T} = \bar{T}_2 \end{aligned}\right\} \quad \bar{u}_k' = \bar{T}_k' = 0; \qquad k = 1;2. \tag{4.2}$$

By solving the system of equation (4.1), one obtains differential equations of the same form for $\tilde{\pi}$ and ϕ. Quite generally, the asymptotic behavior of all Eigenfunctions $q(y)$ is expressed by

$$q'' - \omega_k^2 q = 0 \quad \text{with} \quad \omega_k^2 = \alpha^2 \cdot \frac{G_k}{\bar{T}_k} = R_{kr} + iR_{ki}; \quad k = 1;2. \tag{4.3}$$

Since $\omega_k = \pm \sqrt{R_k} = \omega_{kr} + i\omega_{ki}$, there are two fundamental solutions to (4.3). The general solution is a linear superposition of these fundamental solutions:

$$q = Ae^{+\omega_k y} + Be^{-\omega_k y}, \qquad A \text{ and } B \text{ complex constants.} \tag{4.4}$$

In order to satisfy the boundary conditions, we set $\omega_{kr} > 0$ and then obtain

$$\begin{aligned} &y \to +0 \qquad q = Be^{-\omega_1 y} \qquad B = B_r + iB_i, \\ &y \to -0 \qquad q = Ae^{+\omega_2 y} \qquad A = A_r + iA_i. \end{aligned} \tag{4.5}$$

we obtain ω_k as

$$\omega_k = \omega_{kr} + i\omega_{ki} = \pm \sqrt{\tfrac{1}{2}(|R_k| + R_{kr})} + i \operatorname{sgn}\langle R_{ki}\rangle \sqrt{\tfrac{1}{2}(|R_k| - R_{kr})}, \qquad k = 1;2, \tag{4.6}$$

where /30

$$\begin{aligned} R_{kr} &= \alpha_r^2 \left[\frac{\alpha_r^2 + \gamma^2}{\alpha_r^2} - \frac{M^2}{\bar{T}_k}\left(\bar{u}_k - \frac{\beta}{\alpha_r}\right)^2\right] + \alpha_i^2\left(\frac{M^2}{\bar{T}_k}\bar{u}_k^2 - 1\right), \\ R_{ki} &= 2\alpha_i\alpha_r\left[1 - \frac{M^2}{\bar{T}_k}\bar{u}_k\left(\bar{u}_k - \frac{\beta}{\alpha_r}\right)\right], \qquad k = 1;2, \\ \operatorname{sgn}\langle R_{ki}\rangle &= \operatorname{sgn}\langle \omega_{ki}\rangle = \operatorname{sgn}\langle \alpha_i\left[\bar{T}_k - M^2\bar{u}_k\left(\bar{u}_k - \frac{\beta}{\alpha_r}\right)\right]\rangle \end{aligned} \tag{4.7}$$

The sign of ω_{ki} is indeterminate for neutral disturbances ($\alpha_i = 0$). Since we are only interested in those neutral disturbances which form the limiting case of amplified disturbances ($\alpha_i < 0$), however, we write

$$\operatorname{sgn}\langle \omega_{ki} \rangle = \operatorname{sgn} \langle M^2 \bar{u}_k \left(\bar{u}_k - \frac{\beta}{\alpha_r}\right) - \bar{T}_k \rangle, \qquad k = 1;2 \tag{4.8}$$

for equation (4.7) and thus obtain a uniform representation of the asymptotic solution for amplified disturbances, including their limiting case, the neutral disturbance.

4.2 Physical Character of the Asymptotic Solutions

One can best see the physical character of the asymptotic solution by substituting (4.5) into (3.26):

$$\begin{aligned} y \to +\infty \quad & \mathcal{R}e\langle Q' \rangle = |B| e^{-\alpha_i x - \omega_{1r} y} \cos(\alpha_r x + \gamma z - \omega_{1i} y - \beta t + \iota_B), \\ y \to -\infty \quad & \mathcal{R}e\langle Q' \rangle = |A| e^{-\alpha_i x + \omega_{2r} y} \cos(\alpha_r x + \gamma z + \omega_{2i} y - \beta t + \iota_A), \end{aligned} \tag{4.9}$$

with $\iota_A = \arctan \frac{A_i}{A_r}$; $\iota_B = \arctan \frac{B_i}{B_r}$.

The curves of constant phase are straight lines in the ξ, y system:

$$\begin{aligned} y \to +\infty \quad & \bar{\alpha_r}\, \xi - \omega_{1i} y - \beta t + \iota_B = \text{const}, \\ y \to -\infty \quad & \bar{\alpha_r}\, \xi + \omega_{2i} y - \beta t + \iota_A = \text{const}. \end{aligned} \tag{4.10}$$

/31

For $\omega_{ki} > 0$, one obtains waves entering the boundary layer, and for $\omega_{ki} < 0$, waves leaving the boundary layer, with the phase velocity

$$c_{Ph_k} = \frac{\beta}{\sqrt{\alpha_r^2 + \gamma^2 + \omega_{ki}^2}}, \qquad k = 1;2. \tag{4.11}$$

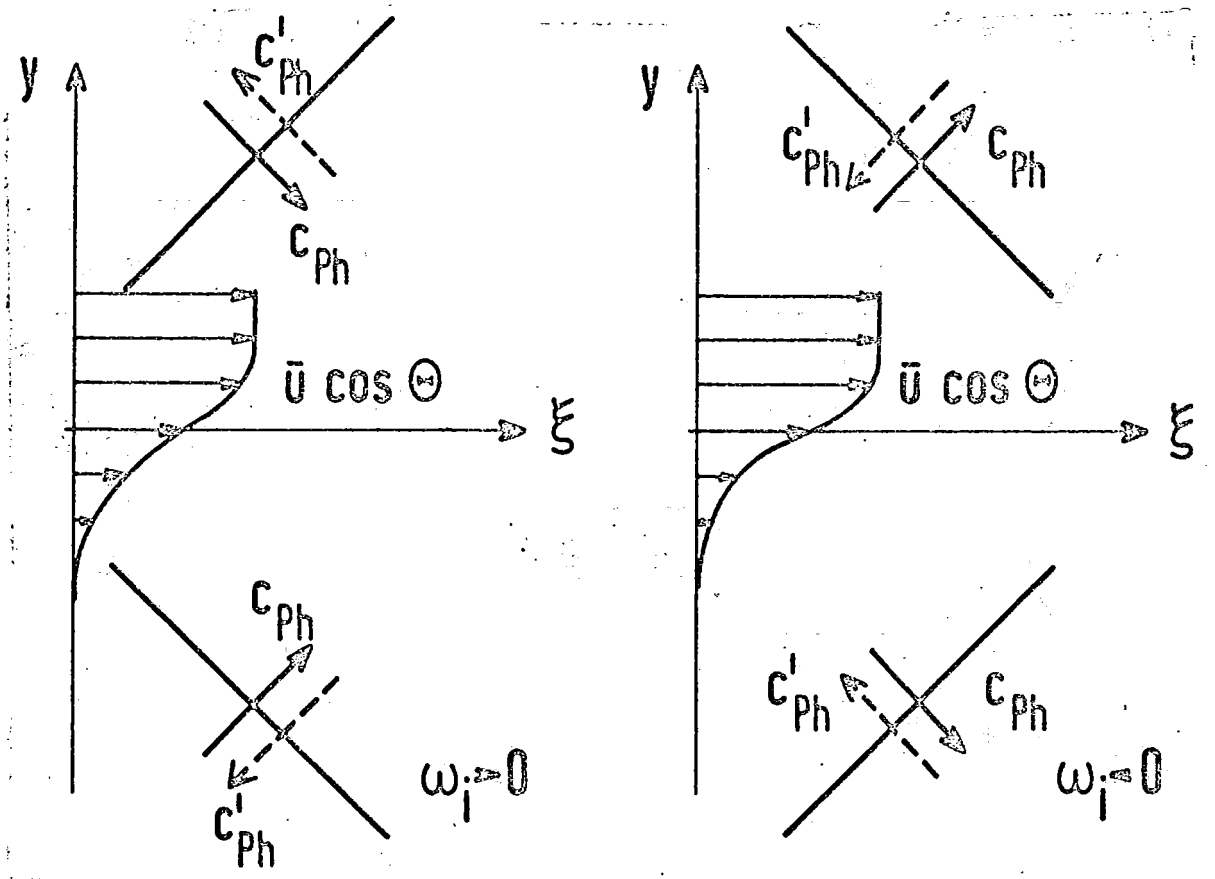

However, this conception is reversed for an observer moving with a relative system (ξ', y) in the ξ direction with flow velocity $\bar{u}_1 \cos\Theta = \cos\Theta$:

$$\xi = \xi' + t\cos\Theta. \tag{4.12}$$

For the lines of constant phase, one obtains, with (3.29) in the relative system, /32

$$y \to +\infty \quad \overline{\alpha_r}\ \xi' - \omega_{1i} y + \alpha_r (1 - c_r) t + \iota_B = \text{const},$$

$$y \to -\infty \quad \overline{\alpha_r}\ \xi' + \omega_{2i} y + \alpha_r (1 - c_r) t + \iota_A = \text{const}. \tag{4.13}$$

The numerical results (c.f. Section 8 and Appendix 9.1) show that $c_r < 1$. Thus in (4.13) the sign of the time-dependent term changes relative to (4.10), however, and the relationships are reversed. The phase velocity c'_{ph} in the relative system is then

$$c'_{ph_k} = \frac{\alpha_r (1 - c_r)}{\sqrt{\alpha_r^2 + \gamma^2 + \omega_{ki}^2}} \qquad k = 1;2. \tag{4.14}$$

Evaluation of (4.8) shows that for $y = -\infty$, $\omega_{2i} < 0$, so a stationary observer there always sees a wave leaving the jet.

Particularly demonstrative results are obtained for the neutral disturbances with $\alpha_r = \alpha_N$ and $\alpha_i = 0$. Then ω_k^2 is real, and for (4.6), one can write

$$\omega_k = \alpha_r \sqrt{\frac{\alpha_r^2 + \gamma^2}{\alpha_r^2} - \frac{M^2}{\bar{T}_k} \left(\bar{u}_k - \frac{\beta}{\alpha_r}\right)^2} = \overline{\alpha_r} \sqrt{1 - \left(\frac{\bar{u}_k \cos \Theta - \bar{c}_{ph_k}}{\bar{a}_k}\right)^2}, \qquad k = 1;2, \tag{4.15}$$

where the local sonic velocity $\bar{a} = \sqrt{\bar{T}}/M$ has been introduced. According to (4.15), ω_k is real as long as the relative velocity of the disturbance relative to the flowing medium is smaller than or equal to the local sonic velocity. These disturbances are to be called neutral disturbances with subsonic or sonic character. In contrast, ω_k is imaginary if the relative velocity is greater than the local sonic velocity. Neutral disturbances with supersonic character are then involved. The sign of ω_{ki} is again determined by equation (4.8). Neutral sonic and supersonic disturbances

are waves of constant amplitude, at infinite distance and the associated Eigenfunctions according to (4.5) do not satisfy the boundary conditions (3.27). In Section 5.1 it is shown that the neutral disturbances with supersonic character are identical to the singular neutral solutions mentioned in the Introduction. With equations (4.11) and (4.14), one obtains, for the phase velocity of these singular neutral disturbances in the absolute and relative systems, /33

$$\begin{aligned} y \to +\infty \quad & c_{ph_1} = \frac{c_r}{1-c_r}\,\bar{a}_1, \qquad c'_{ph_1} = \bar{a}_1, \\ y \to -\infty \quad & c_{ph_2} = \bar{a}_2 \qquad c'_{ph_2} = \frac{1-c_r}{c_r}\,\bar{a}_2. \end{aligned} \tag{4.16}$$

For the angle σ between the wave front and the negative part of the ξ-axis, moreover, one obtains

$$\sin \sigma_k = \frac{1}{\dfrac{\bar{u}_k \cos\Theta - \bar{c}_{ph_k}}{\bar{a}_k}} \qquad k = 1; 2, \tag{4.17}$$

i.e., the reciprocal of the Mach number, which characterizes the relative motion of the disturbance with respect to the flowing medium. The singular neutral disturbances thus behave at infinite distance like Mach waves moving at sonic velocity relative to the flowing medium, perpendicular to their length, the disturbance amplitudes remain constant, since they can not be damped by interference effects as in the case of neutral subsonic disturbances. The damping of the disturbances, as must be required for a real gas, would only be achieved by incorporating damping friction terms in the disturbance computation.

5. Discussion on the Neutral Disturbances

5.1 Determination of the Phase Velocity of Neutral Disturbances

The differential equation (3.19) for the Eigenfunction $\phi(y)$ is regular for amplified disturbances with $\alpha_i \neq 0$ at every point y. For neutral disturbances with real $\alpha = \alpha_N$ and phase velocity $c_N = (\beta/\alpha)_N$, however, (3.19) can become singular at the points $G = 0$ and $\bar{u} - c_N = 0$. The expression G from (3.16) can be rewritten using (3.29) and introducing the local sonic velocity $\bar{a}$:

$$G(\alpha_i = 0) = \frac{\bar{T}}{\cos^2 \Theta} \left[1 - \left(\frac{\bar{u} \cos \Theta - \bar{c}_{ph_N}}{\bar{a}}\right)^2\right], \qquad (5.1)$$

/34

with

$$\bar{c}_{ph_N} = c_N \cos \Theta.$$

Thus the transition from the subsonic to the supersonic range of disturbance in the flow field is characterized by G = 0. This point G = 0 has no significance for the differential equation, since only an apparent singularity is involved which occurs as the result of solving the systems of equations (3.17) for ϕ. Equation (3.17) shows that the point $\bar{u} - c_N = 0$ is the only singularity. The neutral phase velocity for the inequality $0 \leqq c_N \leqq 1$ must be sufficient for the occurrence of this singularity. The general proof that the phase velocity of each disturbance lies within the limits

$$\bar{u}_{min} \leqq c_r \leqq \bar{u}_{max} \qquad (5.2)$$

could previously be demonstrated only for timewise-amplified disturbances in incompressible media (see Lin [29]). Adaptation of this proof to spacially amplified disturbances in incompressible or compressible fluids yields only the lower limit for c_r (see Appendix 9.1); to be sure, the existence of the upper limit for c_r is verified by the results of the numerical study on the Eigenvalue problem (see Section 8). Equation (3.19) thus becomes singular at the point $\bar{u} = c_N$ or $y = y_c$ (the so-called critical layer) if it is not simultaneously true that $\phi(y_c) = \phi_c$, or the expression $(\bar{u}'/\bar{T})'_c$ disappears. Lees and Lin [19] have shown analytically that $\phi_c \neq 0$ if ϕ satisfies the boundary conditions. Since a constant transition from the regular, amplified solutions to the neutral solution can now be expected, the expression $(\bar{u}'/\bar{T})'$ must disappear in the critical layer for the neutral case.

The expression $(\bar{u}'/\bar{T})'$ disappears for the Lock profile for every combination of Mach number M and environment temperature $\bar{T}_2$, at least at the point $\bar{u} = c_s$, which is given by the equation:

$$\left(\frac{\bar{u}'}{\bar{T}}\right)'_{\bar{u} = c_s} = 0 \qquad (5.3)$$

or, with equations (2.14) and (2.27), /35

$$\frac{(1+\frac{1}{b})(1-c_s)^{1/b}-1}{(1-c_s)[1-(1-c_s)^{1/b}]} - 2\frac{\frac{\varkappa-1}{2}M^2(1-2c_s)+1-\bar{T}_2}{(\frac{\varkappa-1}{2}M^2c_s+\bar{T}_2)(1-c_s)+c_s} = 0. \qquad (5.4)$$

Figure 7 shows curves of the function $(\bar{u}'/\bar{T})'$ versus y for various Mach numbers M and environment temperatures $\bar{T}_2$. For $M > 3$ and $\bar{T}_2 < 0.6$, this function has several solutions for c_s. Figure 8 shows the solution c_s to (5.3) as a function of Mach number and environment temperature in a three-dimensional representation, in which the additional solutions occurring only at higher Mach numbers have not been taken into consideration.

The calculations have shown, however, that a neutral disturbance with phase velocity $c_N = c_s$ is not associated with every solution c_s. Section 5.2 shows for which values c_s corresponding neutral solutions have been found. From the fact that (5.3) can have several zero points, it would be possible to conclude the existence of several amplified disturbance modes and thus several neutral disturbances. Mack [32] has shown, for compressible wall boundary layers, that this speculation is generally not born out.

For the environment temperature $\bar{T}_2 = 1$ and low flow velocities with $M = 0$, equation (5.3) yields

$$\bar{u}''_{\bar{u}=c_s} = 0.$$

The phase velocity c_N of a possible neutral disturbance is thus equal to the velocity c_s at the inflection point of the boundary-layer profile. Tollmien [54] has shown, for velocity profiles with inflection points in incompressible fluids, that a neutral disturbance with phase velocity $c_N = c_s$ is the only neutral solution which satisfies the boundary conditions and remains regular over the entire flow range. Tollmien has also shown that in incompressible media, the existence of an inflection point in the velocity profile represents a necessary and sufficient condition for the occurrence of timewise-amplified disturbances (c.f. Section 1). One may assume that the existence of a point in the velocity profile at which the expression /36
$(\bar{u}'/\bar{T})'$ disappears has a significance for the stability of a compressible flow which is similar to the significance of an inflection point with

$\bar{u}'' = 0$ for an incompressible flow. This is also verified by all numerical studies; the rigorous proof of this hypothesis has as yet not been found.

According to (5.1), the neutral disturbance has subsonic character relative to the flow if $G > 0$, i.e.

$$|\bar{u} - c_N| < \frac{\bar{a}}{\cos\Theta}. \tag{5.5}$$

The neutral disturbance thus has subsonic character within the entire flow if its phase velocity satisfies the condition

$$1 - \frac{\bar{a}_1}{\cos\Theta} < c_N < \frac{\bar{a}_2}{\cos\Theta} \tag{5.6}$$

For two-dimensional disturbances, these limites are given by

$$1 - \frac{1}{M} < c_N < \frac{\sqrt{\bar{T}_2}}{M}; \quad (\Theta = 0°). \tag{5.7}$$

These values yield boundary curves in Figure 8 on which the associated neutral disturbance assumes sonic character within the jet or at the outer edge of the jets. Only the limit $c_N = \bar{a}_2/\cos\Theta$ has proved to be meaningful for the numerical calculation of the Eigenvalues within the Mach and temperature ranges studied.

The calculations for amplified disturbances show that the phase velocity c_r for $\alpha_i \to 0$ actually approaches a limiting value c_N. It has been shown, however, that the phase velocity c_N is only a solution to equation (5.3) if the disturbance has subsonic or sonic character throughout the entire flow region. Only then is the differential equation (3.19) thus regular in the critical layer. If the neutral disturbance, on the other hand, assumes supersonic character at some point in the flow (this always occurred first at the outer edge of the boundary layer for the parameter combinations studied), equation (5.3) is not satisfied by $\bar{u} = c_N$, and (3.19) becomes singular. The results can be summarized as

$$\left(\frac{\bar{u}'}{\bar{T}}\right)'_{\bar{u}=c_N} = 0 \quad \text{and} \quad c_N = c_s \quad \text{for } c_N \leqq \bar{a}_2/\cos\Theta,$$

$$\left(\frac{\bar{u}'}{\bar{T}}\right)'_{\bar{u}=c_N} < 0 \quad \text{and} \quad c_N > c_s \quad \text{for } c_N > \bar{a}_2/\cos\Theta. \tag{5.8}$$

/37

Neutral disturbances with supersonic character are thus called singular neutral disturbances (see Section 1). The associated Eigenvalues can only be determined approximately through extrapolation from the neighboring weakly amplified disturbances.

5.2 Discussion on the Singular Neutral Disturbances

5.2.1 Behavior of the Differential Equation (3.19) in the Critical Layer

In the following material, the behavior of the differential equation (3.19) near the critical layer $y = y_c$ is to be studied for neutral supersonic disturbances. It is assumed that the coefficients in (3.19) can be expanded in terms of powers of $y - y_c$ in the vicinity of $y = y_c$ (see Appendix Section 9.2). A fundamental system of solutions can then be given near the critical layer (Tollmien [54], Lees and Lin [19]):

$$\varphi_1 = (y - y_c)\, g_1 (y - y_c)$$

$$\varphi_2 = D\,\varphi_1 \log (y - y_c) + g_2 (y - y_c); \qquad D = \frac{\bar{T}_c}{\bar{u}'_c}\left(\frac{\bar{u}'}{\bar{T}}\right)'_c. \tag{5.9}$$

Here g_1 and g_2 are power series in $y - y_c$ which both assume the value of 1 in the critical layer. The general solution is obtained through linear superposition of the fundamental solutions, (5.9):

$$\varphi = \nu_1 \varphi_1 + \nu_2 \varphi_2. \tag{5.10}$$

According to (5.9), ϕ is regular in the critical layer, while all derivatives of ϕ become logarithmically singular. For neutral subsonic and sonic disturbances, $D = 0$ is always true, so the derivatives also remain

regular. The logarithm occurring in the solution is defined only for positive arguments $y > y_c$. According to Tollmien [54], the analytical extension of the logarithm in this case is given by /38

$$\log (y - y_c) = \ln |y - y_c| - i\pi \tag{5.11}$$

for negative arguments $y \leqq y_c$. For supersonic disturbances, all Eigenfunctions are thus also complex in the neutral case. The free constants ν_1 and ν_2 in (5.10) are thus also to be made complex, i.e., $\nu_1 = \nu_{1r} + i\nu_{1i}$ and $\nu_2 = \nu_{2r} + i\nu_{2i}$. If the solution (5.10) is resolved into a real component and an imaginary component, one obtains for $y > y_c$

$$\begin{aligned} \varphi_r &= \nu_{1r}(y - y_c)g_1 + \nu_{2r}[D(y - y_c)g_1 \ln (y - y_c) + g_2], \\ \varphi_i &= \nu_{1i}(y - y_c)g_1 + \nu_{2i}[D(y - y_c)g_1 \ln (y - y_c) + g_2], \end{aligned} \tag{5.12}$$

and for $y \leqq y_c$

$$\begin{aligned} \varphi_r &= \nu_{1r}(y - y_c)g_1 + \nu_{2r}[D(y - y_c)g_1 \ln |y - y_c| + g_2] + \pi\nu_{2i}D(y - y_c)g_1, \\ \varphi_i &= \nu_{1i}(y - y_c)g_1 + \nu_{2i}[D(y - y_c)g_1 \ln |y - y_c| + g_2] - \pi\nu_{2r}D(y - y_c)g_1. \end{aligned} \tag{5.13}$$

It follows from this that ϕ remains constant in the critical layer, while ϕ' makes a jump, and

$$\lim_{\varepsilon \to 0} [\varphi'(y_c + \varepsilon) - \varphi'(y_c - \varepsilon)] = i\pi\nu_2 D = i\pi\varphi_c D. \tag{5.14}$$

For the Eigenfunction f(y) of the u' disturbance, according to (3.20), this discontinuity in ϕ' means a discontinuity in the critical layer which, to be sure, occurs only for neutral supersonic disturbances.

5.2.2 Wronskian Determinate for the Fundamental System

In the case of a neutral disturbance, all coefficients of the differential equation (3.19) are real. The real component ϕ_r and the imaginary component ϕ_i of a complex solution of ϕ are thus not coupled and must satisfy the differential equation independently of each other. It is possible for ϕ_r and ϕ_i to form a fundamental system for which the Wronskian determinate W of the differential equation (3.19) is not identically zero. The Wronskian determinate of (3.19), according to Szabo [52], is then /39

$$W = \varphi_r \varphi_i' - \varphi_i \varphi_r' = \exp\left(\int \frac{G'}{G}\, dy\right) = KG, \tag{5.15}$$

where K in this case is a real constant.

Since the fundamental system ϕ_r and ϕ_i is known near the critical layer, the Wronskian determinant W in accordance with (5.15) can be calculated out for this solution for ϕ, and information is thus obtained regarding the constant K. If ϕ_r and ϕ_i, according to (5.12) and (5.13) are successively substituted into (5.15) and the boundary transition $y \to y_c$ is carried out, the result is

$$\begin{aligned} W(y_c + 0) &= v_{1r} v_{2i} - v_{1i} v_{2r} = \operatorname{Im} \langle \bar{v}_1 v_2 \rangle, \\ W(y_c - 0) &= \operatorname{Im} \langle \bar{v}_1 v_2 \rangle - \pi |\varphi_c|^2 D. \end{aligned} \tag{5.16}$$

The Wronskian determinant thus jumps in the critical layer by the amount

$$W(y_c + 0) - W(y_c - 0) = \pi |\varphi_c|^2 D. \tag{5.17}$$

For the constant K above and below the critical layer, we thus have the values

$$y > y_c \qquad K = \frac{\mathrm{Im} < \bar{v}_1 v_2 >}{G_c} ,$$

$$y \leqq y_c \qquad K = \frac{\mathrm{Im} < \bar{v}_1 v_2 > - \pi |\varphi_c|^2 D}{G_c} . \tag{5.18}$$

One can conclude from this that for all values of y, linearly independent solutions ϕ_r and ϕ_i can exist; on the other hand, the Wronskian determinant in accordance with (5.15) also disappears for $G = 0$, i.e., at the point in the flow field at which the disturbance assumes sonic character. Since the solution $\phi(y)$ always remains regular at the point $G = 0$ however, as was shown by Lees and Lin [19], the constant K does not change in value at this point. /40

The asymptotic behavior of the Eigenfunction is described by equation (4.5). Resolution into a real component and an imaginary component yields a fundamental system ϕ_r and ϕ_i for $y \to \pm\infty$; care must be taken here to see that ω_k^2 is real in the neutral case. If the Wronskian determinant is now evaluated, it is necessary to decide whether subsonic, sonic or supersonic character is present. The results are

Subsonic	$\omega_k^2 > 0$	$W_k = 2\omega_{kr}\, \mathrm{Im} < A\bar{B} > = 2\omega_{kr}(A_i B_r - A_r B_i),$
Sonic	$\omega_k^2 = 0$	$W_k = 0,$
Supersonic	$\omega_k^2 < 0$	$W_k = \omega_{ki}(\|A\|^2 - \|B\|^2), \quad k = 1;2.$

(5.19)

If the boundary conditions are taken into consideration for the Eigenfunction (3.27), the following tabulation applies for the Wronskian determinant W_k:

	$y \to +\infty;\ A = 0$	$y \to -\infty;\ B = 0$
Subsonic	$W_1 = 0$	$W_2 = 0$
Sonic	$W_1 = 0$	$W_2 = 0$
Supersonic	$W_1 = -\omega_{1i} \lvert B \rvert^2$	$W_2 = \omega_{2i} \lvert A \rvert^2$

(5.20)

On the other hand, it follows from equation (5.15) that $W_k = KG$, so equation (5.20) can be used now to provide approximate information regarding the constant K above and below the critical layer. Three characteristic special cases of neutral disturbances will be discussed in detail.

5.2.3 Discussion of Several Characteristic Neutral Disturbances

1. The neutral disturbance has subsonic character at both flow edges. For the constant K, equations (5.15) and (5.18) yield

$$y > y_c \qquad K = \frac{W}{G} = \frac{\mathrm{Im} \langle \bar{\nu}_1 \nu_2 \rangle}{G_c} = 0 \qquad \text{/41}$$

(5.21)

$$y \leqq y_c \qquad K = \frac{W}{G} = \frac{\mathrm{Im} \langle \bar{\nu}_1 \nu_2 \rangle - \pi \lvert \varphi_c \rvert^2 D}{G_c} = 0 .$$

From this follow the conditions

$$\mathrm{Im} \langle \bar{\nu}_1 \nu_2 \rangle = 0 \quad \text{and} \quad D = \frac{\bar{T}_c}{\bar{u}'} \left(\frac{\bar{u}'}{\bar{T}} \right)'_c = 0. \tag{5.22}$$

The second condition means that the expression $(\bar{u}'/\bar{T})'$ must disappear in the critical layer. The neutral phase velocity c_N is then a solution to (5.3), and the differential equation (3.19) is regular for all y values. One can thus take ϕ as real without limiting generality, i.e., one sets $\nu_{1i} = \nu_{2i} = 0$. In this way the first condition is also satisfied. The same statement applies for the case in which the disturbance exhibits sonic character at both edges.

2. The neutral disturbance has supersonic character at both flow edges. One then obtains for the constant K

$$y > y_c \qquad K = \frac{W}{G} = \frac{\mathrm{Im}\langle \bar{v}_1 v_2 \rangle}{G_c} = -\frac{\omega_{1i}|B|^2}{G_1},$$

$$y \leqq y_c \qquad K = \frac{W}{G} = \frac{\mathrm{Im}\langle \bar{v}_1 v_2 \rangle - \pi |\varphi_c|^2 D}{G_c} = \frac{\omega_{2i}|A|^2}{G_2}. \tag{5.23}$$

The disturbance amplitudes $|A|$ and $|B|$ at the flow edges are then related to the function value $|\phi_c|$ by the following equation:

$$\frac{\pi |\varphi_c|^2 D}{G_c} = -\frac{\omega_{1i}|B|^2}{G_1} - \frac{\omega_{2i}|A|^2}{G_2}. \tag{5.24}$$

It follows from this that the function value $|\phi_c|$ in the critical layer is only determined by stipulating the disturbance amplitudes $|A|$ and $|B|$.

3. The neutral disturbance has subsonic character inside the jet and supersonic character at the outer flow edge. Only this type of supersonic disturbance occurred in the numerical calculations. For the constant K, one obtains /42

$$y > y_c \qquad K = \frac{W}{G} = \frac{\mathrm{Im}\langle \bar{v}_1 v_2 \rangle}{G_c} = 0,$$

$$y \leqq y_c \qquad K = \frac{W}{G} = \frac{\mathrm{Im}\langle \bar{v}_1 v_2 \rangle - \pi |\varphi_c|^2 D}{G_c} = \frac{\omega_{2i}|A|^2}{G_2}. \tag{5.25}$$

It follows from this that

$$\mathrm{Im}\langle \bar{v}_1 v_2 \rangle = 0 \quad \text{and} \quad -\frac{\pi |\varphi_c|^2 D}{G_c} = \frac{\omega_{2i}|A|^2}{G_2}. \tag{5.26}$$

From the first condition, one again concludes, as in the first example, that e.g. it is possible to set $\nu_{1i} = \nu_{2i} = 0$ so that ϕ is completely real for $y > y_c$, while ϕ remains complex for $y \leq y_c$. The second condition states that the disturbance amplitude $|A|$ at the supersonic edge again determines the function value $|\phi_c|$ in the critical layer. The sign of the expression $(\bar{u}'/\bar{T})'_c$ in the critical layer can also be determined from (5.26): ω_{2i} is negative due to the way in which the signs are established in (4.8), and G_2 is likewise negative, due to the supersonic character of the disturbance, so D and thus $(\bar{u}'/\bar{T})'$ must also become negative in the critical layer. According to Figure 7, it follows that $c_N > c_s$ must always be true for the parameter combinations M and $\bar{T}_2$ which were calculated (cf. equation (5.8)). The calculations have shown the correctness of these results.

5.3 Energy Balance of the Disturbance Motion for Neutral Disturbances

Additional insight into the character of the neutral solutions is obtained from an accounting of the disturbance-motion energy. The same considerations have been applied by Lees and Lin [19] for the compressible wall boundary layer. If one calculates the substantial variation in the timewise mean value of the kinetic energy of the disturbance, from the energy equation of mechanics, one obtains, in a dimensionless representation (see Appendix Section 9.3),

$$\bar{\rho}\left(\frac{\partial}{\partial t} + \bar{u}\frac{\partial}{\partial x}\right)\left(\frac{\overline{u'^2 + v'^2 + w'^2}}{2}\right) = -\bar{\rho}\,\overline{u'v'}\frac{d\bar{u}}{dy} - \frac{1}{\varkappa M^2}\overline{\left(u'\frac{\partial p'}{\partial x} + v'\frac{\partial p'}{\partial y} + w'\frac{\partial p'}{\partial z}\right)}. \quad (5.27)$$ /43

Betchov and Criminale [2] provide a clear physical explanation of the terms on the right side of this equation. The first term characterizes the energy transfer between the principal flow and the disturbance motion, resulting from the Reynolds shear stresses

$$\tau_R = -\bar{\rho}\,\overline{u'v'}. \quad (5.28)$$

The energy transfer remains limited to the boundary layer, since only there is the vortex strength $\bar{u}' \neq 0$. For $\tau_R > 0$, the principal flow provides energy for the disturbance motion, and for $\tau_R < 0$, energy from the disturbance motion is transferred to the principal flow. The second term characterizes the loss or gain in kinetic energy of the disturbance which is connected

with a particle transfer among areas of higher or lower pressure. According to Lees and Lin [19], this term is in particular a measure of the disturbance energy radiated away via sonic waves (see Appendix Section 9.5).

For neutral disturbances, the substantial change in disturbance energy must be zero to comply with definition. This is verified with the aid of results from the linearized stability computation in Appendix Section 9.3. For neutral subsonic and sonic disturbances, the terms on the right side of (5.27) disappear individually, whereas for neutral supersonic disturbances only the sum of the two terms becomes zero. Thus, as for amplified disturbances, an energy transfer between the principal flow and the disturbance motion takes place via momentum exchange for neutral supersonic disturbances, the direction of the transfer being determined by the sign of the Reynolds shear stresses τ_R. With the results of the linearized stability theory, according to equation (5.25) and (9.16) one obtains, for the type of supersonic disturbance covered as Example 3 in Section 5.2.3,

$$y > y_c \quad \tau_R = 0, \tag{5.29}$$

/44

$$y \leqq y_c \quad \tau_R = \frac{1}{2}\alpha_N K = -\frac{\alpha_N \pi |\varphi_c|^2 D}{2G_c} > 0.$$

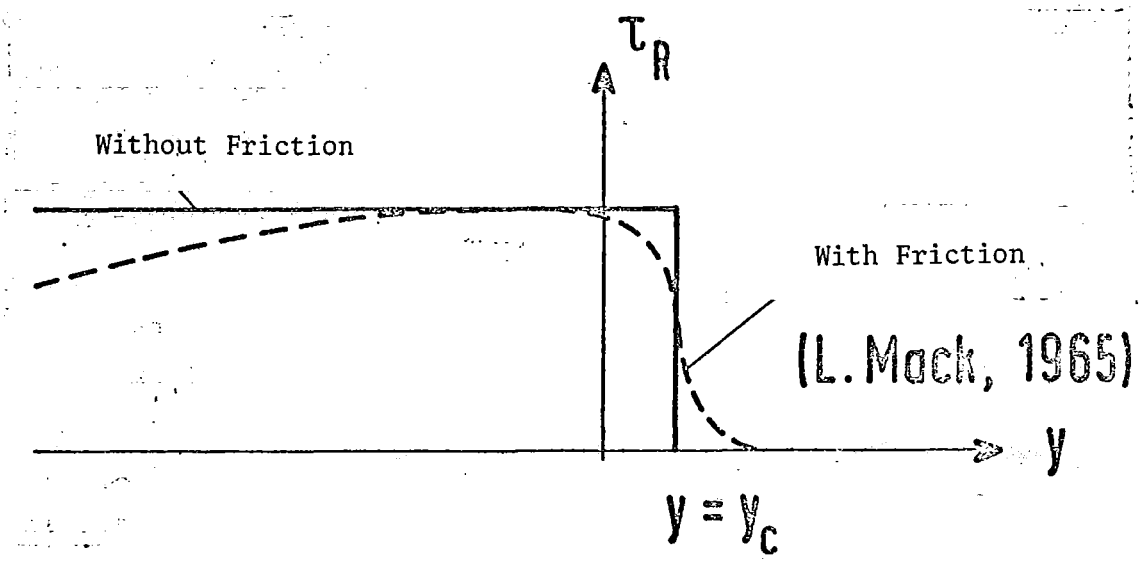

Only in the outer portion of the boundary layer, $y \leq y_c$, is fluctuation energy removed from the principal flow by the Reynolds shear stresses τ_R; the energy is brought back in by the formation of a corresponding distribution of pressure fluctuations in the principal flow. It should be taken into consideration that the result for τ_R found by Mack [32] for wall boundary layers can be converted to free boundary layers. The graphs shows this result schematically. One can see that fluid friction makes the singularity in the critical layer disappear and τ_R becomes zero at the outer edge of the boundary layer.

5.4 Behavior of the Eigenfunctions in the Critical Layer

It has been shown that the Eigenfunction ϕ remains regular for all neutral disturbances, whereas the derivatives of ϕ remain regular only for neutral subsonic and sonic disturbances and become singular for neutral supersonic disturbances. This result applies for two-dimensional and three-dimensional disturbances.

The behavior of the remaining Eigenfunctions, relative to neutral disturbances, can be seen from equations (3.20) through (3.24). The Eigenfunctions Θ and r for the temperature and density fluctuations become singular relative to any neutral disturbance in the critical layer, as long as $\overline{T}'_c$ does not disappear, which generally is not the case, however. The Eigenfunctions f and h for the velocity fluctuations in the x and z directions become singular for all three-dimensional neutral disturbances. Moreover, f becomes singular for all neutral disturbances with supersonic character. Only the Eigenfunction $\tilde{\pi}$ for the pressure fluctuations remains regular in all cases. /45

For an incompressible, free shear layer with a special velocity profile, Stuart [51] was able to give an exact solution to the nonlinear disturbance equation for a neutral, three-dimensional disturbance which is regular throughout. From this solution it is possible to see that the singularity which the solution to the linearized disturbance equation exhibits in the critical layer is obviously only a result of linearizing the equation. It is therefore to be supposed that in the compressible case, the singularity of the neutral Eigenfunctions is likewise to be attributed to the linearization of the equations, at least for subsonic disturbances.

In the case of the Eigenfunctions Θ and r for the temperature and density fluctuations, it is possible that the singularity does not arise from linearization of the disturbance equation, but rather is a result of neglecting the effect of heat conductivity upon the disturbance motion. For Prandtl numbers close to 1, however, the thermal-conductivity term in the energy equation, like the dissipation term, is on the order of magnitude of Re^{-1}. It thus appears as though the effect of thermal conductivity upon the stability of free boundary layers can be neglected in the same manner as the

friction effect. The additional singularities which occur for neutral supersonic disturbances, on the other hand, are possibly to be attributed to the neglect of friction, since the disturbances in this case do not disappear at infinite distance.

6. Stability Behavior of a Free Shear Layer Relative to Long-Wave Disturbances /46

6.1 Effect of the Velocity Profile with Long-Wave Disturbances

The stability behavior of a free shear layer relative to long-wave disturbances can be described analytically with relative ease, since the Eigenvalue equation can be given in closed form. Drazin and Howard [8] compared the stabilities of various velocity profiles in plane, free shear layers relative to two-dimensional, timewise-amplified disturbances in incompressible media. It was found that the various profiles exhibit similar stability behavior relative to long-wave disturbances, i.e., the amplification of the disturbances and their phase velocities show approximate agreement. They concluded from this that the form of the velocity profile has no effect upon the stability behavior of the disturbance if the disturbance wave length is large relative to a characteristic length of the profile (e.g. the boundary-layer thickness). Their explanation can easily be extended to cover three-dimensional disturbances and is independent of whether the disturbances are amplified timewise or spacially.

Since the wave number of the disturbance is inversely proportional to its wavelength, long-wave disturbances are notable for small wave numbers $\bar{\alpha}_r$. According to (3.29), the resultant wave number is $\bar{\alpha}_r = \sqrt{\alpha_r^2 + \gamma^2}$, so for long-wave disturbances the wave numbers α_r and γ in the x and z directions must be small. Since the phase velocity in the direction of flow, $c_r = \beta/\alpha_r$, remains limited, the frequency β must likewise assume small values for small wave numbers α_r. Long-wave disturbances are thus characterized by low frequencies β and small wave numbers α_r and γ. If dimensional quantities are again introduced for the velocity profile $\bar{u}(y)$, the disturbance frequency β and the wave numbers α and γ, then

$$\bar{u}^*(y^*) = \bar{u}_1^*\left(\frac{y^*}{l^*}\right); \quad \beta^* = \beta\,\frac{\bar{u}_1^*}{l^*}; \quad \alpha^* = \frac{\alpha}{l^*}; \quad \gamma^* = \frac{\gamma}{l^*}. \tag{6.1}$$

If, for fixed disturbance frequency β^* and fixed disturbance wave numbers /47 α^* and γ^*, the reference length l^* is made to approach zero, the dimensionless velocity profile $\bar{u}(y)$ becomes a discontinuous profile (plane vortex layer)which is described by

$$y > 0 \qquad \bar{u} = \bar{u}_1 = 1,$$

$$y < 0 \qquad \bar{u} = \bar{u}_2 = 0. \tag{6.2}$$

The dimensionless quantities β, α and γ approach zero of fixed β^*, α^* and γ^*, while the expressions

$$\frac{\beta}{\alpha} = \frac{\beta^*}{\alpha^*} \cdot \frac{1}{\bar{u}_1^*} \qquad \frac{\gamma}{\alpha} = \frac{\gamma^*}{\alpha^*} \tag{6.3}$$

are not affected by the limiting transition $1^* \to 0$. The stability behavior of the velocity profile $\bar{u}^*(y^*)$ relative to three-dimensional disturbances at low disturbance frequencies β^* and thus small disturbance wave numbers α^* and γ^* can therefore be obtained from a stability study of the vortex layer. Since the vortex layer possesses no characteristic length, the Eigenvalue equation can only remain a function of the quantities β/α and γ/α, which according to (6.3) are independent of the reference length.

6.2 Eigenvalue Equation for the Compressible Vortex Layer

In the following, the stability behavior of the compressible vortex layer is determined relative to spacially amplified, three-dimensional disturbances. A check is then made as to how well the results for the vortex layer describe the stability behavior of the Lock profile being studied for low disturbance frequencies. For the vortex layer, $\bar{u}' = \bar{u}'' = 0$ for $y \neq 0$, so the differential equation (3.19) for Eigenfunction ϕ assumes (cf. equation (4.3)) the form

$$\varphi_k'' - \omega_k^2 \varphi_k = 0, \qquad k = 1; 2. \tag{6.4}$$

If one takes into consideration the boundary conditions (3.27), $\phi(\pm\infty) = 0$, one obtains the following solution for ϕ (cf. equation (4.5)):

$$\varphi_1 = Be^{-\omega_1 y}; \qquad \varphi_2 = Ae^{\omega_2 y}, \quad \text{A and B complex constants,} \tag{6.5}$$

/48

where ω_k is determined from equation (4.7) and (4.8); in particular, again $\omega_{kr} > 0$. Both solutions must satisfy the following relationship conditions at the vortex layer ($y = 0$):

1. The velocity component normal to the deflected vortex layer must be the same on both sides of the vortex layer. This is identical to the requirement that the vortex layer be formed by the same fluid particles at all times.

2. The pressure must be equal on both sides of the vortex layer.

These relationship conditions lead to a linear, homogeneous system of equations for the free constants A and B which has non-zero solutions only for certain Eigenvalues $\beta/\alpha = f(M, \overline{T}_2, \Theta)$. These Eigenvalues β/α are solutions to the so-called Eigenvalue equation.

For the equation for the disturbed vortex layer, one can set

$$H(x,y,z,t) = y - \eta(x,z,t) = 0 \tag{6.6}$$

with $$\eta = C \exp[i(\alpha x + \gamma z - \beta t)], \quad C = \text{const.}$$

The first condition, that the vortex layer always deforms by the same fluid particles, is then identical to the requirement

$$\frac{DH}{Dt} = \frac{\partial H}{\partial t} + u\frac{\partial H}{\partial x} + v\frac{\partial H}{\partial y} + w\frac{\partial H}{\partial z} = 0. \tag{6.7}$$

If the disturbance equation (3.2) is substituted into (6.7) and the equation is linearized in terms of the disturbance quantities, the result is

$$\frac{\partial \eta}{\partial t} + \bar{u}\frac{\partial \eta}{\partial x} = v'. \tag{6.8}$$

From this one obtains, with equations (3.5) and (6.6), the first relationship condition

$$\frac{\varphi_1(y=0)}{\bar{u}_1 - \frac{\beta}{\alpha}} = \frac{\varphi_2(y=0)}{\bar{u}_2 - \frac{\beta}{\alpha}}. \tag{6.9}$$

/49

The second condition, that of pressure equality on both sides of the vortex layer, is identical to the requirement that the amplitude functions $\tilde{\pi}_1$ and $\tilde{\pi}_2$ for the pressure disturbances in both areas be equal at the vortex layer. Thus from (3.17) the second relationship condition is found to be

$$\frac{\bar{u}_1 - \frac{\beta}{\alpha}}{G_1}\,\varphi_1'(y=0) = \frac{\bar{u}_2 - \frac{\beta}{\alpha}}{G_2}\,\varphi_2'(y=0). \tag{6.10}$$

If the solutions (6.5) for Eigenfunction ϕ in the two areas are substituted into equations (6.9) and (6.10), two equations are obtained for determining the constant A and B:

$$\begin{aligned} &\frac{1}{\bar{u}_2 - \frac{\beta}{\alpha}} \cdot A - \frac{1}{\bar{u}_1 - \frac{\beta}{\alpha}} \cdot B = 0, \\ &\frac{\bar{u}_2 - \frac{\beta}{\alpha}}{\bar{T}_2 \omega_2} \cdot A + \frac{\bar{u}_1 - \frac{\beta}{\alpha}}{\bar{T}_1 \omega_1} \cdot B = 0. \end{aligned} \tag{6.11}$$

This homogeneous system of equations has nontrivial solutions for A and B only if the coefficient determinant disappears. From this one obtains the Eigenvalue equation

$$\frac{(\bar{u}_1 - \frac{\beta}{\alpha})^2}{\bar{T}_1\,\omega_1} + \frac{(\bar{u}_2 - \frac{\beta}{\alpha})^2}{\bar{T}_2\,\omega_2} = 0 \tag{6.12}$$

or, written out with equations (3.16) and (4.3),

$$\frac{(1 - \frac{\beta}{\alpha})^2}{\sqrt{\frac{\alpha^2+\gamma^2}{\alpha^2} - M^2(1-\frac{\beta}{\alpha})^2}} + \frac{(\frac{\beta}{\alpha})^2}{\sqrt{\bar{T}_2\,[\bar{T}_2\,\frac{\alpha^2+\gamma^2}{\alpha^2} - M^2(\frac{\beta}{\alpha})^2]}} = 0. \tag{6.13}$$

/50

6.3 Solutions to the Eigenvalue Equation

The solutions to the Eigenvalue equation have been discussed by Pai [41], Miles [39, 40] and Lessen, Fox and Zien [23, 24] among others. For low velocities with compressibility effects approaching zero (M = 0), equation (6.13) assumes the form

$$(1 - \frac{\beta}{\alpha})^2 + \frac{1}{\bar{T}_2}(\frac{\beta}{\alpha})^2 = 0, \tag{6.14}$$

i.e. the angle of incidence Θ of the disturbance as given by (3.29) no longer occurs in the Eigenvalue equation. One then obtains for the Eigenvalue

$$\frac{\beta}{\alpha} = \frac{\bar{T}_2 + i\sqrt{\bar{T}_2}}{1+\bar{T}_2}. \tag{6.15}$$

Here, that solution is selected which leads to a negative α_i for spacial amplification. The incompressible vortex layer is thus unstable relative to all disturbance frequencies, as has already been shown by Rayleigh [43]. The Eigenvalue equation (6.13) is generally not soluble in closed form for arbitrary Mach numbers M and environment temperatures $\bar{T}_2$. For two-dimensional disturbances, Miles [39] gives the closed solution for two special cases. For $\bar{T}_2 = 1$, he finds the Eigenvalue as a function of Mach number to be

$$\frac{\beta}{\alpha} = \frac{1}{2} + i\sqrt{\frac{1}{1+\sqrt{M^2+1}} - \frac{1}{4}}. \tag{6.16}$$

According to (6.16), the compressible vortex layer for $\bar{T}_2 = 1$ becomes more and more stable with increasing Mach number M (for spacial and timewise amplification) and is stable relative to all disturbance frequencies for $M > 2\sqrt{2}$. Miles also finds that for arbitrary $\bar{T}_2$, the compressible vortex layer is stable relative to two-dimensional disturbances for /51

$$M \geq (1+\bar{T}_2^{1/3})^{3/2}. \tag{6.17}$$

The solutions to equation (6.13) have been determined numerically for arbitrary combinations of Mach number M and environment temperature $\bar{T}_2$, and two-dimensional disturbances ($\gamma = 0$). From the complex solutions for β/α, it is possible to obtain the phase velocity and the degree of amplification for disturbances amplified spacially and timewise by making either α or β complex. Figures 9 and 10 show the wave number α_r/β and the amplification parameter $-\alpha_i/\beta$ for two-dimensional, spacially amplified distrubances as a function of Mach number M and environment temperature $\bar{T}_2$ in three-dimensional form. One can see that the amplification increases sharply in the region

of low Mach numbers and low environment temperatures. For $\bar{T}_2 > 2$, the environment temperature has only a slight effect upon the amplification parameter. With increasing Mach number, the amplification parameters decrease continuously at constant $\bar{T}_2$, i.e., the compressible vortex layer becomes more stable with increasing Mach number. Finally, as a certain Mach limit, given by (6.17) is exceeded, it becomes stable relative to all disturbance frequencies. In both figures, those points are marked at which the disturbances within the range 1 ($y > 0$) or the range 2 ($y < 0$) first assume supersonic character with increasing Mach number. These points are connected by the lines $\bar{u}_1 - c_r = \bar{a}_1$ and $c_r = \bar{a}_2$. One can see that the neutral disturbances in both ranges have supersonic character. This is informative, since the Eigenvalue equation (6.12) can only have real solutions if ω_1 and ω_2 are imaginary and opposite signs result from equation (4.8) for the two of them.

For two-dimensional disturbances ($\gamma = 0$), it has been shown that it makes no difference to the solution of the Eigenvalue equation (6.13) whether one uses disturbances which are amplified timewise or spacially. If three-dimensional disturbances ($\gamma \neq 0$) are taken into consideration, on the other hand, this differentiation is important, since the ratio of wave numbers γ/α is real for timewise amplification and complex for spacial amplification. For timewise-amplified disturbances, i.e., α real, it is possible to substitute the disturbance angle Θ given by equation (3.29) into (6.13): /52

$$\frac{\alpha^2 + \gamma^2}{\alpha^2} = \frac{1}{\cos^2 \Theta}. \tag{6.18}$$

The solutions β/α (M, $\bar{T}_2$) to equation (6.13), calculated for two-dimensional disturbances, are thus also valid for timewise-amplified three-dimensional disturbances if the Mach number M is replaced by $M\cos\Theta$. In particular, the compressible vortex layer, according to (6.17), is stable relative to timewise-amplified disturbances (Miles [40]) for Mach numbers:

$$M \geqq \frac{1}{\cos \Theta}\left(1 + \bar{T}_2^{1/3}\right)^{3/2}. \tag{6.19}$$

For spacial amplification, on the other hand, the solutions to the Eigenvalue equation (6.13) must be calculated anew as functions of the disturbance incidence angle Θ. Figure 11 shows the amplification parameter $-\alpha_i/\beta$ for spacially amplified disturbances and an angle of incidence of

$\Theta = 45°$. The stability limit is reached only at a higher Mach number than given by (6.19) for timewise amplification.

Figure 12 shows the dependence of the spacial amplification - α_i/β upon the angle of incidence Θ of the disturbance for various Mach number M and environment temperatures $\overline{T}_2$. The stabilizing effect of the Mach number upon the compressible vortex layer disappears with increasing angle of incidence Θ. For $\Theta > 45°$, the Mach number even has a pronounced destabilizing effect, particularly for low environment temperatures. The amplification reaches a maximum for a certain angle Θ, which lies between 45° and 70° for the parameter range under study.

At the beginning of this section, the hypothesis was proposed that the form of the velocity profile in an arbitrary free shear layer is of no consequence if the disturbance wavelength is large relative to a characteristic profile length. Drazin and Howard [8] have verified the hypothesis for timewise-amplified disturbances in compressible media. For spacial amplification, the stability behavior of the Lock profile relative to long-wave disturbances or low disturbance frequencies was compared with the vortex-layer behavior. Figure 13 shows this comparison for several combinations of Mach number M and environment temperature $\overline{T}_2$ for two-dimensional /53 disturbances. Agreement is satisfactory for disturbance frequencies $\beta < 0.005$.

7. Numerical Treatment of the Eigenvalue Problem

7.1 Transformation of the Initial Equations

In Section 3.6, the Eigenvalue problem was formulated in the following manner: For a given frequency β and a given disturbance angle of incidence Θ, the Eigenvalues α_r and α_i are to be so determined that the Eigenfunctions $q_r(y)$ and $q_i(y)$ satisfy the boundary conditions (3.27). To this end, one could start with the differential equation (3.19) for the Eigenfunction ϕ, which is linear and second-order. Through resolution into real and imaginary components, it is possible to obtain from this a system of coupled differential equations for $\phi_r(y)$ and $\phi_i(y)$. For the numerical treatment it is desirable (see Betchov and Criminale [2]), to transform equation (3.19) into a first-order differential equation by introducing a new variable $\Phi = \phi'/\phi$; to be sure, the equation is not linear, but is of the Riccati type. However, it is possible to reduce the system of equations (3.17) for the Eigenfunctions $\tilde{\pi}$ and ϕ to a first-order differential equation of the Riccati type directly, by introducting a new variable χ defined as follows:

$$\chi = \chi_r + i\chi_i = i\frac{\tilde{\pi}}{\varphi}. \qquad (7.1)$$

The advantage of the χ transformation relative to the Φ transformation becomes apparent in the numerical treatment of neutral supersonic disturbances. As was shown in Section 5.2, ϕ' becomes singular in the critical layer, whereas ϕ and $\bar{\pi}$ remain regular. For neutral supersonic disturbances, therefore, Φ is singular in the critical layer, and χ remains regular (see Appendix Section 9.4).

With (7.1), the system of equations (3.17) becomes a differential equation for χ:

$$\chi' = \alpha^2 \frac{\bar{u} - \frac{\beta}{\alpha}}{\bar{T}} - \chi \frac{G\chi + \bar{u}'}{\bar{u} - \frac{\beta}{\alpha}}. \tag{7.2}$$

In Section 4.1 it was shown that the asymptotic behavior of all Eigenfunction described by (4.5). The function χ from (7.1) must therefore approach a constant value asymptotically for $y \to \pm \infty$, and its derivative must disappear. Equation (7.2) thus yields /54

$$y \to \pm \infty \qquad \chi_k = (-1)^k \frac{\alpha^2 (\bar{u}_k - \beta/\alpha)}{\bar{T}_k \omega_k}; \quad \chi'_k = 0 \qquad k = 1; 2, \tag{7.3}$$

where the signs are again specified such that $\omega_{kr} > 0$ and the sign of ω_{ki} is determined by (4.8).

It is desirable in the numerical treatment of the Eigenvalue problem to change the independent variables in equation (7.2). According to Section 2, the velocity profile $\bar{u}(y)$ becomes independent of the Mach number M and the environment temperature $\bar{T}_2$ as the result of introducing the new variable Y in accordance with equation (2.16). If the differential equation (7.2) is transformed using (2.16), the result is

$$\frac{d\chi}{dY} = \alpha^2 (\bar{u} - \frac{\beta}{\alpha}) - \chi \frac{G\bar{T}\chi + \frac{d\bar{u}}{dY}}{\bar{u} - \frac{\beta}{\alpha}}. \tag{7.4}$$

The Mach number M, the environment temperature $\bar{T}_2$ and the isentropic exponent κ are now contained only in the expression $G \cdot \bar{T}$ (see equation (2.14) and (3.15)). The universal velocity profile $\bar{u}(Y)$ is given by equation (2.27).

7.2 Calculation of the Eigenvalues

Calculation of the Eigenvalues α_r and α_i for the differential equation (7.4) for given values of β and Θ is carried out using the method given by Michalke [38]. The velocity $\bar{u}$ is substituted into (7.4) as a new independent variable; this reduces the range of integration $-\infty \leq Y \leq +\infty$ to $\bar{u}_2 \leq \bar{u} \leq \bar{u}_1$ with $\bar{u}_1 = 1$ and $\bar{u}_2 = 0$.

One obtains /55

$$\frac{d\chi}{d\bar{u}} = \frac{1}{N(\bar{u})}\left[\alpha^2\left(\bar{u}-\frac{\beta}{\alpha}\right) - \chi\,\frac{G\bar{T}\chi + N(\bar{u})}{\bar{u}-\frac{\beta}{\alpha}}\right], \tag{7.5}$$

where, according to (2.27),

$$N(\bar{u}) = \frac{d\bar{u}}{dY} = 2ab(1-\bar{u})\left[1-(1-\bar{u})^{1/b}\right] \tag{7.6}$$

The boundary values $\chi(\bar{u}_1)$ and $\chi(\bar{u}_2)$ follow from (7.3):

$$\chi\Big|_{\bar{u}=\bar{u}_{1;2}} = \frac{\alpha^2(\bar{u}-\beta/\alpha)}{\bar{T}\omega}\Bigg|_{\bar{u}=\bar{u}_{1;2}} \tag{7.7}$$

The derivative of the function $\chi(\bar{u})$ at the boundaries must be determined in accordance with l'Hospital's rule, since in (7.5) both the bracketed expression and the function $N(\bar{u})$ disappear, according to (7.6) and (7.7) for $\bar{u}_1 = 1$ and $\bar{u}_2 = 0$.

$$\frac{d\chi}{d\bar{u}}\Big|_{\bar{u}=\bar{u}_{1;2}} = \frac{2\alpha^2(\bar{u}-\frac{\beta}{\alpha}) - \chi\left[\chi\,\frac{d(G\bar{T})}{d\bar{u}} + \frac{dN}{d\bar{u}}\right]}{\frac{dN}{d\bar{u}}(\bar{u}-\frac{\beta}{\alpha}) + 2\chi G\bar{T}}\Bigg|_{\bar{u}=\bar{u}_{1;2}} \tag{7.8}$$

Resolution of (7.5) into real and imaginary components again leads to a system of coupled differential equations for χ_r and χ_i. Correspondingly, the boundary values $\chi_r(\bar{u}_{1,2})$ and $\chi_i(\bar{u}_{1,2})$, as well as the derivative at the boundaries, are obtained through the resolution of equations (7.7) and (7.8).

The differential equation (7.5) is now integrated stepwise, beginning at the two boundaries $\bar{u}_1 = 1$ and $\bar{u}_2 = 0$, up to a value $\bar{u}_2 < \bar{u}_0 < \bar{u}_1$ for two arbitrary pairs of values $\alpha = \alpha_r + i\alpha_i$, and in each case the complex difference

$$\Delta(\alpha_r,\alpha_i) = \chi(\bar{u}_0 + 0) - \chi(\bar{u}_0 - 0), \tag{7.9}$$

which must become zero for the Eigenvalues α_r and α_i being sought, is calculated. For the given pairs of values α_1 and α_2, the differences Δ_1 and Δ_2, from which an improved pair of values α_3 is obtained by linear interpolation, are calculated from equation (7.9). Through renewed integration of the differential equation (7.5) with the pair of values α_3, the associated difference Δ_3 is obtained. A further improvement in α results from repeated parabolic interpolation until the difference $|\Delta| < \varepsilon$ with $\varepsilon = 10^{-7}\ |\chi(\bar{u}_0)|$. The integration is accomplished using a Runge-Kutta method with automatic step selection. The calculations were carried out on a digital computer with nine decimal places. /56

For calculating the Eigenvalues of the neutral disturbances with $\alpha_i = 0$ as the limiting case of amplified disturbances, it is again necessary to differentiate between subsonic, sonic and supersonic character. As was demonstrated in Section 5.1, the phase velocity c_N of the neutral disturbance in the direction of flow is a solution to (5.3) only for subsonic and sonic disturbances. In this case, the solution curve $\chi(\bar{u})$ to the differential equation (7.5) is regular with all derivatives in the critical layer and real over the entire range of integration, i.e., $\chi_i(\bar{u} \equiv 0$ (see Appendix Section 9.4). The boundary values given by (7.7) and (7.8) for the solution $\chi(\bar{u})$ are likewise real, since $\omega_k^2 \geq 0$ for neutral subsonic and sonic disturbances. Since the neutral phase velocity $c_N = \beta_N/\alpha_N$ can be determined from (5.3), only the neutral wave number α_N still appears as an Eigenvalue in the differential equation (7.5). The Eigenvalue α_N can be calculated using the method given above as the function of the disturbance angle of incident Θ.

In Section 5.2, the study of neutral disturbances with supersonic character showed that their phase velocity c_N can not satisfy (5.3), so the differential equation (7.5) becomes singular in the critical layer. In Appendix Section 9.4 it is shown that χ remains regular in the critical

layer, whereas all derivatives of χ become singular logarithmically. Moreover, χ must also be taken as complex for neutral supersonic disturbances. Due to this singular character of the solutions, these neutral disturbances cannot be calculated exactly. The Eigenvalues of the neutral supersonic disturbances can only be determined approximately through interpolation from /57
the neighboring, weakly amplified disturbances, whose solution curves $\chi(\bar{u})$ are always regular

7.3 Calculation of the Eigenfunction

The Eigenfunctions associated with the Eigenvalues were determined by integrating the system of coupled differential equations (3.17) for the complex Eigenfunctions $\tilde{\pi}(y)$ and $\phi(y)$. Here, too, it is desirable to introduce the independent variable Y, given by (2.16), in place of y, since the velocity profile $\bar{u}(y)$ is independent of the Mach number M and the environment temperature $\bar{T}_2$. To be sure, only a plot of the Eigenfunctions versus y is physically meaningful, so the curve of y(Y) must likewise be determined from (2.16). The following system of equations must then be integrated:

$$\frac{d\tilde{\pi}}{dY} = \alpha^2 \left(\bar{u} - \frac{\beta}{\alpha}\right)\varphi,$$

$$\frac{d\varphi}{dY} = \frac{iG\bar{T}\tilde{\pi} + \frac{d\bar{u}}{dY}\varphi}{\bar{u} - \frac{\beta}{\alpha}}, \qquad (7.10)$$

$$\frac{dy}{dY} = \bar{T}.$$

Through resolution of the first two equations of (7.10) into real and imaginary components, a system of four coupled first-order differential equations is obtained for the Eigenfunctions

$\tilde{\pi}_r(Y)$, $\tilde{\pi}_i(Y)$, $\varphi_r(Y)$ and $\varphi_i(Y)$.

The system of equations (7.10) has three free constants, of which one, according to (2.16), is determined by the requirement $y(Y = 0) = 0$, whereas the others can be chosen arbitrarily. Consequently, the integration must start at Y = 0. The complex function values $\tilde{\pi}(0)$ and $\phi(0)$ are, according to (7.1), linked by the condition

$$\chi_r(0) + i\,\chi_i(0) = i\,\frac{\tilde{\pi}_r(0) + i\,\tilde{\pi}_i(0)}{\varphi_r(0) + i\,\varphi_i(0)} \cdot \qquad (7.11)$$

The complex function value $\chi(0)$ is obtained by integrating the differential equation (7.5) from one of the two boundaries $\bar{u}_1$ or $\bar{u}_2$ to the value $\bar{u}(Y = 0)$. If, corresponding to the two free constants, $\phi_r(0) = 1$ and $\phi_i(0) = 0$ are now chosen, the integration begins at $Y = 0$ with the following values for $\tilde{\pi}$, ϕ and y: /58

$$\varphi_r(0) = 1;\ \varphi_i(0) = 0;\ \tilde{\pi}_r(0) = \chi_i(0);\ \tilde{\pi}_i(0) = -\chi_r(0);\ y(0) = 0. \qquad (7.12)$$

The integration is carried out in the positive and negative Y directions until the asymptotic behavior of the Eigenfunctions described by (4.5) is obtained. The integration again was carried out using a Runge-Kutta method. The Eigenfunctions f and Θ were determined simultaneously with the integration, in accordance with (3.20) and (3.23), while the curves of h and r were not determined. In the next section, the numerical results which were obtained are discussed.

8. Discussion of the Numerical Results

The stability behavior of the Lock profile relative to three-dimensional spacially amplified disturbances was studied for Mach numbers $0 \leq M \leq 3$ and environment temperatures $0.6 \leq \bar{T}_2 \leq 2$ for air with $\kappa = 1.4$. Environment temperatures $\bar{T}_2 < 1$ mean a cooled free jet and $\bar{T}_2 > 1$, a heated free jet. The largest portion of the numerical studies were limited to the stability of the Lock profile relative to two-dimensional disturbances ($\Theta = 0$). Consideration of three-dimensional disturbances alters the stability behavior only quantitatively, rather than qualitatively.

Figure 14 shows the amplification parameter $-\alpha_i$ for two-dimensional disturbances as a function of disturbance frequency β and Mach number M for $\bar{T}_2 = 1$ in a three-dimensional representation. For M = const., the amplification increases with increasing frequency β, up to a maximum value, then drops off again and finally becomes zero as the neutral disturbance frequency β_N is reached. The neutral disturbances, as a limiting case of amplified disturbances, are joined by the lines $\alpha_i = 0$. The Lock profile exhibits stable behavior relative to disturbance frequency $\beta > \beta_N$. The stability

behavior of the Lock profile relative to low frequencies has already been determined in Section 6. The amplification parameters $-\alpha_i/\beta(M, \bar{T}_2, \Theta)$ calculated there for the compressible vortex layer are identical to the slope /59
$-(\partial\alpha_i/\partial\beta)_{M,\bar{T}_2,\Theta}$ of the amplification curve for the Lock profile at the point $\beta = 0$.

One can see that the maximum amplification is greatest for M = 0 and falls off sharply with increasing Mach number. The region of amplified frequencies β is likewise greatest for M = 0 and becomes smaller with increasing Mach number. The Lock profile thus becomes more and more stable with increasing Mach number. Since the phase velocity c_r does not exceed the value of 1, all disturbances have subsonic character at both edges of the boundary layer M < 1. If the Mach number is increased at constant disturbance frequency, the disturbances first assume sonic character at the outer boundary-layer edge, corresponding to reaching the line $c_r = \bar{a}_2$. In particular, $c_N = \bar{a}_2$ applies for the neutral disturbance on this line. If the Mach number is further increased, then $c_N > \bar{a}_2$, i.e., the neutral disturbances are now singular and can only be calculated approximately. The singular neutral disturbances are connected via the dashed line $\alpha_i = 0$. One can see that the region of amplified frequencies becomes smallest for those Mach numbers for which the associated amplification curve $-\alpha_i(\beta)$ leads to the neutral sonic disturbance with $c_N = \bar{a}_2$. For higher Mach numbers, the frequency range of amplified disturbances again increases slowly.

After the line $c_r = \bar{a}_2$ is passed on the lines of constant disturbance frequency β, all disturbances have supersonic character at the outer edge of the boundary layer. For disturbance frequencies $\beta < 0.02$ and Mach numbers M > 2, moreover, the disturbances assume supersonic character inside the jet. This is characterized by crossing over the line $\bar{u}_1 - c_r = \bar{a}_1$. In the region of supersonic disturbances, the amplification parameter is relatively small, and a rise in the Mach number has only a slight stabilizing effect. Characteristic of the supersonic region is the fact that the amplification curves $-\alpha_i(\beta)$ can exhibit two relative maxima for M - const. The maxima in the amplification curves have been connected by dashed lines.

Figures 15 and 16 show the amplification parameter $-\alpha_i$ for the environment temperature $\bar{T}_2 = 0.6$ (cooled free jet) and $\bar{T}_2 = 2$ (heated free jet). Comparison with the results for $\bar{T}_2 = 1$ show that the amplification of disturbances is increased sharply by cooling the free jet and the region of amplified frequencies is reduced. Heating of the free jet has the effect of /60
weaker amplification of the disturbances, while the region of amplified frequencies become larger. The cooled free jet (Figure 15) exhibits a

discontinuous increase in the range of amplified frequencies for increasing Mach number near the neutral sonic disturbance, with $c_N = \bar{a}_2$. This discontinuous rise is also somewhat less marked for $\overline{T}_2 = 1$, but it is no longer perceptible for $\overline{T}_2 = 2$. A more exact study shows that this pronounced change in the neutral disturbance frequency is caused by the occurrence of a second disturbance mode which is generally amplified more weakly than the first mode, represented in Figures 14, 15 and 16, and thus was not shown. Apparently the second mode also has an appreciable effect only upon the stability behavior of the cooled free-jet boundary layer. The lines β = const. were therefore dashed in the region of neutral sonic disturbance, since they only provide an approximate representation of the true curve. The characteristic features of the second mode are discussed below.

Figures 17, 18 and 19 show the wave number α_r of the two-dimensional disturbances as functions of disturbance frequency β and Mach number M for the environment temperature $\overline{T}_2 = 1$, $\overline{T}_2 = 0.6$ and $\overline{T}_2 = 2$. The disturbance wave numbers $\alpha_r/\beta(M, \overline{T}_2\ \Theta)$ calculated for the compressible vortex layer are identical to the slopes $(\partial\alpha_r/\partial\beta)_{M,\overline{T}_2,\Theta}$ of the curves for $\beta = 0$. Figures 20, 21 and 22 show the phase velocity $c_r = \beta/\alpha_r$ of the disturbances as a function of disturbance frequency β and Mach number M for the environment temperatures $\overline{T}_2 = 1$, $\overline{T}_2 = 0.6$ and $\overline{T}_2 = 2$ in a three-dimensional representation. For $\beta = 0$, the phase velocity c_r as a function of M and $\overline{T}_2$ could again be taken from the stability-study results for the compressible vortex layer.

The results up to now show that the principal flow being studied is stabilized by increasing the Mach number and the environment temperature, at least for low Mach numbers. If the vortex strength $\Omega(y) = -du/dy$ of the principal flow is calculated for various combinations of M and T_2, one sees that the maximum vortex strength of the profiles is likewise reduced by increasing the Mach number and the environment temperature (see Figure 23). It is apparent, however, not only that the vortex-strength distribution is responsible for the instability of the free boundary layer, as in the case of incompressible flow without thermal conductivity, but also that the density distribution $\bar{\rho}(y)$ at the temperature distribution $\overline{T}(y)$ have an appreciable effect (see equation (2.13)). For the case $M \to 0$, therefore, an attempt was made to give special treatment to the effect of the vortex-strength distribution and that of the density distribution. Initially, the effect of various density distributions upon the stability of a free boundary layer with a particular velocity profile was studied. The velocity profiles for M = 0 and $\overline{T}_2 = 1$ was chosen for this. Figure 24 shows the amplification curves for three different temperature profiles ($\overline{T}_2 = 0.6$, 1, 2). One can see that even at Mach number M = 0, heating the boundary layer

/61

has a stabilizing effect. In general, the vortex-strength distribution and the density distribution are coupled via the velocity and temperature profiles, however. According to Figure 25, this boundary-layer stabilization effect is increased even more by heating, due to coupling of the velocity and temperature profiles.

The effect of Mach number upon the amplification parameter $-\alpha_i$ is represented for constant environment temperature $\bar{T}_2$ in Figure 26 for the constant disturbance frequency $\beta = 0.08$. It is found that the free jet is made very much more stable by heating (raising $\bar{T}_2$) for Mach numbers $M < 1.5$, whereas heating has the opposite effect for higher Mach numbers. Figure 26 also makes it clear that a rise in Mach number has a great stabilizing effect for $M < 1.5$; for higher Mach numbers, the stabilizing effect is slight. The dashed curve shows the amplification of the second mode for $\bar{T}_2 = 0.6$. For other environment temperatures, the second mode has not been calculated.

The effect of the isentropic exponent κ for the flowing gas upon the stability of the flow is shown in Figure 27. In free boundary layers in gases with $\kappa = 1.10$ (e.g. freon), the amplification parameter for two-dimensional disturbances is generally greater than in air. The deviations increase with increasing Mach number and decreasing environment temperature.

In the following, the characteristic features of the second disturbance mode are explained. This second mode always occurs around the neutral sonic disturbance $c_N = \bar{a}_2$ and is limited to a narrow range of Mach numbers. Figure 28 shows the amplification parameter $-\alpha_i$ as a function of disturbance /62
frequency β for the first and second modes in the Mach-number range $1.4 \leq M \leq 2$ for the environment temperature $\bar{T}_2 = 0.6$. Figure 28 thus represents a magnified section of Figure 15; the plot here is two-dimensional, though. For the environment temperature under study, $\bar{T}_2 = 0.6$, the second mode first occurs at $M \approx 1.54$ as the Mach number is increased. The second mode is amplified only within a small frequency range, which includes the corresponding neutral disturbance frequency of the first mode. The amplification curve - $\alpha_i(\beta)$ of the second mode thus possess two neutral disturbances with $\beta_N > 0$. As the Mach number is further increased, the second mode is amplified more and more sharply, and the amplified frequency range becomes wider. The corresponding amplification curves of the first and second modes intersect for Mach numbers $M \leq 1.64$. For a particular disturbance frequency β, therefore, the disturbances of both modes experience the same spacial amplification; however, the two disturbances are propagated with different phase velocities. Figure 29 shows the associated phase velocity for disturbances of the first and second modes. For $M \leq 1.64$, all disturbances of the first mode have subsonic character over the entire flow region, whereas all disturbances of the second mode assume supersonic character at the outer

boundary-layer edge. The neutral disturbances of the first mode therefore lie along the line $c_N < \bar{a}_2$ for $M \leq 1.64$, whereas the two neutral disturbances of the second mode lie along the line $c_N > \bar{a}_2$. The line $c_N > \bar{a}_2$ was dashed in to indicate that singular neutral disturbances are involved.

The two modes fuse for Mach numbers $M > 1.64$, and simultaneously split up again. Figure 28 shows that the amplification curve for the two modes no longer intersect following the transformation process. It is characteristic of the transformation process that the neutral disturbance frequency of both modes changes discontinuously, a fact which has already been pointed out in the discussion on Figure 15. The neutral disturbance of the first mode assumes supersonic character for the first time here, while now the second mode now possesses a neutral subsonic and a neutral supersonic disturbance for $M > 1.64$. The second mode falls off very sharply for $M > 1.64$. For $M = 1.728$, the neutral phase velocity c_N calculated in accordance with (5.3) is just equal to the sonic velocity $\bar{a}_2$; i.e., for $\bar{T}_2 = 0.6$, there are regular neutral disturbances only for $M \leq 1.728$. Since the second mode possesses a regular neutral disturbance following the transformation process, one can assume that the second mode is no longer amplified for $M \geq 1.728$. The curve dashed in for $M = 1.67$ was not calculated. /63

The effect of Mach number upon the neutral wave number α_N is shown in Figure 30 for various environment temperatures $\bar{T}_2$. It was shown, at the same time, how α_N changes with the disturbance angle of incidence Θ. The approximative calculation of neutral supersonic disturbances ($c_N > \bar{a}_2$), however, was carried out only for the angle of incidence $\Theta = 0°$. For $\bar{T}_2 = 0.6$ and $\Theta = 0°$, three neutral wave numbers are found in the range $1.54 < M < 1.73$, corresponding to the occurrence of the second mode. This range becomes smaller and smaller for higher environment temperatures and is no longer perceptible for $\bar{T}_2 = 2$. In Figure 31, the calculated neutral wave numbers for the Lock profile are compared with the results of Lessen, Fox and Zien [25]. The deviations can apparently be explained by the fact that Lessen, Fox and Zien have calculated the velocity profile exactly from the differential equation (2.20), whereas the approximative equation (2.27) was used for the velocity profile in the author's calculations.

The effect of the three-dimensionality of the disturbances upon the stability of the Lock profile is shown in Figures 32 through 34. They thus supplement the representation of profile stability relative to two-dimensional disturbances in Figures 14 through 16. For low Mach numbers, the maximum amplification becomes smaller as the disturbance angle of incidence Θ increases. At the same time, the range of amplified frequencies becomes smaller. This result coincides with the statement made by Squire's theorem [50] for $M = 0$ (see Section 1). For higher Mach numbers, however, the relationships can be reversed, so that three-dimensional disturbances are

amplified more markedly than two-dimensional. In the Lock profile studied, this is even the case for M = 2; the results were magnified in Figure 35 for this Mach number. The effects of three-dimensionality of the disturbances is greatest at $\bar{T}_2 = 0.6$ for the cooled free jet; here disturbances which are propagated at an angle of $\Theta = 50°$ to 60° relative to the direction of flow are amplified the most. Calculations show that all disturbances which are propagated at this angle still have subsonic character over the entire flow field even at M = 2. Interestingly, the second mode found for $\bar{T}_2 = 0.6$ and $\Theta = 30°$ is amplified almost as sharply as the first mode of the two-dimensional disturbances. /64

The Eigenvalues were calculated from the differential equation (7.5) for $\chi(\bar{u})$ using the method given in Section 7. The curves of the complex function $\chi(\bar{u})$ were plotted in Figure 36 for various disturbance frequencies β and for a principal flow with M = 1.6 and $\bar{T}_2 = 0.6$ in which the two disturbance modes are amplified. χ is a pure real for the neutral disturbance freqeuncy β_N of the first mode (Case 3); on the other hand, χ is complex for the two singular neutral solutions of the second mode (Cases 4 and 7).

The curves of several complex Eigenfunctions were determined for the maximum amplified disturbance frequency in each case for various Mach numbers M and the environment temperature $\bar{T}_2 = 1$. The real and imaginary components of the Eigenfunctions $f(y)$, $\alpha\phi(y)$, $\tilde{\pi}(y)$ and $\Theta(y)$ were plotted in Figures 37 and 38 for u', v', p' and T' disturbances. According to (3.4), the complete solution for a particular disturbance value Q' is composed of the complex Eigenfunction q(y) and the complex exponential term $\exp[i(\alpha x + \gamma z - \beta t)]$. To be sure, only the real component of the disturbance value Q' is of physical significance in the sense of a measurable value; it is calculated using Equation (3.26). Accordingly, the amplitude distribution of the disturbance in a particular cross section x = const. of the free jet is proportional to the magnitude of the complex Eigenfunction $|q(y)|$, whereas the phase angle ι is determined by the relationship between the imaginary and real components of the Eigenfunction. The corresponding amplitude distributions and the phase angle of the disturbances were therefore calculated once more from the Eigenfunctions shown in Figures 37 and 38 for the maximally amplified disturbance frequency in each case.

Figures 39 and 40 show the amplitude distribution of u', v', p' and T' disturbances, while the phase distribution of the u' disturbance has been plotted in Figure 41. One can see in Figure 37 that for M = 0 (Case 1) the real component f_r and the imaginary component f_i of the u' disturbance have a common zero point for $y < 0$. It follows from this that the associated amplitude distribution of the disturbance (Figure 39) likewise becomes zero at this point and that the disturbance phase is rotated through an angle of 180° (Figure 41). This zero point in the amplitude distribution of the u' disturbance, as well as the associated phase rotation, were also found by /65

Freymuth [11] in an experimental study on the stability of the free-jet boundary layer at low velocities (see Section 1). Figure 39 shows that the zero point disappears under the effect of compressibility and the amplitude subsequently exhibits only a relative minimum which becomes less and less pronounced as Mach number increases. Correspondingly, the phase distribution of the disturbance exhibits no phase discontinuity for $M > 0$, but rather only a steep phase slope which likewise disappears with increasing Mach number (Figure 41).

Figure 42 shows a comparison of the amplitude and phase distributions of the u' and v' disturbances of the first and second mode at Mach number $M \doteq 1.6$ and environment temperature $\bar{T}_2 = 0.6$ for the drawn-in disturbance frequency $\beta = 0.0542$. Both disturbance modes are amplified to an equal extent for this disturbance frequency.

9. Appendix

9.1 A Lower Limit for the Phase Velocity of Spacially Amplified Disturbances

If the differential equation (3.19) is rewritten by introducing a function

$$\Psi = \frac{\varphi}{\bar{u} - \frac{\beta}{\alpha}} \tag{9.1}$$

the result is

$$L(\Psi) = \left[\frac{\Psi'(\bar{u} - \frac{\beta}{\alpha})}{G}\right]' - \alpha^2 \frac{(\bar{u} - \frac{\beta}{\alpha})^2}{\bar{T}} \Psi = 0. \tag{9.2}$$

If the integral expression

$$\int_{-\infty}^{+\infty} [\bar{\Psi} L(\Psi) - \Psi \overline{L(\Psi)}]\, dy = 0, \tag{9.3}$$

is now formulated and the boundary conditions (3.27) are taken into consideration, the result is /66

$$4i\alpha_i\alpha_r\int_{-\infty}^{+\infty}\left[|\psi'|^2\bar{T}\cdot\frac{\alpha_r^2}{|\alpha|^4}\cdot\frac{c_r\left(\frac{\alpha_i}{\alpha_r}\right)^2\bar{u}+(\bar{u}-c_r)\left(\bar{u}\,\frac{\gamma^2}{\alpha_r^2}+c_r\right)}{|G|^2}+\right.$$

$$\left.+|\psi|^2\cdot\frac{\bar{u}}{\bar{T}}(\bar{u}-c_r)\right]dy=0. \tag{9.4}$$

This integral can only disappear for amplified disturbances if the expression $\bar{u}-c_r$ becomes negative within the flow, so a lower limit is obtained for c_r:

$$c_r>\bar{u}_{min}=0. \tag{9.5}$$

If the imaginary component of the integral expression (9.3) is evaluated for timewise-amplified disturbances, it is possible to derive a lower and upper limit for c_r (see equation (5.2)).

9.2 The Behavior of the Eigenfunction ϕ in the Vicinity of the Critical Layer for Neutral Disturbances

Assuming that the coefficients of the differential equation (3.19) can be expanded in terms of powers of $y-y_c$ in the vicinity of $y=y_c$, one obtains

$$\frac{G'}{G}=\frac{\bar{T}_c'}{\bar{T}_c}+\left(\frac{G'}{G}\right)_c(y-y_c)+\ldots,$$

$$G\left(\frac{\bar{u}'}{G}\right)'=\bar{T}_c\left(\frac{\bar{u}'}{\bar{T}}\right)_c'+\left[G\left(\frac{\bar{u}'}{G}\right)'\right]'(y-y_c)+\ldots, \tag{9.6}$$

$$\frac{G}{\bar{T}}=\frac{\alpha_N^2+\gamma^2}{\alpha_N^2}+\left(\frac{G}{\bar{T}}\right)_c''\frac{(y-y_c)^2}{2}+\ldots,$$

$$\bar{u}-c_N=\bar{u}_c'(y-y_c)+\bar{u}_c''\frac{(y-y_c)^2}{2}+\ldots$$

Thus, as an approximation, it is possible to set /67

$$\varphi'' - C\varphi' - \left(\frac{D}{y - y_c} + E\right)\varphi = 0 \tag{9.7}$$

for (3.19) in the vicinity of $y = y_c$, with

$$C = \frac{\bar{T}_c'}{\bar{T}_c}\ ;\ D = \frac{\bar{T}_c}{\bar{u}_c'}\left(\frac{\bar{u}'}{\bar{T}}\right)_c'\ ;\ E = \frac{1}{\bar{u}_c'}\left[G\left(\frac{\bar{u}'}{G}\right)'\right]_c' + \frac{\alpha_N^2 + \gamma^2}{\alpha_N^2}.$$

According to Kamke [14], this differential equation has the linearly independent solutions

$$\begin{aligned} \varphi_1 &= (y - y_c)\, g_1 (y - y_c), \\ \varphi_2 &= S\varphi_1 \log (y - y_c) + g_2 (y - y_c), \end{aligned} \tag{9.8}$$

with

$$g_1 (y - y_c) = 1 + a_1 (y - y_c) + a_2 (y - y_c)^2 + \ldots,$$

$$g_2 (y - y_c) = 1 + b_1 (y - y_c) + b_2 (y - y_c)^2 + \ldots \tag{9,9}$$

The coefficients a_i and b_i are determined by substituting the solutions (9.8) into equation (9.7):

$$a_1 = \frac{C + D}{2} = \frac{1}{2} \cdot \frac{\bar{u}_c''}{\bar{u}_c'}$$

$$a_2 = \frac{1}{6}\left[(C + D)\left(C + \frac{D}{2}\right) + E\right]$$

$$\vdots$$

$$b_1 = 0$$

$$b_2 = \frac{1}{2}\left[D(C - 3a_1) + E\right]$$

$$\vdots$$

$$S = D = \frac{\bar{T}_c}{\bar{u}_c'}\left(\frac{\bar{u}_c'}{\bar{T}}\right)_c'.$$

In the critical layers, ϕ_1 and ϕ_2 and all derivatives $\phi_1^{(n)}$ are regular, whereas all derivatives $\phi_2^{(n)}$ become singular logarithmically if the coefficient D does not disappear. /68

9.3 The Substantial Change In The Timewise Mean Value of the Kinetic Disturbance Energy

If the first equation of the system (3.1) is multiplied by u, the second equation by v and the third equation by w, and the equation are summed, the mechanics energy equation for frictionless media is obtained:

$$\rho \frac{D}{Dt}\left(\frac{u^2+v^2+w^2}{2}\right) = -\frac{1}{\varkappa M^2}\left(u\frac{\partial p}{\partial x}+v\frac{\partial p}{\partial y}+w\frac{\partial p}{\partial z}\right), \tag{9.10}$$

where

$$\frac{D}{Dt} = \frac{\partial}{\partial t} + u\frac{\partial}{\partial x} + v\frac{\partial}{\partial y} + w\frac{\partial}{\partial z}$$

If the disturbance equation (3.2) is substituted into (9.10), all terms again drop out which contain only principal-flow quantities. If all third and higher order terms in disturbance quantities are neglected, one obtains, through time-averaging,

$$\bar{\rho}\overline{\left(\frac{\partial}{\partial t}+\bar{u}\frac{\partial}{\partial x}\right)\left(\frac{u'^2+v'^2+w'^2}{2}\right)} + \bar{\rho}\,\overline{u'v'}\frac{d\bar{u}}{dy} + \frac{1}{\varkappa M^2}\overline{\left(u'\frac{\partial p'}{\partial x}+v'\frac{\partial p'}{\partial y}+w'\frac{\partial p'}{\partial z}\right)} = \tag{9.11}$$

$$-\bar{\rho}\bar{u}\overline{\left(u'\frac{\partial u'}{\partial x}+v'\frac{\partial u'}{\partial y}+w'\frac{\partial u'}{\partial z}\right)} - \bar{u}\overline{\left(\rho'\frac{\partial u'}{\partial t}+\rho'\frac{\partial u'}{\partial x}+\rho'v'\frac{d\bar{u}}{dy}\right)}.$$

If one uses the disturbance equation (3.2) in the first equation of the system (3.1) and determines the time-average value in the same manner, one can see that the right side of (9.11) becomes zero. One thus obtains

$$\bar{\rho}\overline{\left(\frac{\partial}{\partial t}+\bar{u}\frac{\partial}{\partial x}\right)\left(\frac{u'^2+v'^2+w'^2}{2}\right)} = -\bar{\rho}\,\overline{u'v'}\frac{d\bar{u}}{dy} - \frac{1}{\varkappa M^2}\overline{\left(u'\frac{\partial p'}{\partial x}+v'\frac{\partial p'}{\partial y}+w'\frac{\partial p'}{\partial z}\right)}. \tag{9.12}$$ /69

If the results of the linearized stability study (3.5) are substituted into (9.12), the two terms on the right side are then

$$-\bar{\rho}\,\overline{u'v'}\,\frac{d\bar{u}}{dy} = -\frac{1}{2}\,\bar{\rho}\,\mathcal{R}e<\alpha\varphi\bar{f}>\frac{d\bar{u}}{dy}, \tag{9.13}$$

$$\frac{1}{\varkappa M^2}\overline{\left(u'\frac{\partial p'}{\partial x}+v'\frac{\partial p'}{\partial y}+w'\frac{\partial p'}{\partial z}\right)} = \frac{1}{2}\,\mathcal{R}e<i(\alpha\bar{f}+\gamma\bar{h})\tilde{\pi}+\overline{\alpha\varphi}\,\frac{d\tilde{\pi}}{dy}>.$$

For the special case of neutral disturbance, the disturbance amplitude may not undergo a change, and the left side of (9.12) must disappear. This is verified by calculating out the terms on the right side for $\alpha_i = 0$. After a number of intermediate computations, one obtains

$$-\bar{\rho}\,\overline{u'v'}\,\frac{d\bar{u}}{dy}\bigg|_{\alpha_i=0} = \frac{1}{\varkappa M^2}\overline{\left(u'\frac{\partial p'}{\partial x}+v'\frac{\partial p'}{\partial y}+w'\frac{\partial p'}{\partial z}\right)}_{\alpha_i=0} = \frac{\alpha_N}{2G}\,\mathrm{Jm}<\bar{\varphi}\,\frac{d\varphi}{dy}>\frac{d\bar{u}}{dy}. \tag{9.14}$$

For neutral subsonic and sonic disturbances, ϕ is real, and both terms disappear separately, whereas for neutral supersonic disturbances, only their sum becomes zero. With the aid of (5.15), one can show that for neutral supersonic disturbances, the expression $<\bar{\phi}\phi'>$ is identical to the Wronskian determinant W:

$$\mathrm{Jm}<\bar{\varphi}\,\varphi'> = \varphi_r\,\varphi_i' - \varphi_i\,\varphi_r' = W = KG. \tag{9.15}$$

Thus for the Reynolds shear stresses, one obtains, with (5.21) and (9.14),

$$\tau_R = \frac{1}{2}\,\alpha_N\,\frac{W}{G} = \frac{1}{2}\,\alpha_N\,K. \tag{9.16}$$

9.4 The Behavior of the χ Function in the Vicinity of the Critical Layer For Neutral Disturbances

/70

With the aid of (3.17), it is possible to eliminate the Eigenfunction $\tilde{\pi}$ from (7.1) so that the function χ can be represented in the form

$$\chi = \frac{1}{G}\left[\left(\bar{u} - \frac{\beta}{\alpha}\right)\frac{\varphi'}{\varphi} - \bar{u}'\right]. \tag{9.17}$$

For neutral disturbances, however, the behavior of the Eigenfunction ϕ in the vicinity of the critical layer is known; from equations (5.9), (5.10) and (9.8), one obtains

$$\frac{\varphi'}{\varphi} = \frac{\nu_1 \varphi_1' + \nu_2 \varphi_2'}{\nu_1 \varphi_1 + \nu_2 \varphi_2} = \tag{9.18}$$

$$= \nu_3 g_3(y-y_c) + D\left[g_4(y-y_c) + g_3(y-y_c)\log(y-y_c)\right],$$

with $$g_3(y-y_c) = 1 + 2a_1(y-y_c) + 3a_2(y-y_c)^2 + \ldots,$$

$$g_4(y-y_c) = 1 + \left(a_1 + 2\frac{b_2}{D}\right)(y-y_c) + \left(a_2 + 3\frac{b_3}{D}\right)(y-y_c)^2 + \ldots$$

and $$\nu_3 = \nu_{3r} + \nu_{3i}\, i = \frac{\nu_1}{\nu_2}.$$

For the behavior of the χ function in the vicinity of the critical layer, one thus obtains

$$\chi = -\frac{\bar{u}_c'}{\bar{T}_c}\left\{1 - \nu_3(y-y_c)g_3 - D(y-y_c)\left[g_4 + g_3\log(y-y_c)\right]\right\}. \tag{9.19}$$

χ thus remains regular for all neutral disturbances in the critical layer and assume the value there of

$$\chi_c = -\frac{\bar{u}_c'}{\bar{T}_c}, \tag{9.20}$$

/71

which is independent of the Eigenvalue α. The derivative χ' becomes singular in the critical layer and undergoes a jump, due to the analytical extension of the logarithm, for negative arguments, by the amount

$$\lim_{\varepsilon \to 0} [\chi'(y_c+\varepsilon) - \chi'(y_c-\varepsilon)] = i\pi \frac{\bar{u}'_c}{\bar{T}_c} D. \tag{9.21}$$

For neutral subsonic and sonic disturbances, D = 0, and all derivatives of χ are likewise regular. In accordance with Section 5.2, ν_{3i} can be set equal to 0 in this case, so χ is real over the entire integration range, whereas χ is to be taken as complex for neutral supersonic disturbances.

9.5 The Disturbed Laminar Boundary Layer in Compressible Fluids as an Acoustic Source

From the system of equations (3.3) one obtains, by solving for the pressure fluctuations p', the equation

$$\frac{\partial^2 p'}{\partial t^2} - \bar{a}^2 \left[\left(1 - \frac{\bar{u}^2}{\bar{a}^2}\right) \cdot \frac{\partial^2 p'}{\partial x^2} + \frac{\partial^2 p'}{\partial y^2} + \frac{\partial^2 p'}{\partial z^2}\right] + 2\bar{u} \cdot \frac{\partial^2 p'}{\partial x \partial t} = \tag{9.22}$$

$$= 2\varkappa \frac{d\bar{u}}{dy} \cdot \frac{\partial v'}{\partial x} + \frac{1}{M^2} \frac{d\bar{T}}{dy} \cdot \frac{\partial p'}{\partial y}.$$

At the edges of the boundary layer, this differential equation, with (4.2), becomes

$$y \to +\infty \quad \frac{\partial^2 p'}{\partial t^2} - \bar{a}_1^2 \left[(1-M^2) \cdot \frac{\partial^2 p'}{\partial x^2} + \frac{\partial^2 p'}{\partial y^2} + \frac{\partial^2 p'}{\partial z^2}\right] + 2 \cdot \frac{\partial^2 p'}{\partial x \partial t} = 0 \tag{9.23}$$

and /72

$$y \to -\infty \quad \frac{\partial^2 p'}{\partial t^2} - \bar{a}_2^2 \left[\frac{\partial^2 p'}{\partial x^2} + \frac{\partial^2 p'}{\partial y^2} + \frac{\partial^2 p'}{\partial z^2}\right] = 0. \tag{9.24}$$

One thus obtains the homogeneous acoustics wave equation for the propagation of sound in a fluid flowing in the x direction at Mach number M or for the propagation of sound in a fluid at rest. In the boundary-layer region, however, the inhomogeneous wave equation with the source terms

$$2\varkappa \frac{d\bar{u}}{dy} \cdot \frac{\partial v'}{\partial x} + \frac{1}{M^2} \cdot \frac{d\bar{T}}{dy} \cdot \frac{\partial p'}{\partial y}, \qquad (9.25)$$

applies, i.e., regions within the disturbed laminar, compressible flows with non-zero velocity gradients or temperature gradients are to be considered as source regions for pressure fluctuations and thus as sources in the acoustical sense.

Note /73

This work was carried out in the Hermann-Fottinger Flow Engineering Institute at the Engineering University of Berlin, under the direction of Professor R. Wille, PhD (Engineering). It was undertaken as part of a research program of many years' duration covering the development of turbulence in laminar free-jet boundary layers, carried out jointly with the DVL Turbulence Research Institute. It was therefore possible to base this study upon the results from a large number of scientific projects which have taken place at these two Institutes. I would especially like to thank the director of both Institutes, Professor R. Wille, for his generous support to the work, and to his valuable directions regarding it's implementation. In addition, I would like to thank Dr. A. Michalke, PhD (Engineering), of the DVL Turbulence Research Institute for many discussions and suggestions which have facilitated my work in the field of stability theory, as well as for his enthusiastic support in the solution of a number of problems in the study. I am grateful to the German Research Association, Bad Godesberg, for its financial support in executing the numerical computations.

Diploma Engineer Hans Gropengiesser,
Berlin

REFERENCES

1. Betchov, R. and A. B. Szewczyk, "Stability of a Shear Layer Between Parallel Streams", *Physics of Fluids*, Vol. 6, pp. 1391 to 1396, 1963. /74
2. Betchov, R. and W. O. Criminale, "Stability of Parallel Flows", New York, London: Academic Press, 1967.
3. Brown, G. B., "On Sensitive Flames", *Philosophical Magazine*, Vol. 13, p. 161, 1932.
4. Brown, G. B., "On Vortex Motion in Gaseous Jets and The Origin of Their Sensitivity to Sound", *Proc. Phys. Soc. (London)*, Vol. 47, p. 703, 1935.
5. Brown, W. B., "Stability of Compressible Boundary Layers Including The Effects of Two-Dimensional Linear Flows and Three-Dimensional Disturbances", Northrop Aircraft Inc., Norair Division Rep., 1965.
6. Chapman, D. R., "Laminar Mixing of a Compressible Fluid", NACA TN 1800, 1950.
7. Domm, U., "A Hypothesis Regarding the Mechanism of Turbulence Formation", DVL Report Nr. 23, 1956.
8. Drazin, P. G. and L. N. Howard, "The Instability to Long-Waves of Unbounded Parallel Inviscid Flow", *J. Fluid Mech.*, Vol. 14, pp. 257-283, 1962.
9. Dunn, D. W. and C. C. Lin, "On The Stability of the Laminar Boundary Layer in a Compressible Fluid", *J. Aeronaut. Sci.*, Vol. 22, pp. 455-477, 1955.
10. Fabian, H., "Experimental Studies on Velocity Fluctuations in the Mixing Zone of a Free Jet Near the Nozzle Mouth", DVL Report Nr. 122, 1960.
11. Freymuth, P., "On Transition in a Separated Laminar Boundary Layer", *J. Fluid Mech.*, Vol. 25, pp. 683-706, 1966. /75
12. Gaster, M., "A Note on the Relation Between Temporally-Increasing and Spatially-Increasing Disturbances in Hydrodynamic Stability", *J. Fluid Mech.*, Vol. 14, p. 222, 1962.
13. Helmholtz, H., "Discontinuous Fluid Motions", Monatsberichte Konigl. Akad. Wiss. Berlin, pp. 215-228, 1868.
14. Kamke, E., *Differentialgleichungen, Losungsmethoden und Losungen*, [Differential Equations, Methods of Solution and Solutions], Leipzig, Academic Press, Geest and Portig Co, 1967.
15. Kendall, J. M., "Supersonic Boundary Layer Stability", *Space Prog. Summary*, 37 - 39, Vol. 5, pp. 147-148, 1966.
16. Landau, L. D., "Stability of Tangential Discontinuities in Compressible Fluid", *Dokl. Akad. Nauk. SSSR*, 44, pp. 139-141, 1944.
17. Laufer, J. and T. Vrebalovich, "Stability and Transition of a Supersonic Laminar Boundary Layer on an Insulated Flat Plate", *J. Fluid Mech*, 9, pp. 257-299, 1960.
18. Leconte, J., "On The Influence of Musical Sounds on the Flame of a Jet of Coal Gas", *Philosophical Magazine*, 15, p, 235, 1858.

19. Lees, L. and C. C. Lin, "Investigation of the Stability of the Laminar Boundary Layer in a Compressible Fluid", NACA Techn. Note No. 1115, 1946.
20. Lees, L., "The Stability of the Laminar Boundary Layer in a Compressible Fluid," NACA Techn. Rept. No. 876, 1947.
21. Lees, L. and E. Reshotko, "Stability of the Compressible Laminar Boundary Layer", *J. Fluid Mech.*, 12, pp. 555-590, 1962.
22. Lessen, M., "On the Stability of Free Laminar Boundary Layer Between Parallel Streams", NACA Rep. No. 979, 1950. /76
23. Lessen, M., J. A. Fox and H. M. Zien, "Hydrodynamic Stability", Dept. Aero. Eng. and Dept. Eng. Research, Pennsylvania State Univ., Techn. Rep. No. 2, 1954.
24. Lessen, M., J. A. Fox and H. M. Zien, "The Instability of Inviscid Jets and Wakes in Compressible Fluid", *J. Fluid Mech.*, 21, pp. 129-143, 1965 a.
25. Lessen, M., J. A. Fox and H. M. Zien, "On the Inviscid Stability of the Laminar Mixing of Two Parallel Streams of a Compressible Fluid", *J. Fluid Mech.*, 23, pp. 355-367, 1965 b.
26. Lessen, M. and S.-H. Ko, "Viscous Instability of an Incompressible Fluid Half-jet Flow", *Physics of Fluids*, 9, pp. 1179-1183, 1966 a.
27. Lessen, M., J. A. Fox and H. M. Zien, "Stability of the Laminar Mixing of Two Parallel Streams with Respect to Supersonic Disturbances", *J. Fluid Mech.*, 25, pp. 737-742, 1966 b.
28. Lin, C. C., "On the Stability of the Laminar Mixing Region Between Two Parallel Streams of Gas", NACA Techn. Note No. 2887, 1953.
29. Lin, C. C., The Theory of Hydrodynamic Stability, London and New York: Cambridge University Press, 1955.
30. Lock, R. C., "The Velocity Distribution in the Laminar Boundary Layer Between Parallel Streams", *Quart. J. Mech. Appl. Math*, 4, pp. 42-63, 1935.
31. Mack, L. M., "Numerical Calculation of the Stability of the Compressible Laminar Boundary Layer," California Institute of Technology, Jet Propulsion Laboratory Rept. No. 20-122, 1960.
32. Mack, L. M., "Stability of the Compressible Layer According to a Direct Numerical Solution", Recent Developments in Boundary Layer Research, *AGARDograph*, 97, Part I, pp. 329-362, 1965. /77
33. Mack, L. M., "Viscous and Inviscid Amplification Rates of Two and Three-Dimensional Disturbances in a Compressible Boundary Layer", *Space Prog. Summary*, 42, 4 November, 1966.
34. Michalke, A., "On the Inviscid Instability of the Hyperbolic-Tangent Velocity Profile", *J. Fluid Mech.*, 19, pp. 543-556, 1964 a.
35. Michalke, A., "Vortex Formation in a Free Boundary Layer According to Stability Theory", *J. Fluid Mech*, 22, pp. 371-383, 1964 b.
36. Michalke, A., "Spatially Growing Disturbances in an Inviscid Shear Layer", *J. Fluid Mech.*, 23, pp. 521-544, 1965.
37. Michalke, A. and R. Wille, "Flow Processes in the Laminar-Turbulent Transition Region of Free-Jet Boundary Layers", *Applied Mechanics*, Proc. 11th Internat. Congr. Appl. Mech., Munich, pp. 962-972, ed. H. Gortler, Berlin, Heidelberg, New York: Springer Press, 1966.

38. Michalke, A., "The Influence of the Vorticity Distribution on the Inviscid Instability of a Free Shear Layer", To be published in *Fluid Dynamics Transactions* (Poland).
39. Miles, J. W., "On the Disturbed Motion of a Plane Vortex Sheet", *J. Fluid Mech.*, 4, pp. 538-552, 1958.
40. Miles, J. W., "On the Stability of a Plane Vortex Sheet with Respect to Three-Dimensional Disturbances", *J. Fluid Mech.*, 15, pp. 335-336, 1963.
41. Pai, S. I., "On the Stability of Two-Dimensional Laminar Jet Flow of Gas", *J. Aeronautical Science*, 51, pp. 731-742, 1951. /78
42. Rayleigh, Lord, "On the Instability of Jets", *Scientific Papers*, 1, pp. 361-371, Cambridge University Press, 1878.
43. Rayleigh, Lord, "On the Stability, or Instability, of Certain Fluid Motions," *Scientific Papers*, 1, pp. 474-487, Cambridge University Press, 1880.
44. Reshotko, E., "Stability of the Compressible Laminar Boundary Layer", California Institute of Technology, Guggenheim Aeronautical Laboratory, GALCIT Memo. No. 52, 1960.
45. Sato, H., "Experimental Investigation on the Transition of a Laminar Separated Layer", *J. Phys. Soc. Japan*, 11, pp. 702-709, 1956.
46. Sato, H., "Further Investigation on the Transition of Two-Dimensional Separated Layer at Subsonic Speeds", *J. Phys. Soc. Japan*, 14, pp. 1797-1810, 1959.
47. Sato, H., "The Stability and Transition of a Two-Dimensional Jet", *J. Fluid Mech.*, 7, pp. 53-80, 1960.
48. Schlichting, H., *Grenzschichttheorie, 5th Edition*, [Boundary-Layer Theory, 5th Edition], Karlsruhe: G. Braun Press, 1965.
49. Schubauer, G. B. and H. K. Skramstad, "Laminar Boundary Layer Oscillations and Transition on a Flat Plate", NACA Techn. Rept. No. 090, 1943.
50. Squire, H. B., "On the Stability of Three-Dimensional Disturbances of Viscous Flow Between Parallel Walls", *Proc. Roy. Soc.* (London), A142, pp. 621-628, 1933.
51. Stuart, J. T., "On Finite Amplitude Oscillations in Laminar Mixing Layers", *J. Fluid Mech.*, 29, pp. 417-440, 1967.
52. Szabo, I., *Hohere Mathematik, Teil 6*, [Higher Mathematics, Part 6], R. Rothe, editor, B. G. Teubner Press, 1953. /79
53. Timme, A., "Velocity Distribution in Vortices", *Ing. Archiv*, 15, pp. 205-225, 1957.
54. Tollmien, W., "A General Criterion for the Instability of Laminar Velocity Distributions", *Nachr. Ges. Wiss. Gottingen, Math.-phys. Klasse*, pp. 79-114, 1935.
55. Tyndall, J., "On Sensitive Jets", *Philosophical Magazine*, 33, p. 375, 1867.
56. Wehrmann, O., "Acoustic Control of Turbulent Amplification in the Free Jet", Jahrbuch der WGL, pp. 102-108, 1957.

57. Wehrmann, O. and R. Wille, "Phenomonology of the Laminar-Turbulent Transition in the Free Jet for Low Reynolds Numbers" in book *Grenzschichtforschung*, [Boundary-Layer Research], editor H. Bortler, Springer Press, Berlin, Gottingen, Heidelberg, pp. 387-404, 1958.
58. Wille, R., "Flow Phenomena in the Transition Region from Ordered to Disordered Movement", *Jahrbuch der Schiffbautechnischen Gesellschaft*, 46, pp. 174-187, 1952.
59. Wille, R., "Model Representations for the Laminar-Turbulent Transition", Research Cooperative of the Land of Nordrhein-Westfalen, *Naturwissensch*, No. 72. Cologne and Opladen, West German Press, 1960, DVL Report No. 113, 1960.
60. Wille, R., "Phenomonology of Free Jets", *Z. f. Flugwiss.*, No. 6, pp. 222-233, 11, 1963 a.
61. Wille, R., "Growth of Velocity Fluctuations Leading to Turbulence in Free Shear Flow", AFOSR Techn. Report Contract AF 61(052)-412, 1963 b.

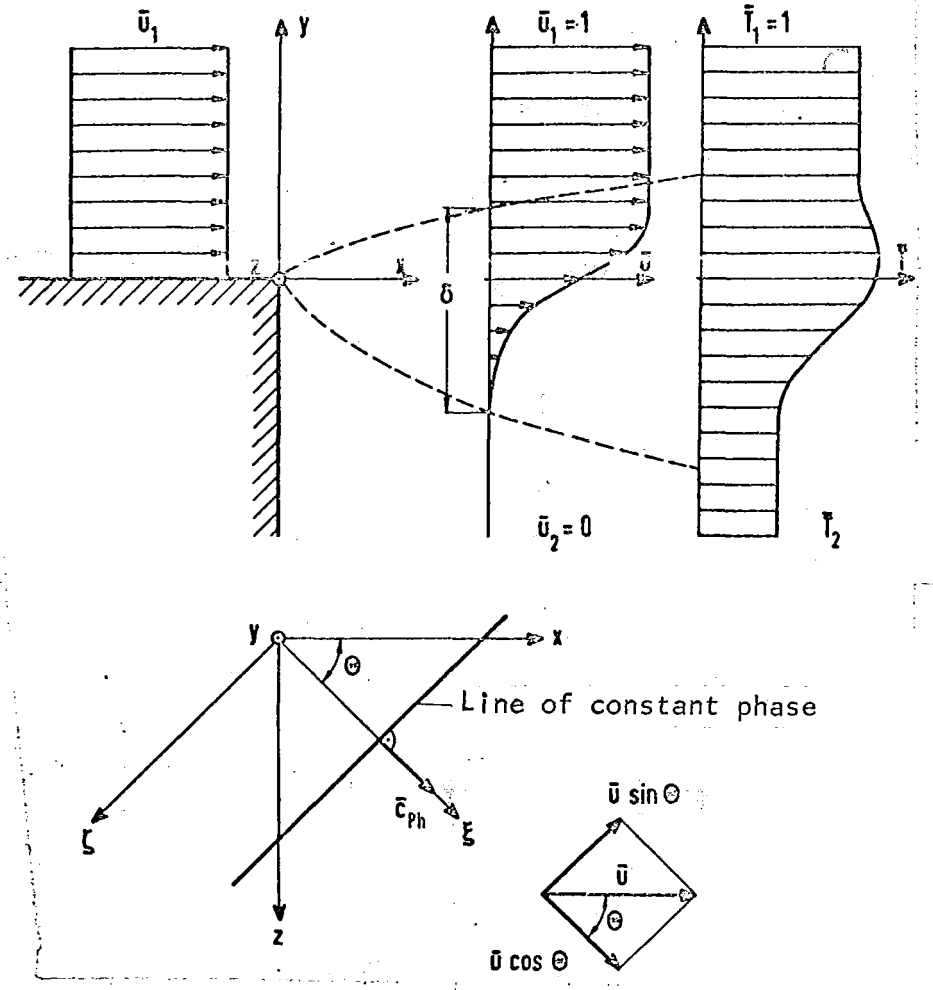

Figure 1. The Development of a Plane Free-Jet Boundary Layer From a Plane Vortex Layer Under the Influence of Fluid Friction (Schematic).

/82

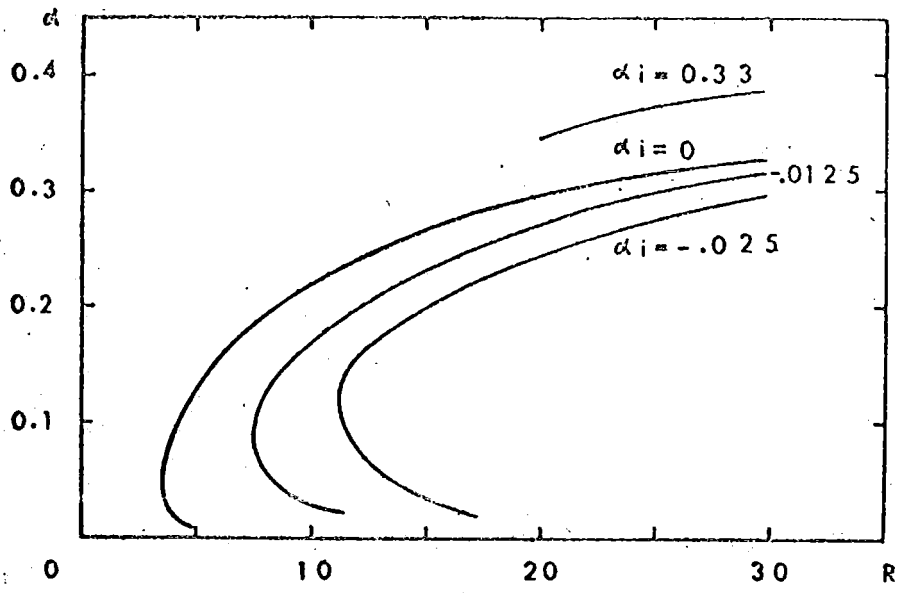

Figure 2 a. The Wave Number α_r of Two-Dimensional, /83
Spacially Amplified Disturbances of the Lock Profile As a Function of Reynolds Number Re for Constant Amplification Parameter α_i in Incompressible Media (According to Lessen and Ko [26]).

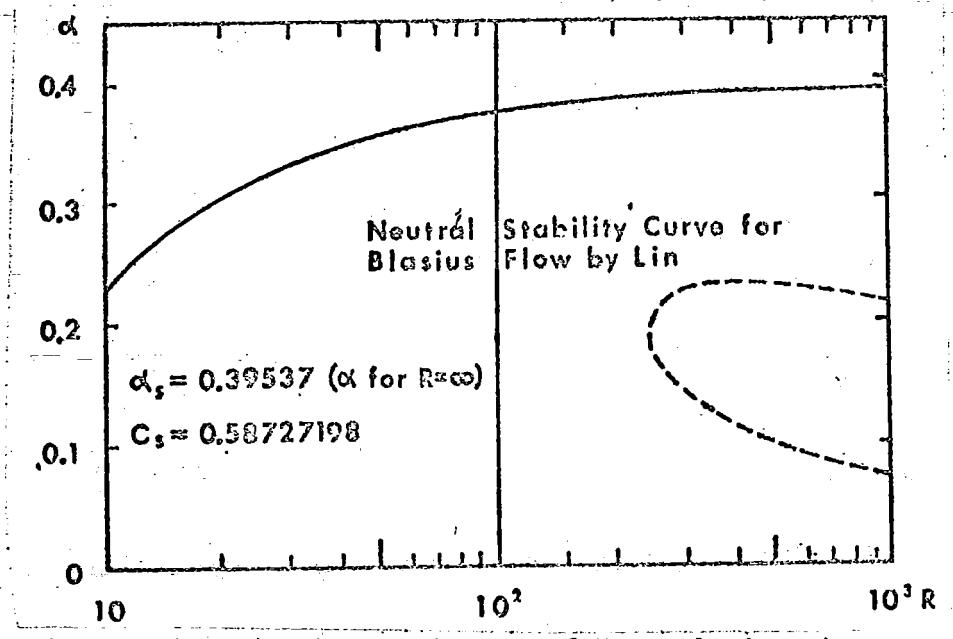

Figure 2 b. The Wave Number α_r of Neutral Disturbances of Lock Profile as a Function of Reynolds Number Re in Incompressible Media (According to Lessen and Ko, [26]).

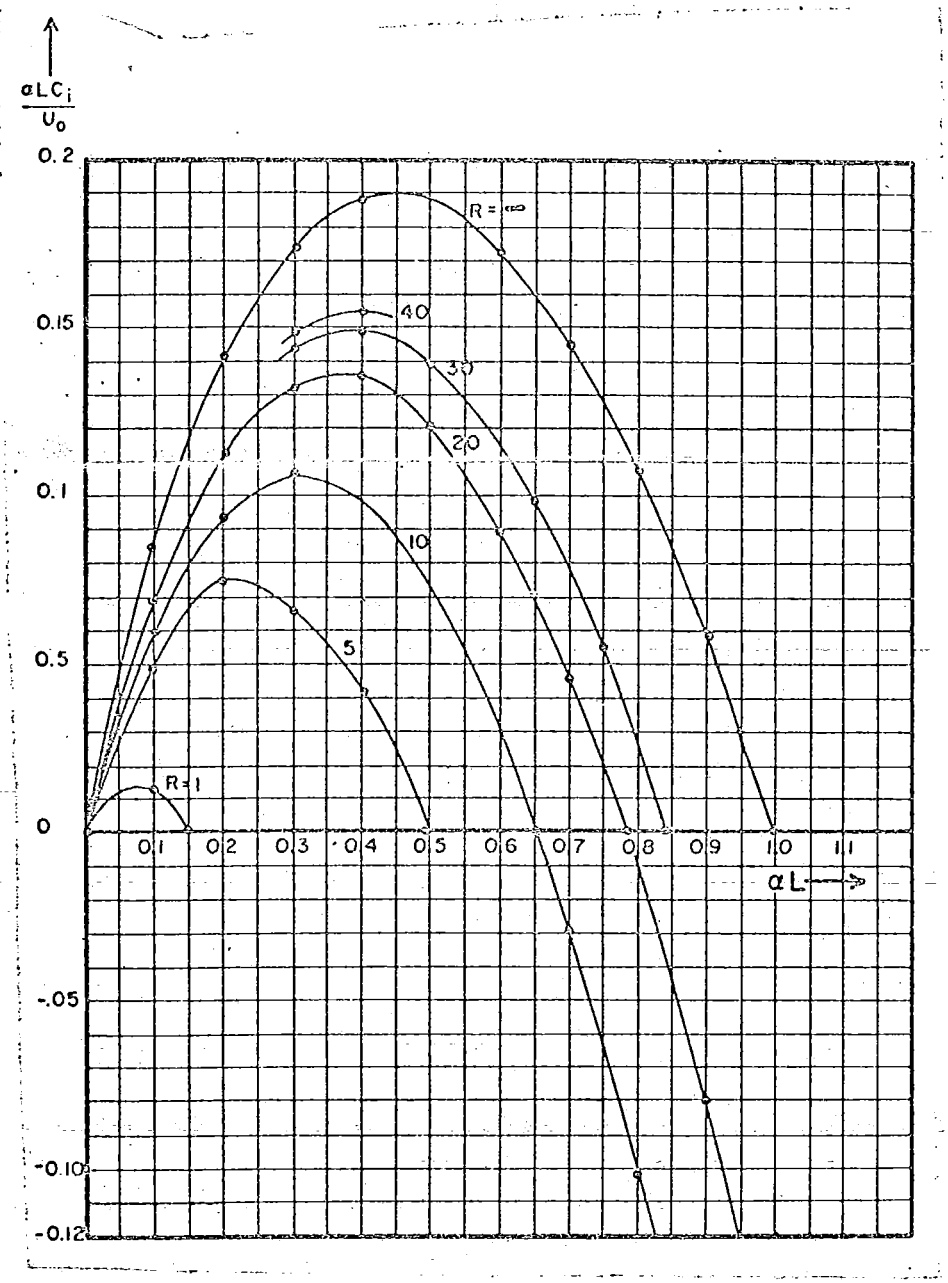

Figure 3. The "Spacial" Amplification Parameter (i.e., The Timewise Amplification Parameter Transformed With The Phase Velocity of the Disturbance) For Two-Dimensional Disturbances of the Hyperbolic-Tangent Profile as a Function of Wave Number for Constant Reynolds Numbers in Incompressible Media (According to Betchov and Szewczyk, [1]).

/84

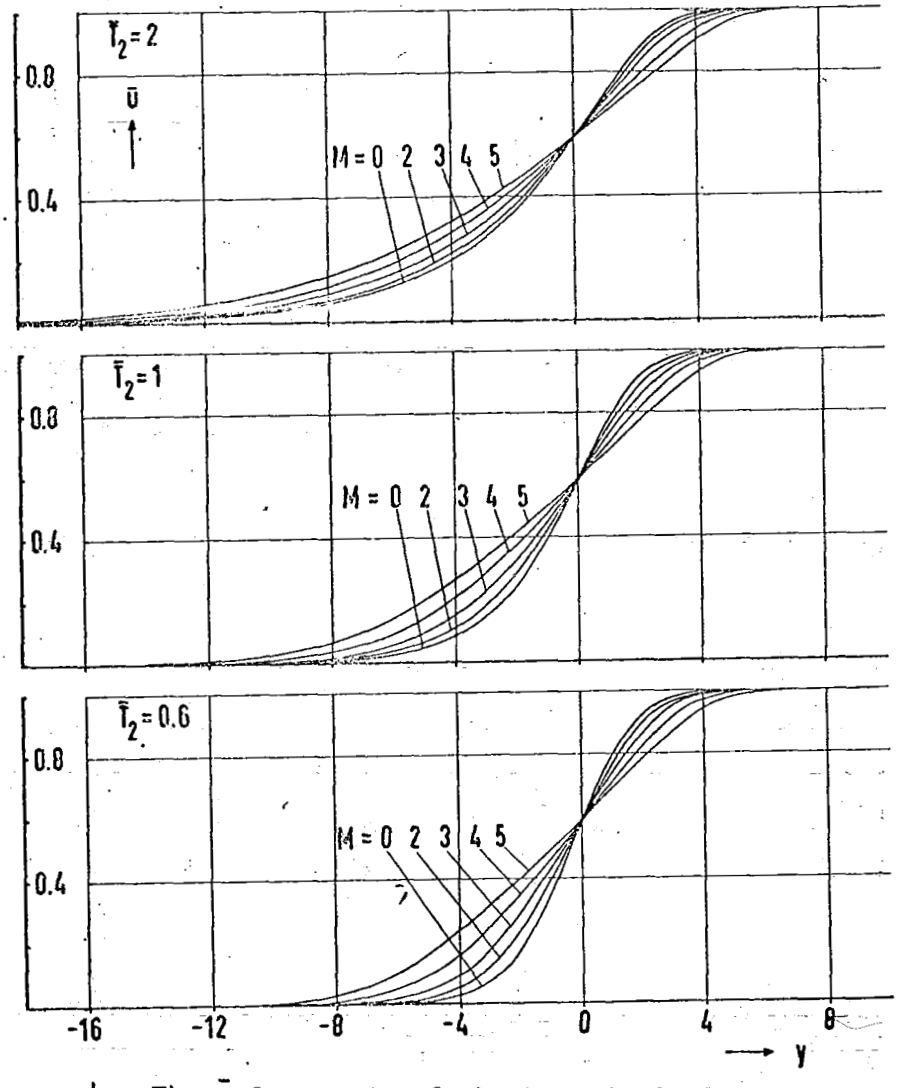

Figure 4. The $\bar{u}$ Component of the Principal Flow (Lock Profile) for Various Mach Numbers M and Environment Temperatures $\bar{T}_2$ for Air.

/85

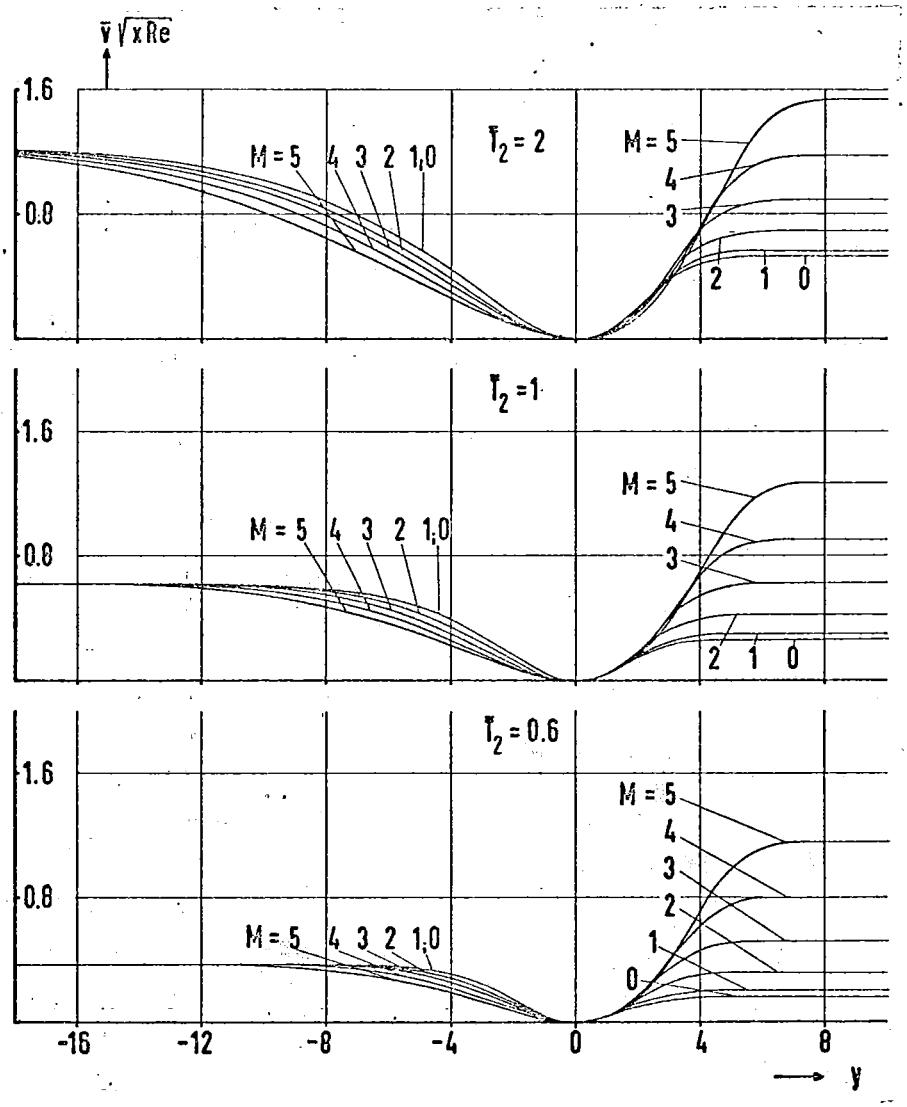

Figure 5. The $\bar{v}$ Component of the Principal Flow For Various Mach Numbers M and Environment Temperatures $\bar{T}_2$ for Air.

/86

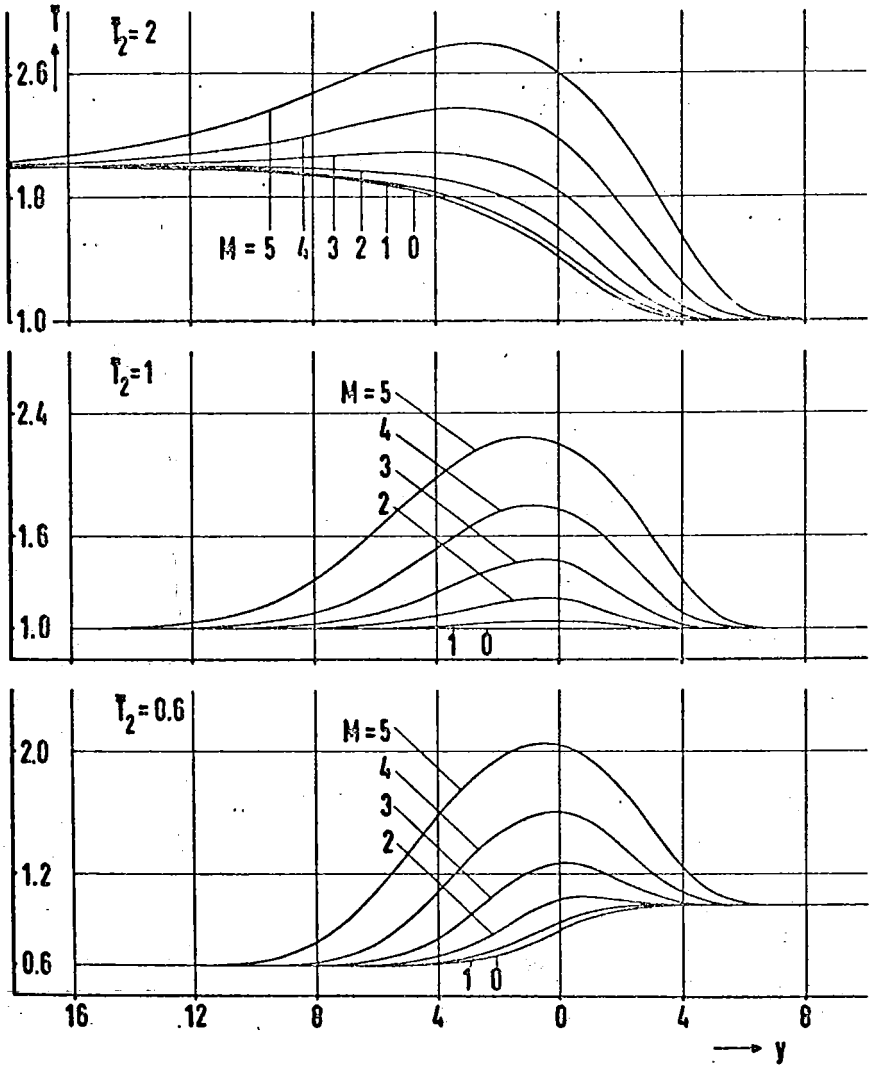

Figure 6. Temperature Profiles $\overline{T}$ of the Principal Flow For Various Mach numbers M and Environment Temperatures $\overline{T}_2$ for Air.

/87

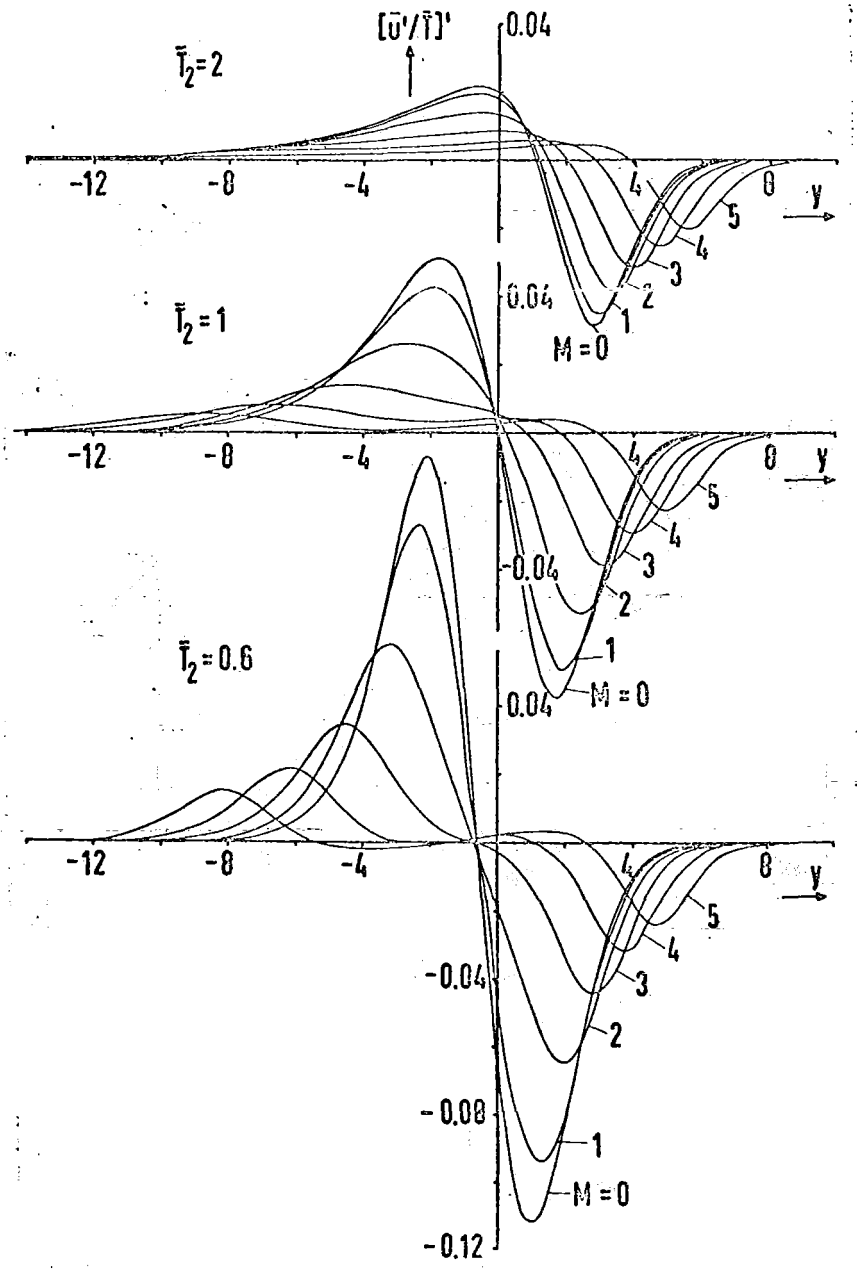

Figure 7. Plot of the Function $(\bar{u}'/\bar{T})'$ Versus y For Various Mach numbers M and Environment Temperatures $\bar{T}_2$ for Air.

/88

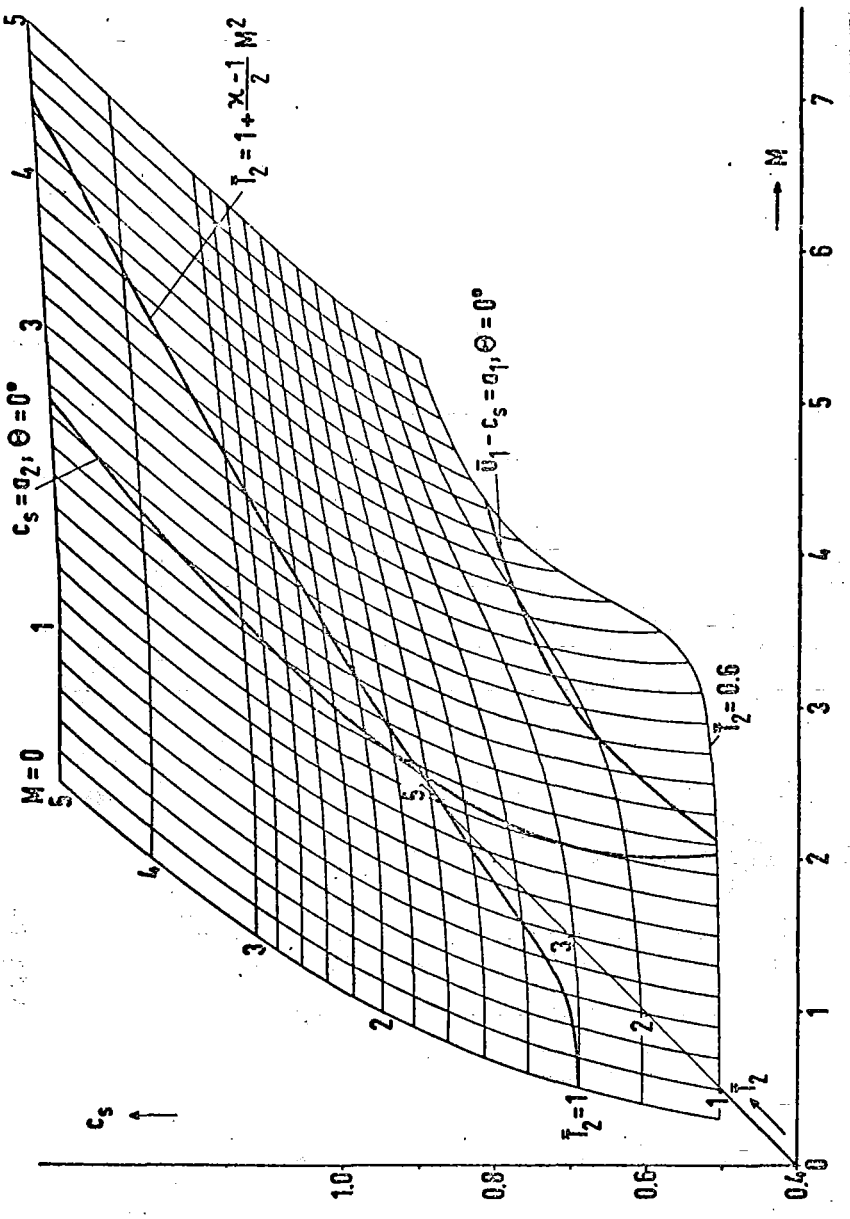

Figure 8. Solution c_s to the Equation $(\bar{u}'/\bar{T})' = 0$ For Various Mach Numbers M and Environment Temperatures $\bar{T}_2$ for Air.

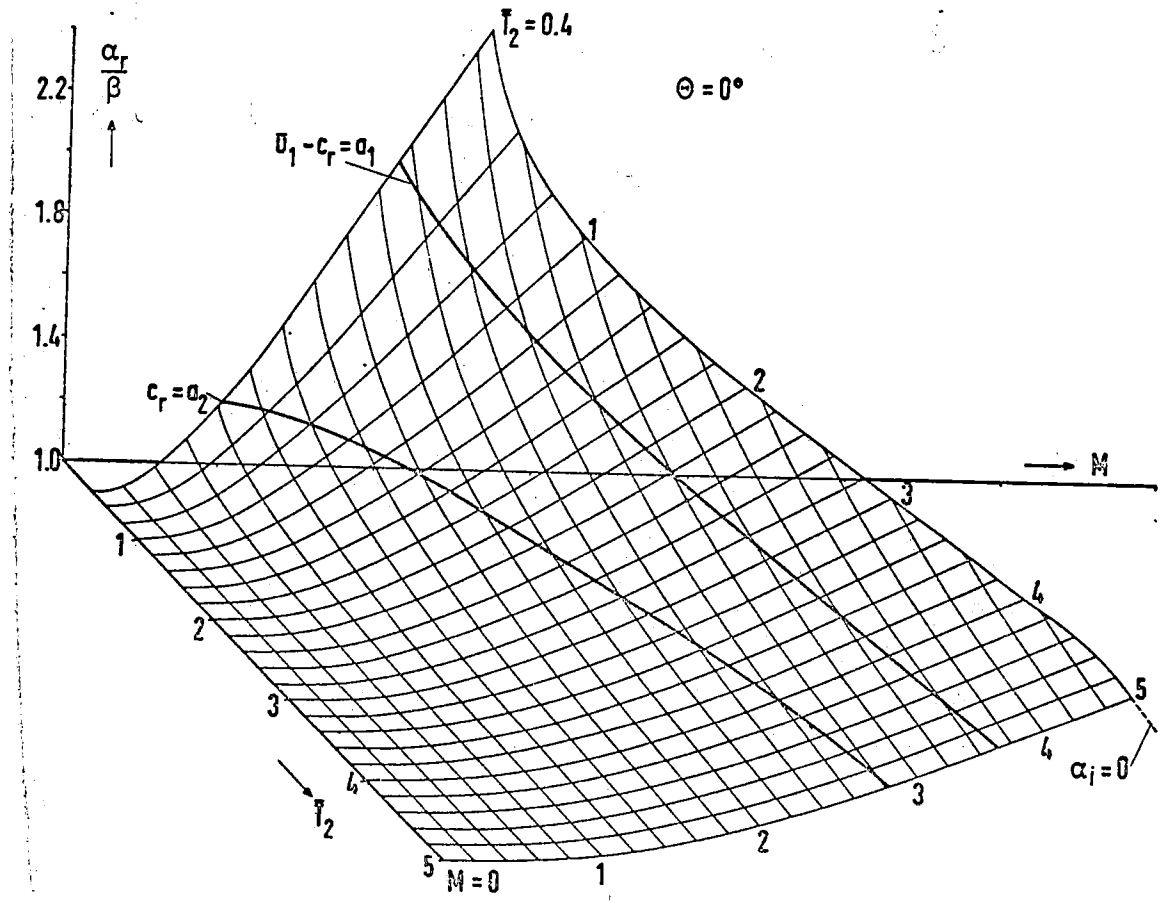

Figure 9. Wave Number α_r/β For Two-Dimensional, Spacially Amplified Disturbances Of The Compressible Vortex Layer as a Function of Mach Number M and Environment Temperature $\bar{T}_2$.

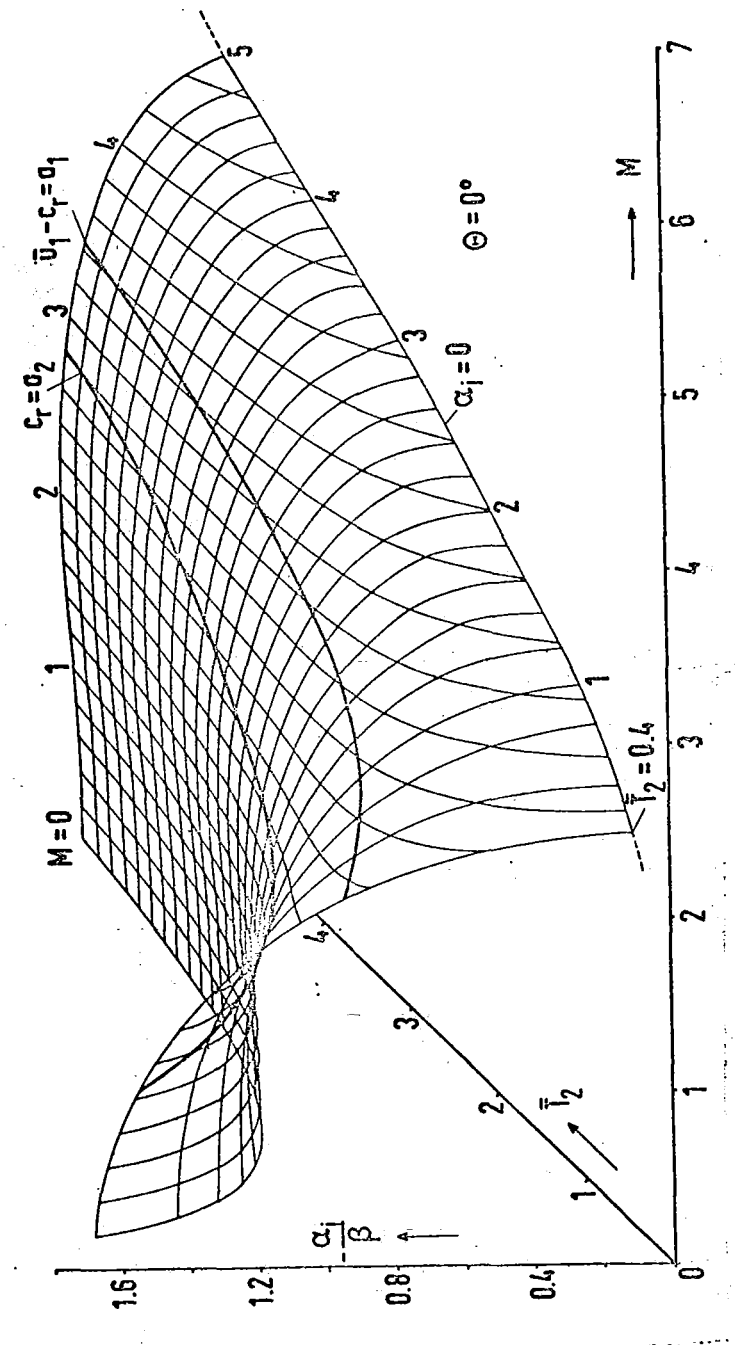

Figure 10. Amplification Parameter $-\alpha_i/\beta$ For Two-Dimensional, Spacially Amplified Disturbances of the Compressible Vortex Layer as a Function of Mach Number M and Environment Temperature $\bar{T}_2$.

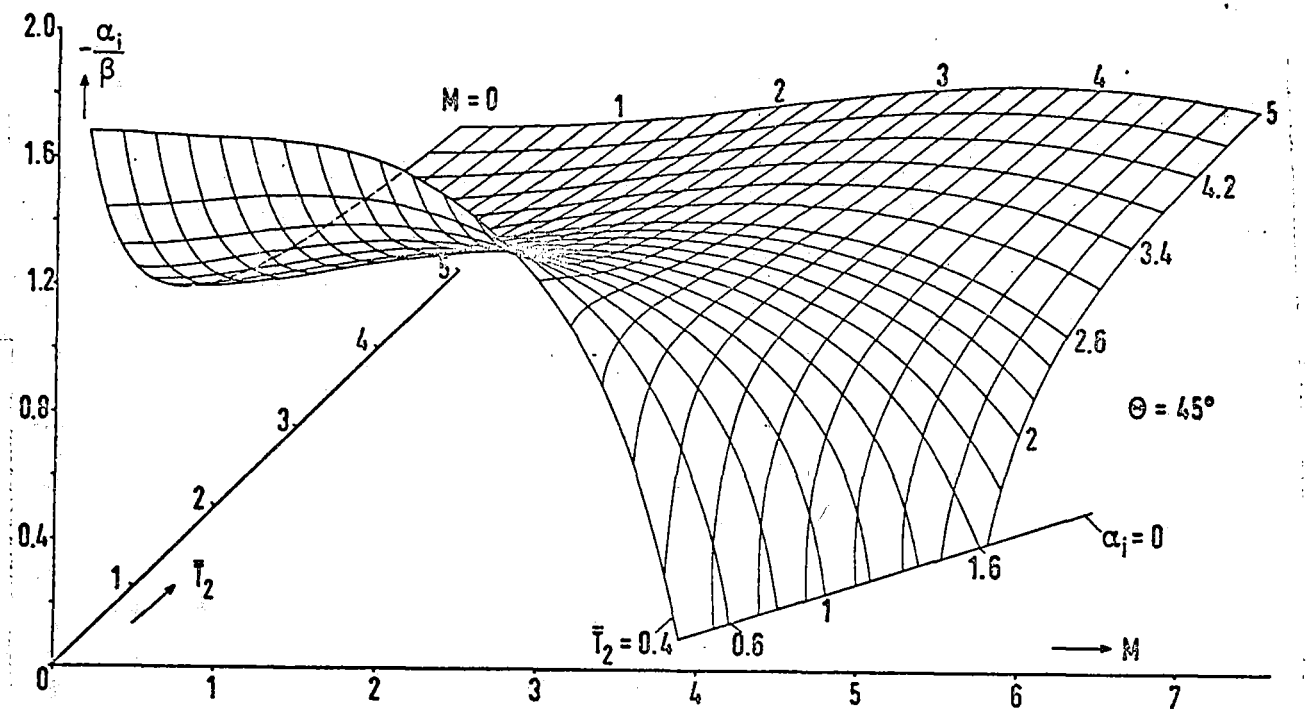

Figure 11. Amplification Parameter $-\alpha_i/\beta$ For Three-Dimensional, Spacially Amplified Disturbances ($\Theta = 45°$) of the Compressible Vortex Layer as a Function of Mach Number M and Environment Temperature $\bar{T}_2$.

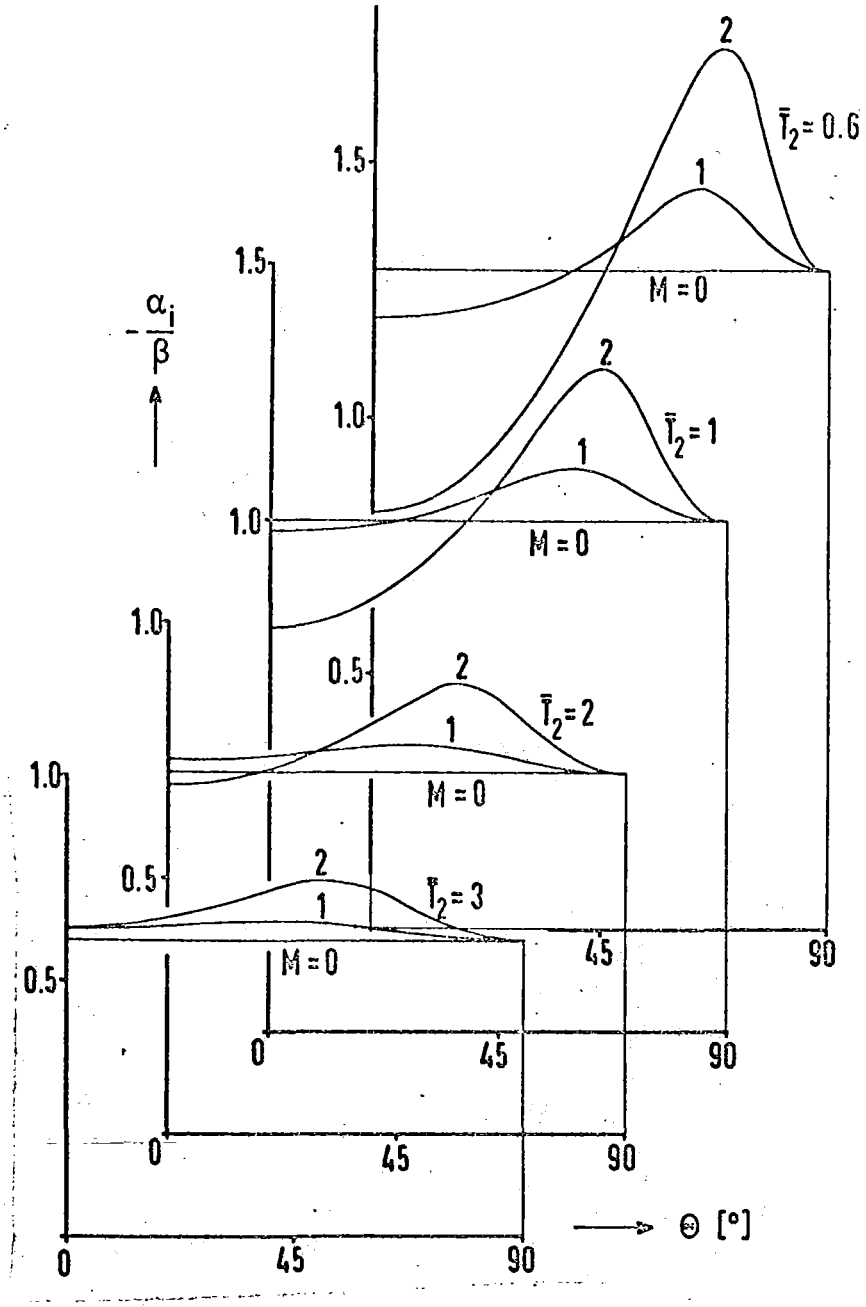

Figure 12. Amplification Parameter $-\alpha_i/\beta$ For Three-Dimensional, Spacially Amplified Disturbances of the Compressible Vortex Layer as a Function of Angle of Incidence Θ With the Mach Number M as a Parameter for Various Environment Temperatures $\bar{T}_2$.

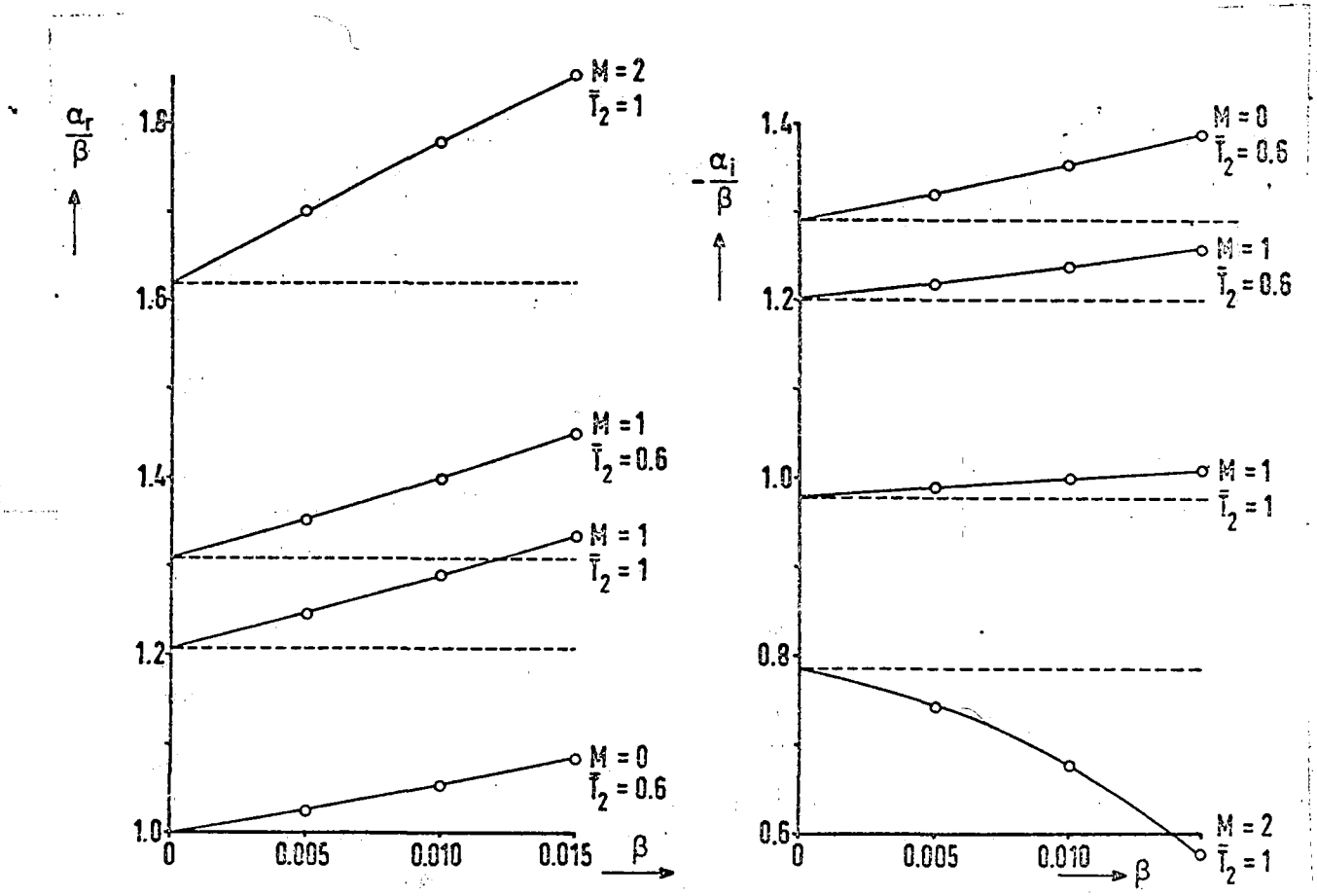

Figure 13. Comparison of Stability Behaviors of the Compressible Vortex Layer (----) With the Lock Profile (——) Relative to Two-Dimensional, Spacially Amplified Disturbances with Low Disturbance Frequencies β For Various Mach Numbers M and Environment Temperatures $\bar{T}_2$.

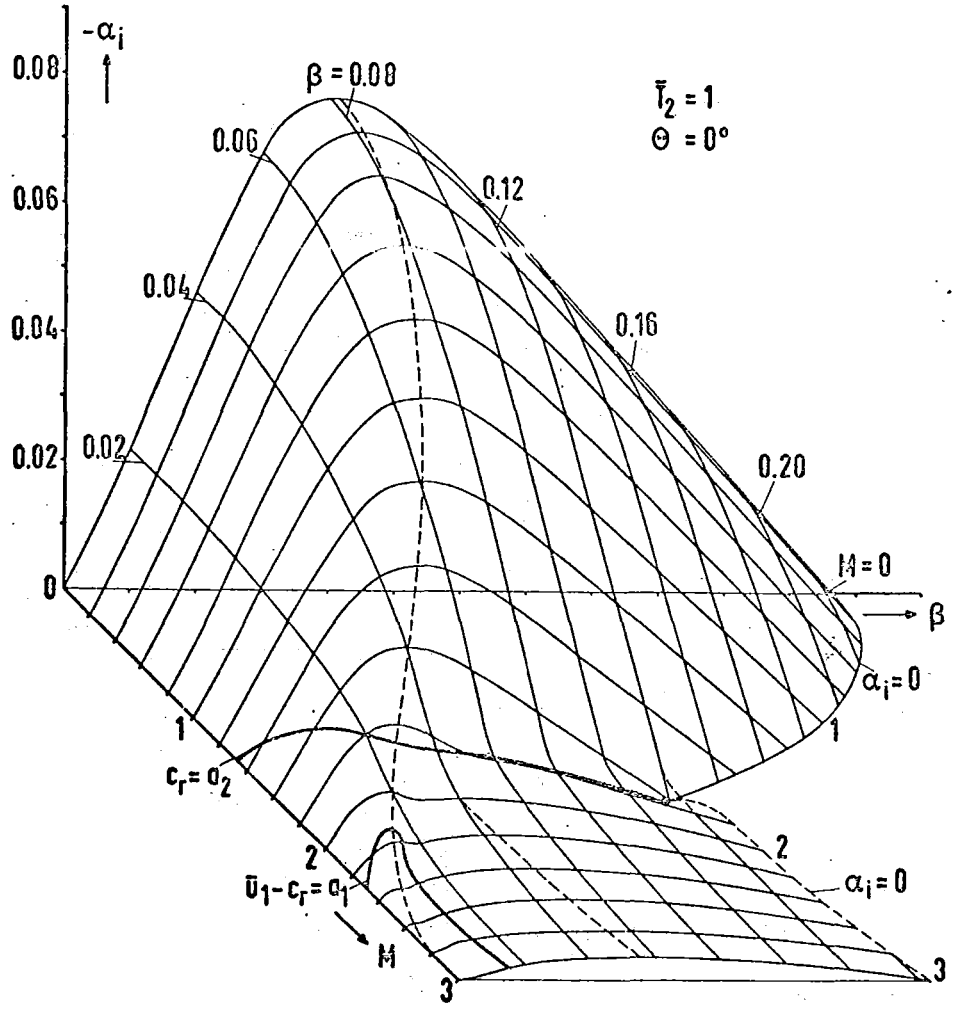

Figure 14. Amplification Parameter $-\alpha_i$ for Two-Dimensional, Spacially Amplified Disturbances of the Lock Profile (First Mode) As a Function of Disturbance Frequency β and the Mach Number M for the Environment Temperature $\bar{T}_2 = 1$.

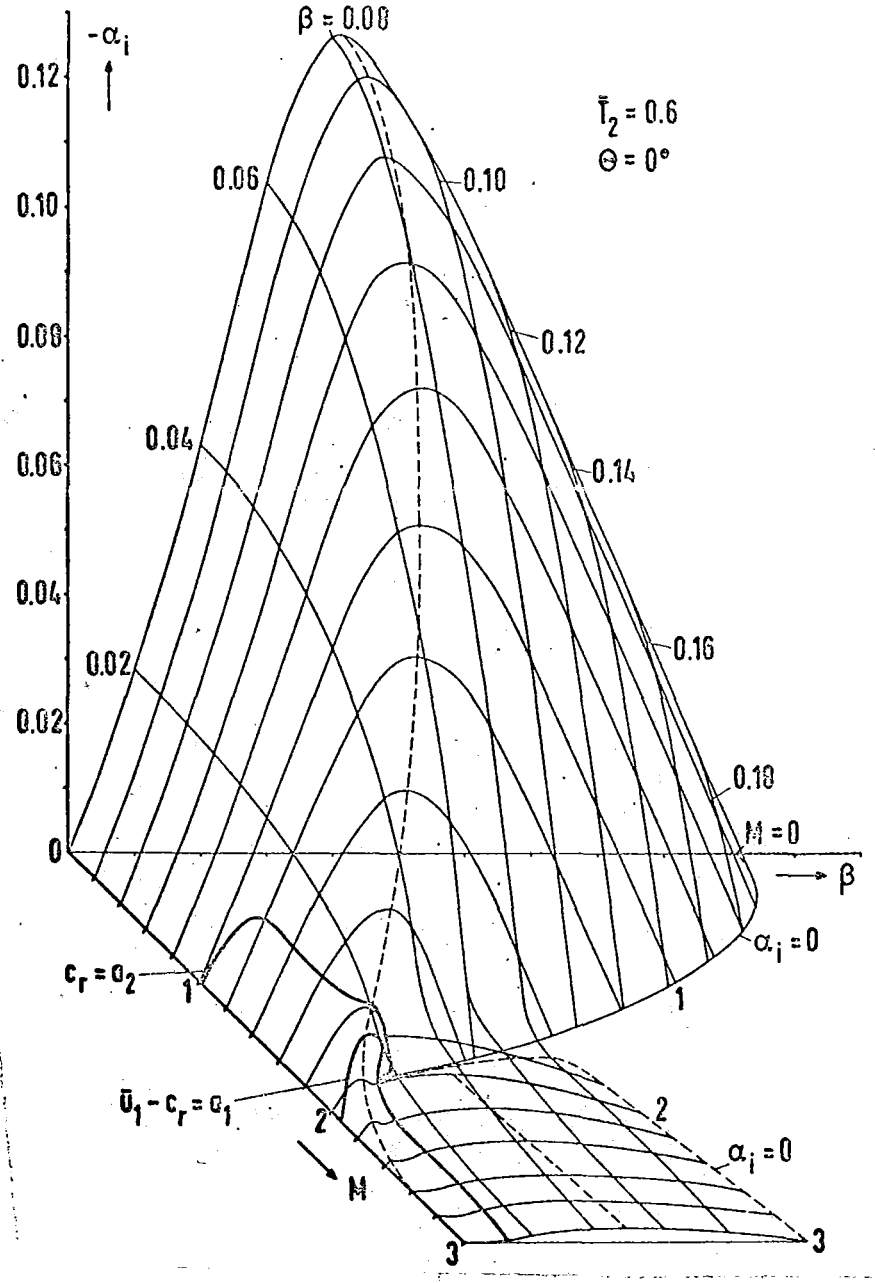

Figure 15. Amplification Parameter $-\alpha_i$ for Two-Dimensional Spacially Amplified Disturbances of the Lock Profile as a Function of Disturbance Frequency β and Mach Number M for the Environment Temperature $\bar{T}_2 = 0.6$ (Cooled Free Jet).

Even Roman odd

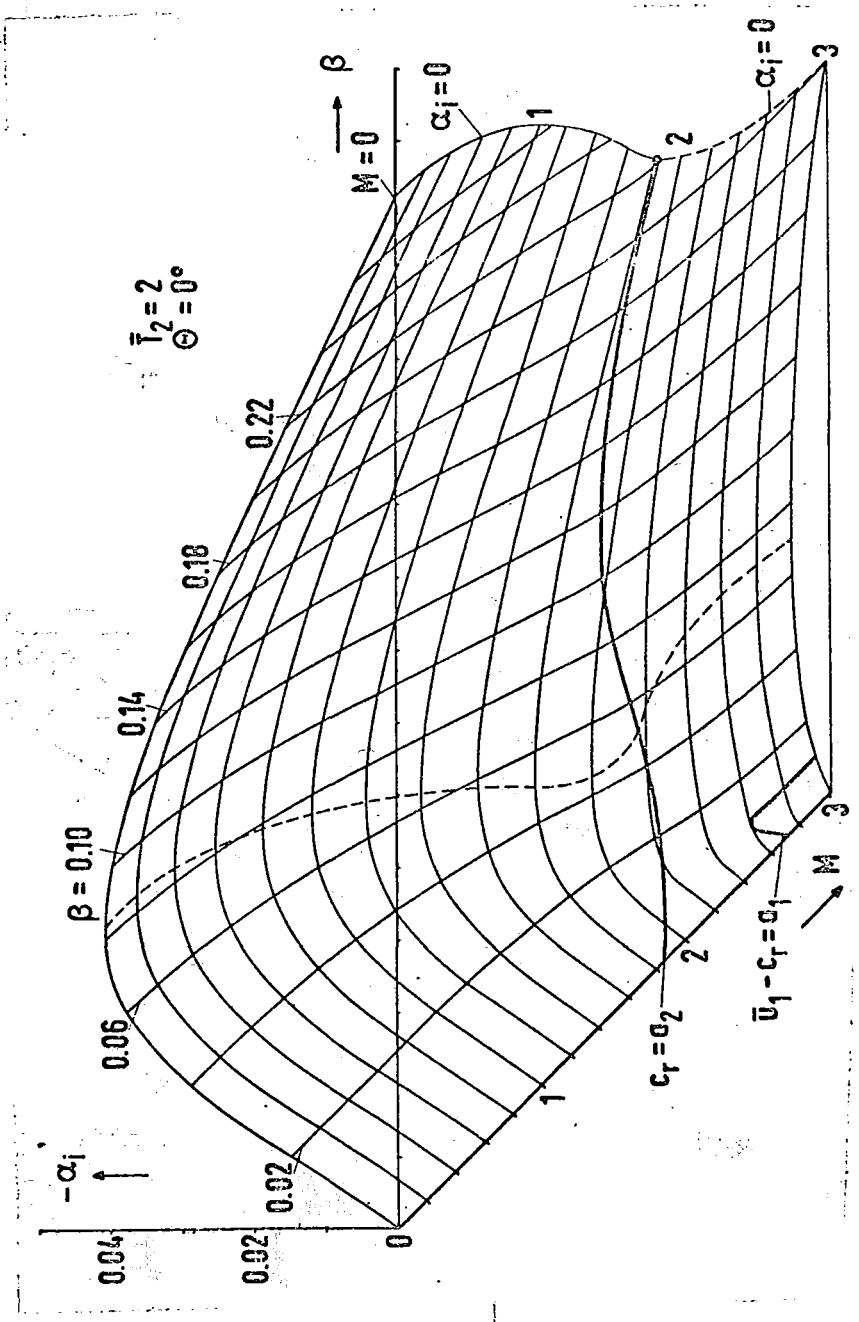

Figure 16. Amplification Parameter $-\alpha_i$ for Two-Dimensional, Spacially Amplified Disturbances of the Lock Profile as a Function of Disturbance Frequency β and Mach Number M for the Environment Temperature $\bar{T}_2 = 2$ (Heated Free Jet).

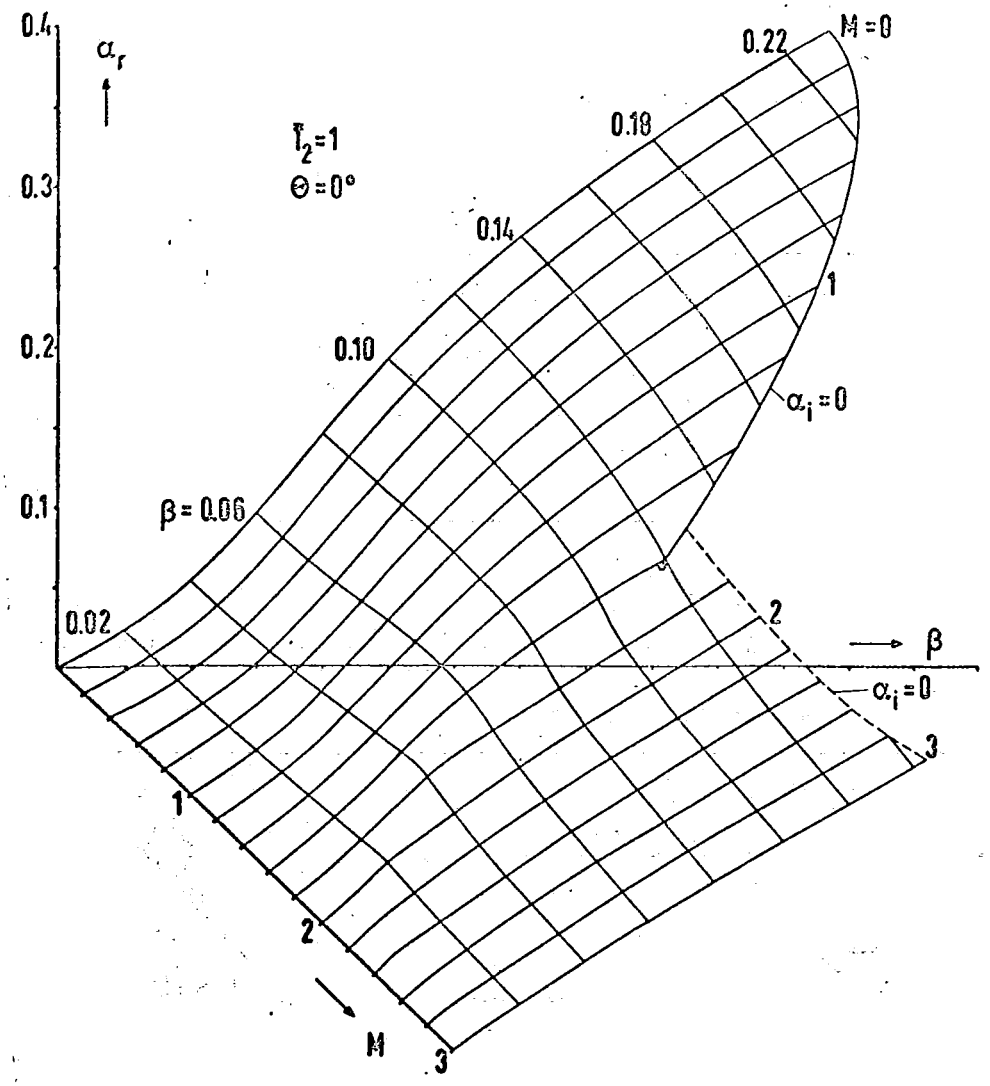

Figure 17. Wave Number α_r for Two-Dimensional, Spacially Amplified Disturbances of the Lock Profile as a Function of Disturbance Frequency β and Mach Number M for the Environment Temperature $\overline{T}_2 = 1$.

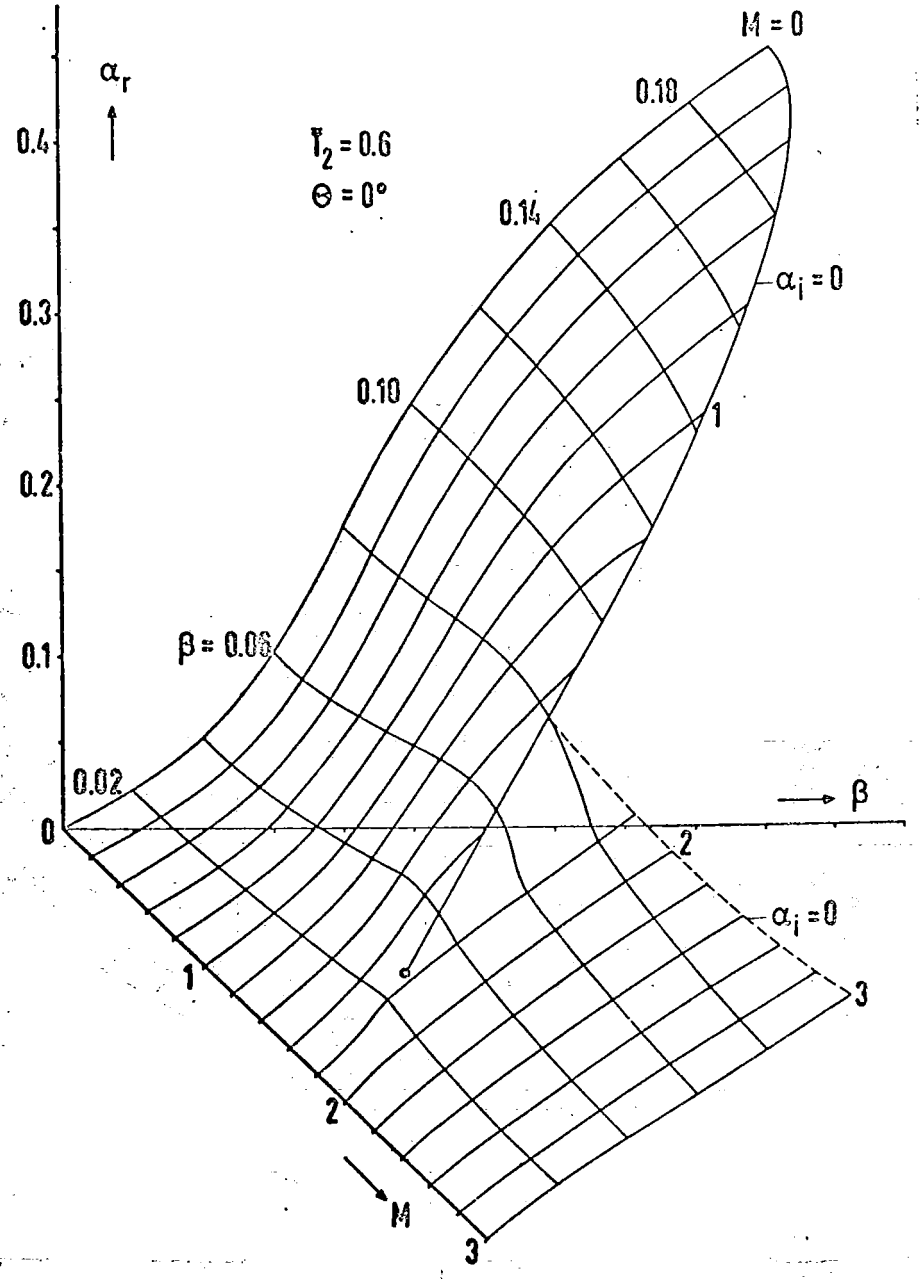

Figure 18. Wave Number α_r for Two-Dimensional, Spacially Amplified Disturbances of the Lock Profile as a Function of Disturbance Frequency β and Mach Number M for the Environment Temperature $\bar{T}_2 = 0.6$ (Cooled Free Jet).

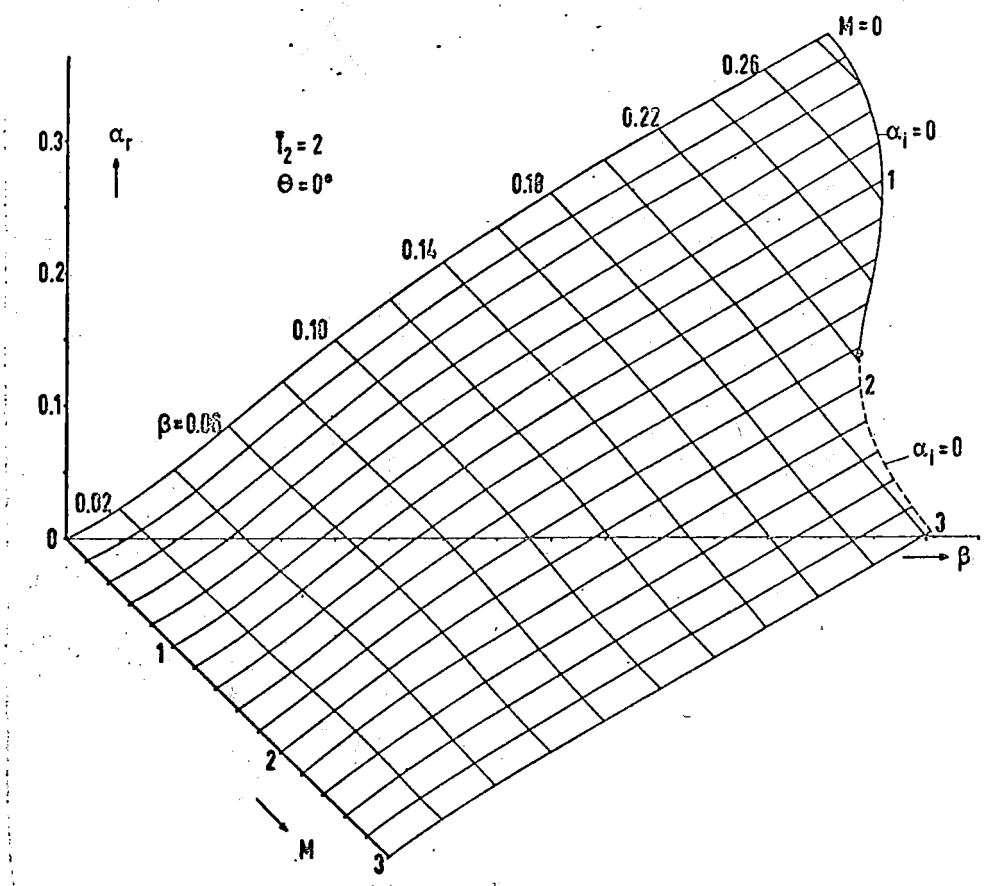

Figure 19. Wave Number α_r for Two-Dimensional, Spacially Amplified Disturbances of the Lock Profile as a Function of Disturbance Frequency β and Mach Number M for the Environment Temperature $\bar{T}_2 = 2$ (Heated Free Jet).

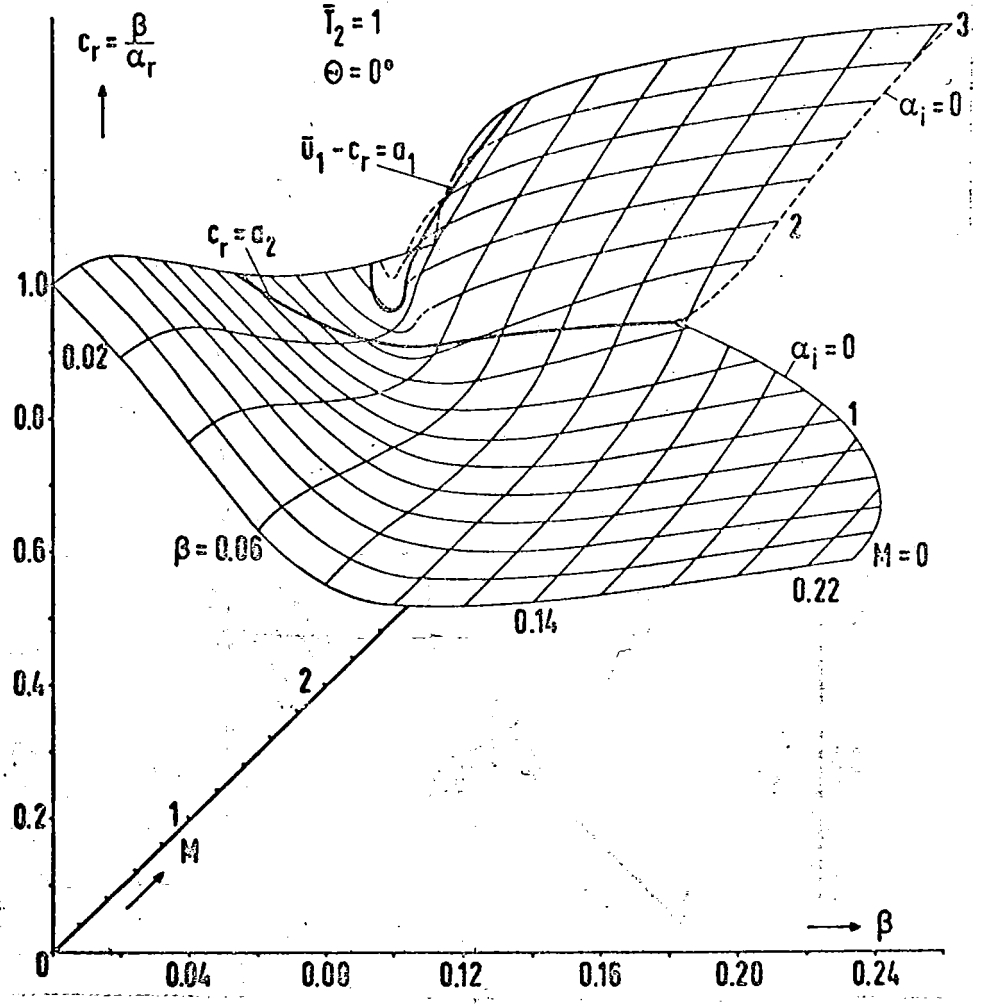

Figure 20. Phase Velocity $c_r = \beta/\alpha_r$ for Two-Dimensional, Spacially Amplified Disturbances of the Lock Profile as a Function of Disturbance Frequency β and Mach Number M for the Environment Temperature $\bar{T}_2 = 1$.

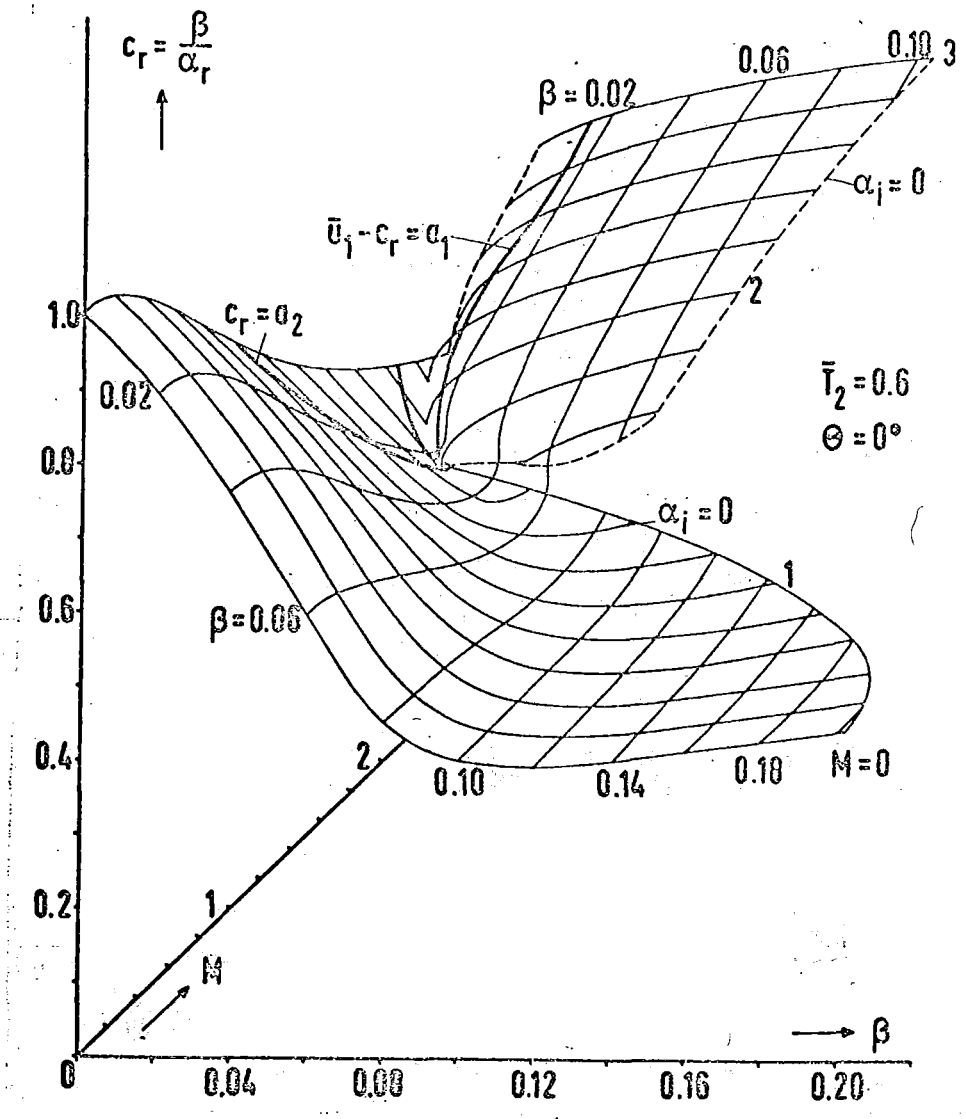

Figure 21. Phase Velocity $c_r = \beta/\alpha_r$ for Two-Dimensional, Spacially Amplified Disturbances of the Lock Profile as a Function of Disturbance Frequency β and Mach Number M for the Environment Temperature $\bar{T}_2 = 0.6$ (Cooled Free Jet).

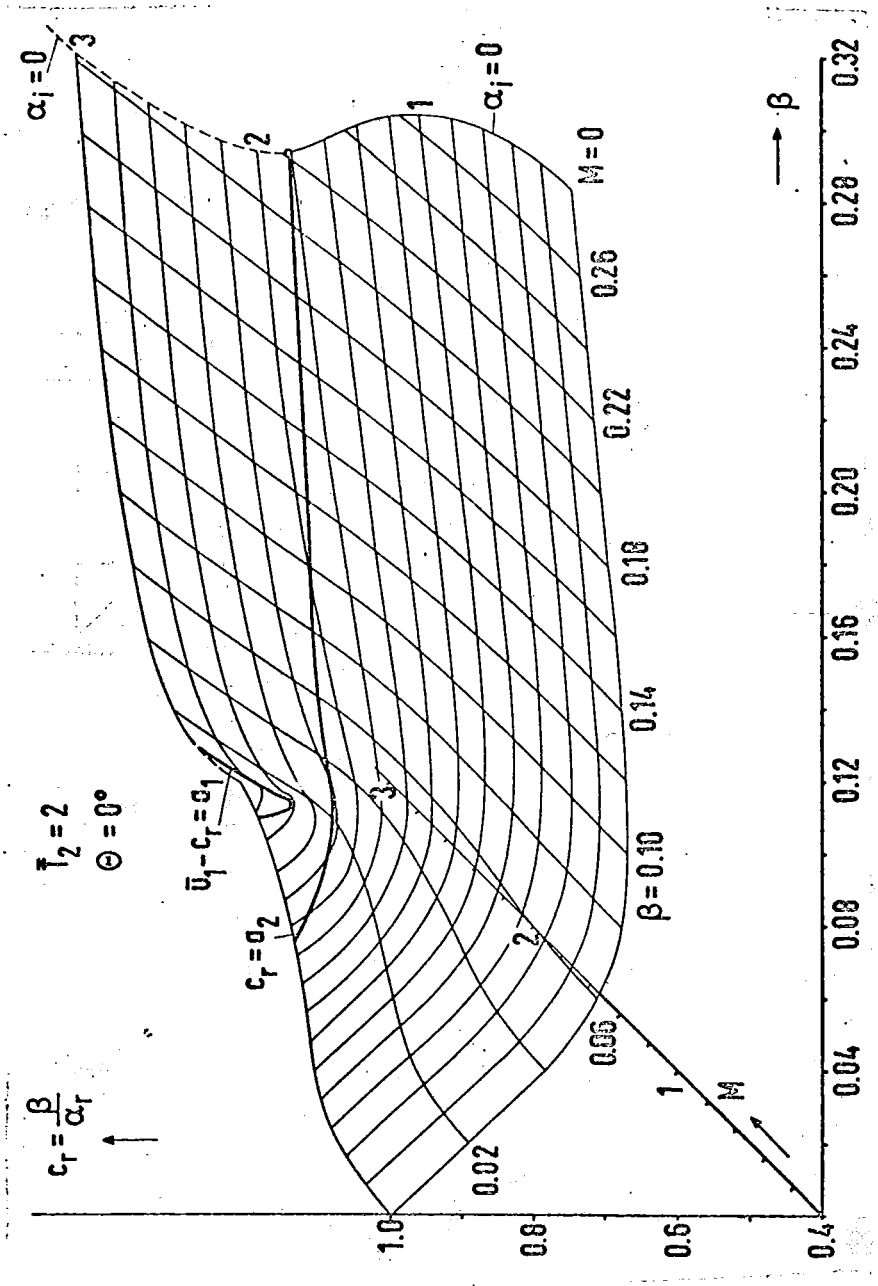

Figure 22. Phase Velocity $c_r = \beta/\alpha_r$ for Two-Dimensional, Spacially Amplified Disturbances of the Lock Profile as a Function of Disturbance Frequency β and Mach Number M for the Environment Temperature $\bar{T}_2 = 2$ (Heated Free Jet).

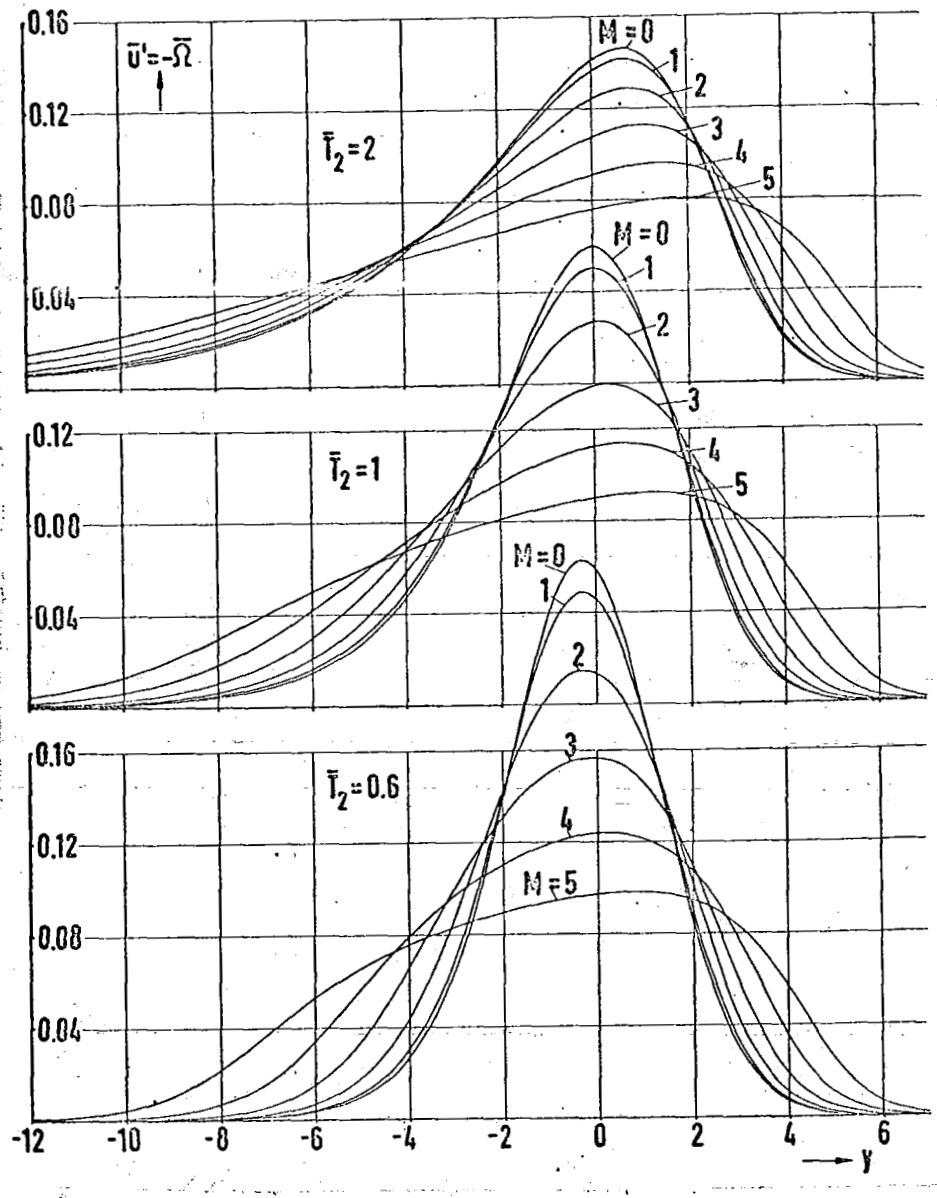

Figure 23. Vortex-Strength Distribution $\Omega(y) = -d\bar{u}/dy$ of the Lock Profile for Various Mach Numbers M and Environment Temperatures $\bar{T}_2$ for Air.

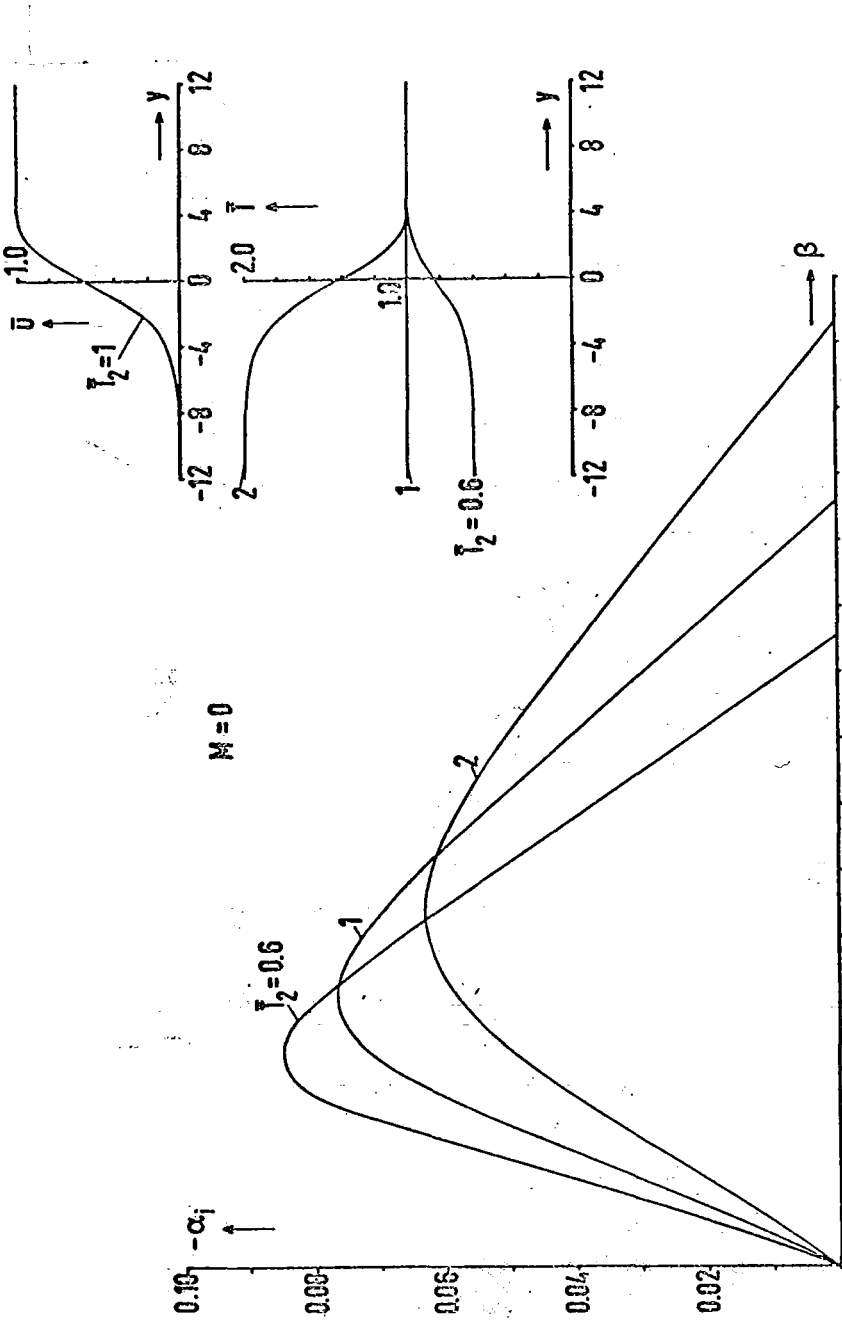

Figure 24. Amplification Parameter $-\alpha_i$ for Two-Dimensional, Spacially Amplified Disturbances of the Lock Profile as a Function of Disturbance Frequency, β for the Mach Number M = 0 and Three Environment Temperatures $\bar{T}_2$ (Velocity and Temperature Profiles not Coupled).

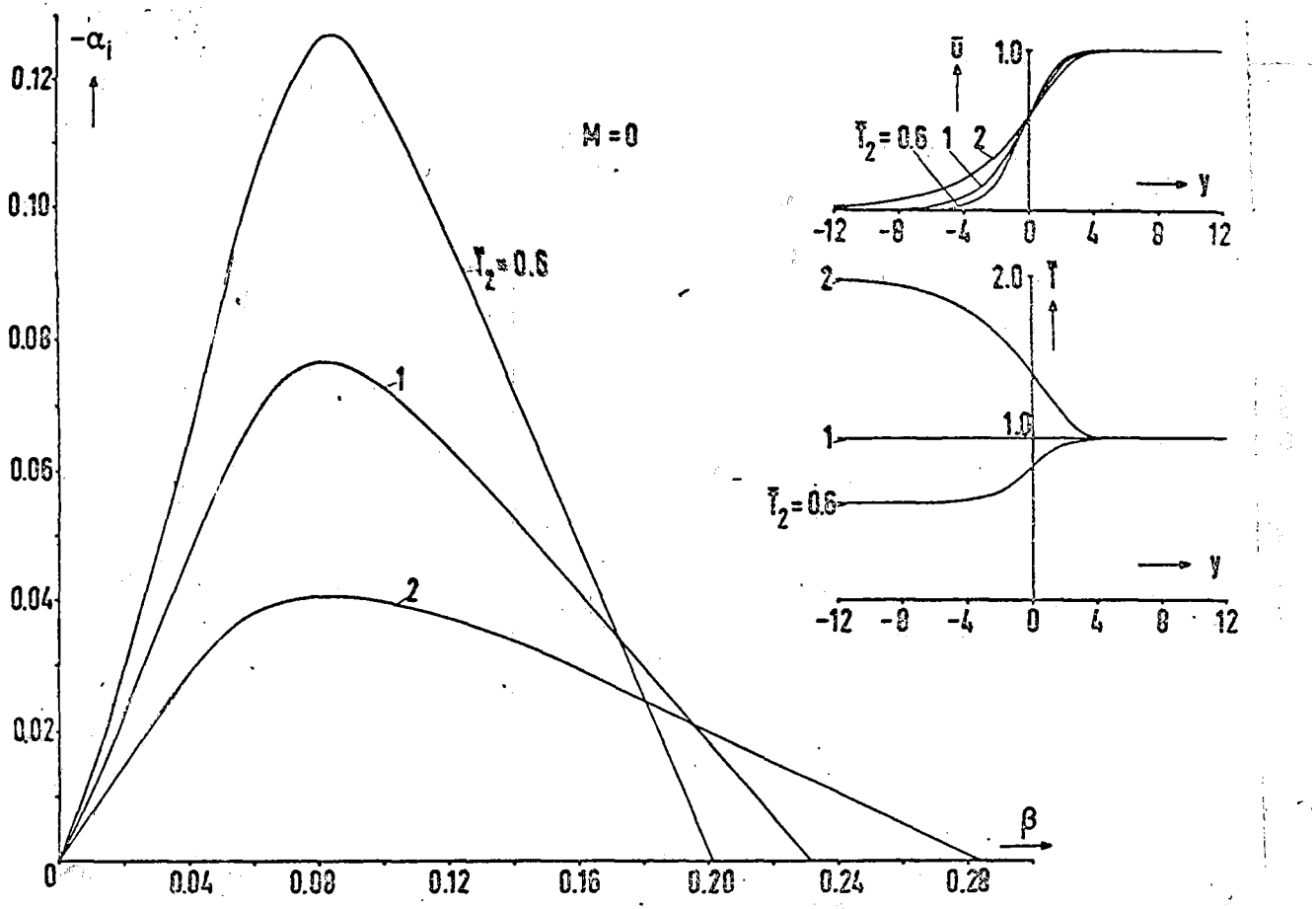

Figure 25. Amplification Parameter $-\alpha_i$ for Two-Dimensional, Spacially Amplified Disturbances of the Lock Profile as a Function of Disturbance Frequency β for the Mach Number M = 0 and Three Environment Temperatures $\overline{T}_2$ (Velocity and Temperature Profiles Coupled).

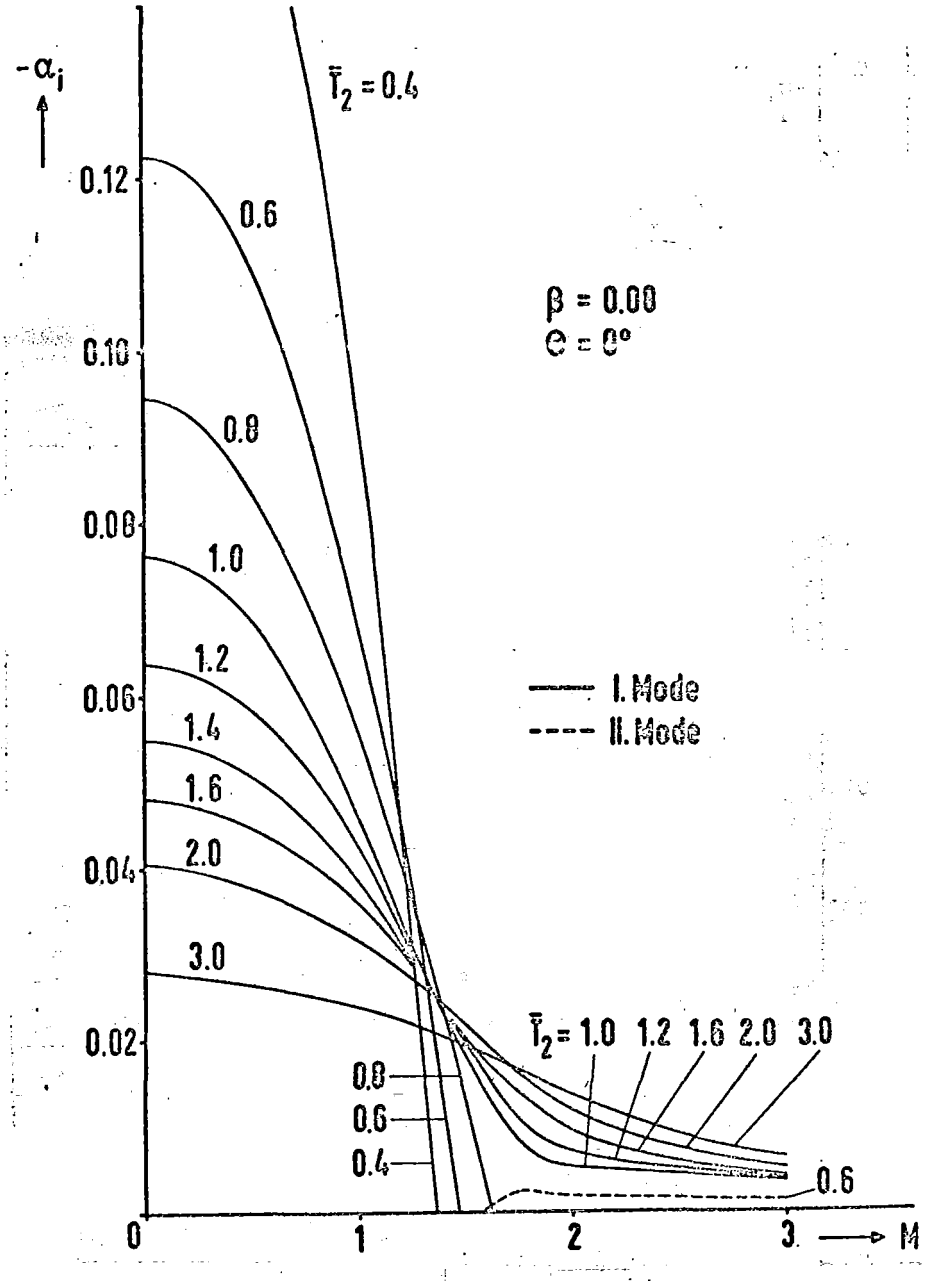

Figure 26. Amplification Parameter $-\alpha_i$ for Two-Dimensional, Spacially Amplified Disturbances of the Lock Profile for Constant Disturbance Frequency $\beta = 0.08$ as a Function of Mach Number M for Various Environment Temperatures $\bar{T}_2$.

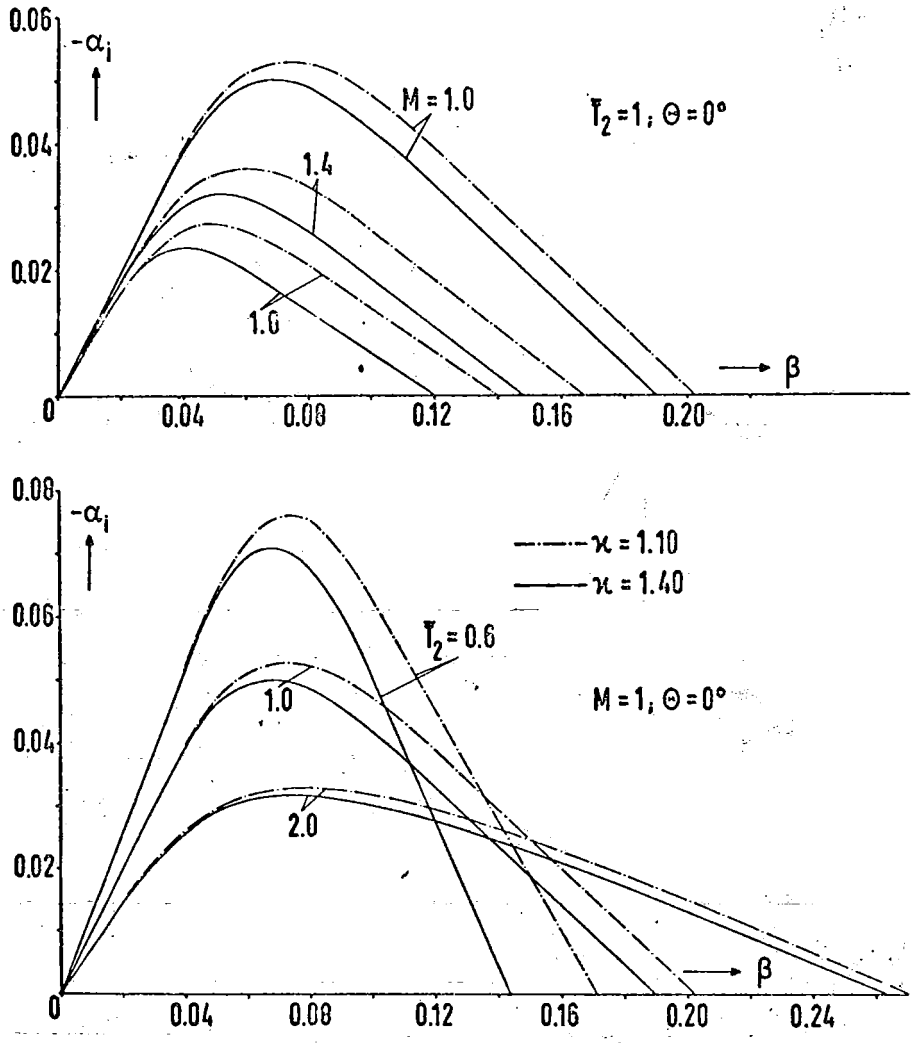

Figure 27. Effect of the Isentropic Exponent κ of the Gas Upon the Amplification Parameter $-\bar{\alpha}_i$ for Two-Dimensional, Spacially Amplified Disturbances of the Lock Profile for Several Values of Mach Number M and Environment Temperature $\bar{T}_2$.

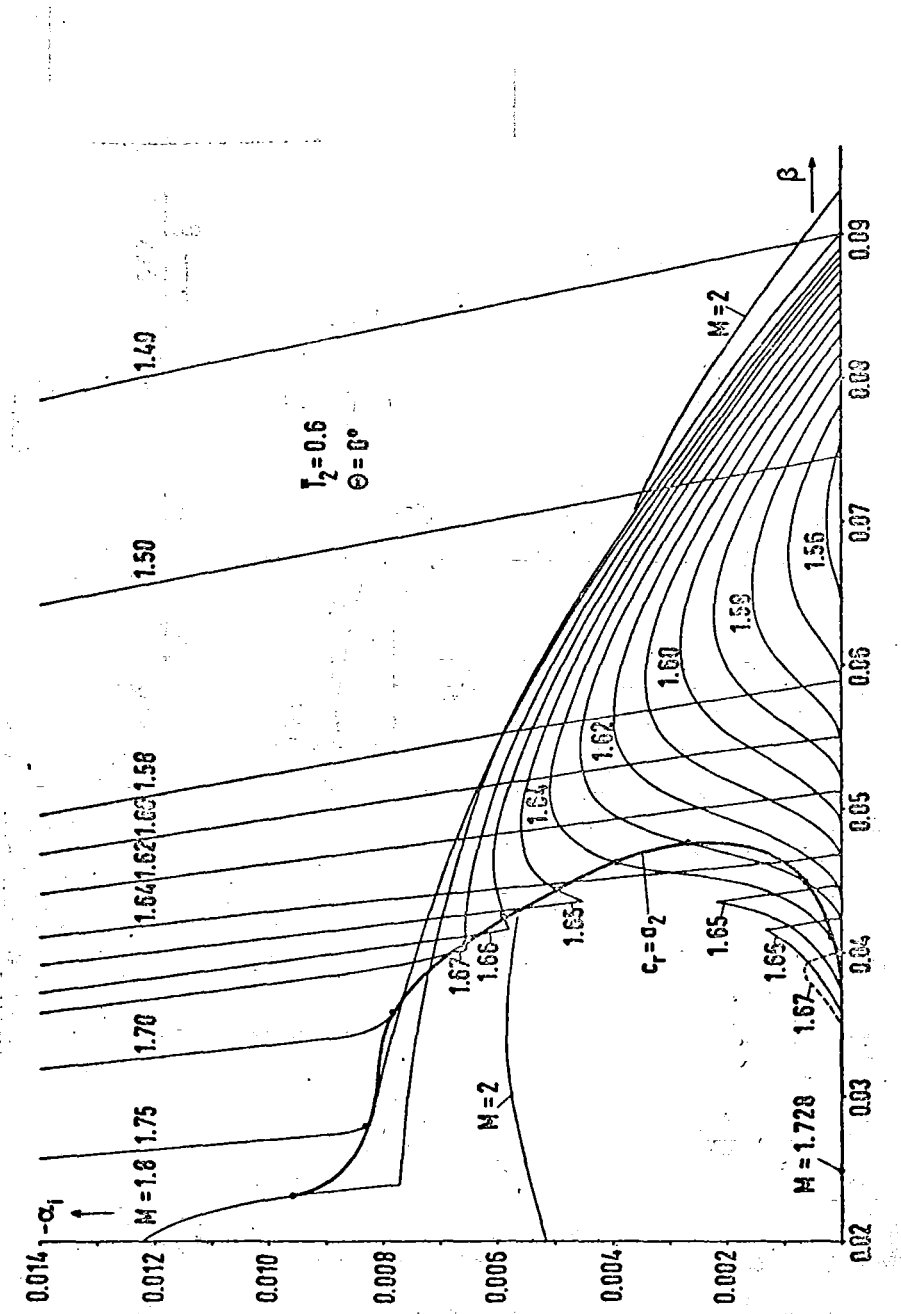

Figure 28. Amplification Parameter $-\alpha_i$ for Two-Dimensional, Spacially Amplified First and Second Mode Disturbances of the Lock Profile as a Function of Disturbance Frequency β for Various Mach Numbers M and the Environment Temperature $\overline{T}_2$ = 0.6.

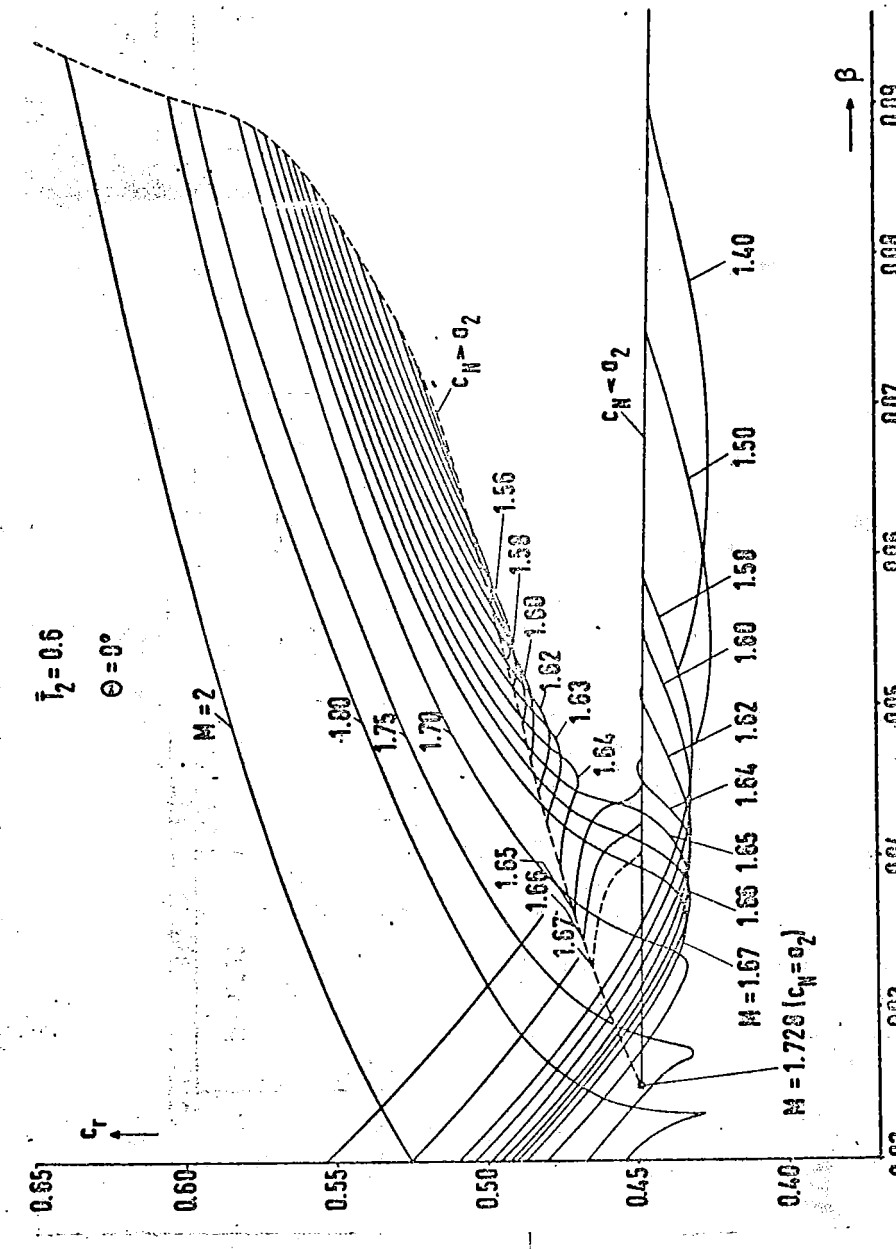

Figure 29. Phase Velocity $c_r = \beta/\alpha_r$ For Two-Dimensional, Spacially Amplified First and Second Mode Disturbances of the Lock Profile as a Function of Disturbance Frequency β for Various Mach Numbers M and the Environment Temperature $\bar{T}_2 = 0.6$.

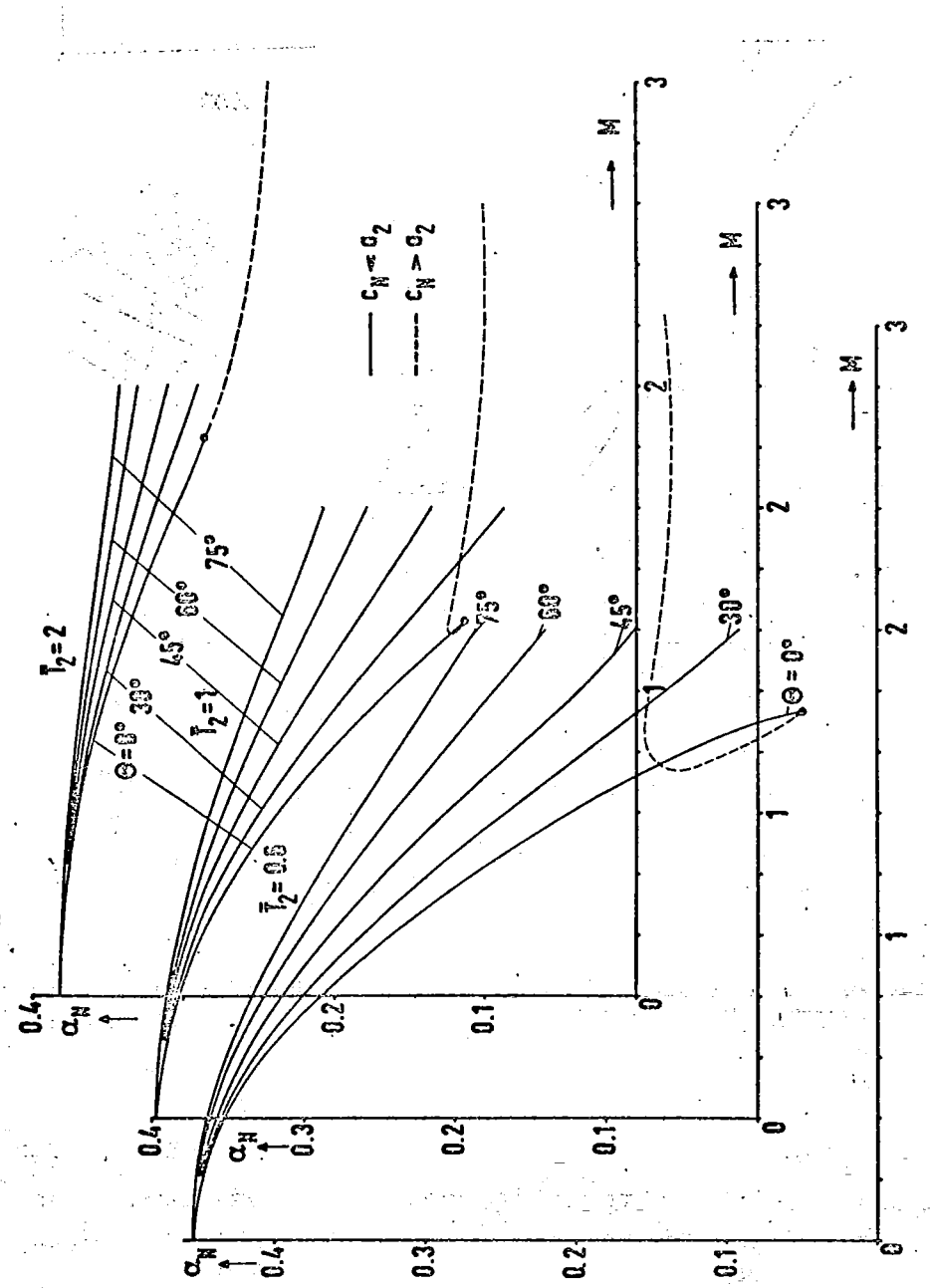

Figure 30. Neutral Wave Numbers α_N of the Lock Profile as a Function of Mach Number M for Various Environment Temperatures $\overline{T}_2$ and Disturbance Angles of Incidence Θ.

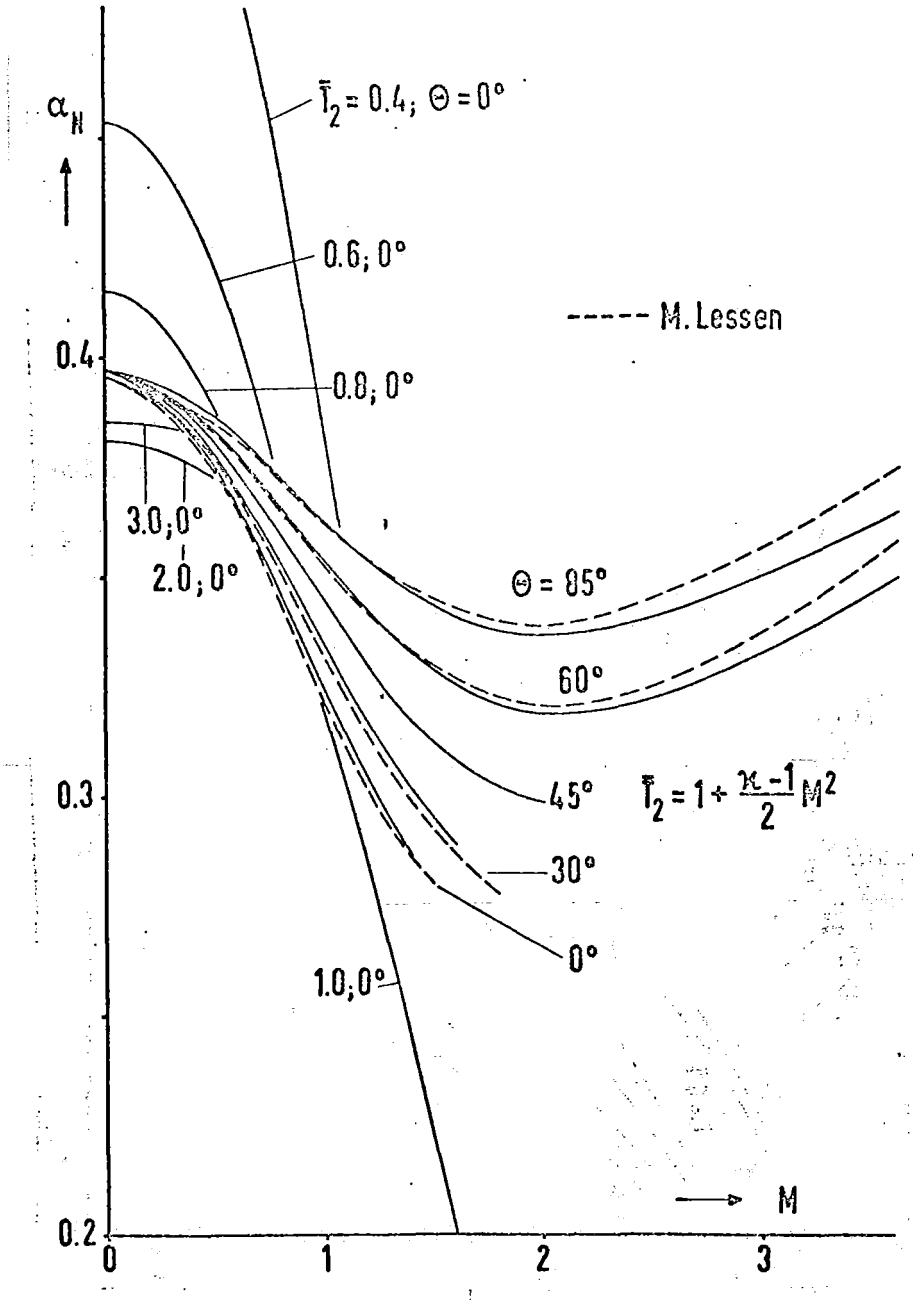

Figure 31. Neutral Wave Numbers α_N of the Lock Profile as a Function of Mach Number M for Various Environment Temperatures $\bar{T}_2$ and Disturbance Angles of Incidence Θ. Comparison With the Results of Lessen, Fox and Zien [25] for $\bar{T}_2 = 1 + \frac{\kappa - 1}{2} M^2$.

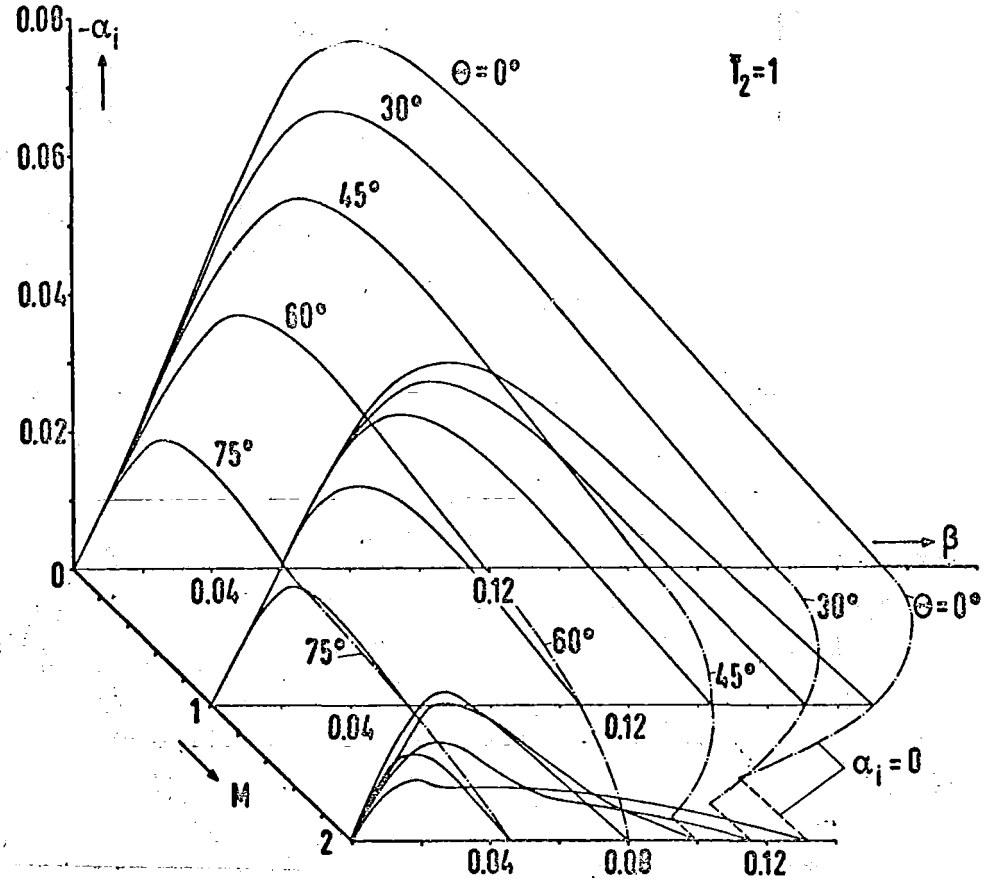

Figure 32. The Amplification Parameter $-\alpha_i$ for Three-Dimensional, Spacially Amplified Disturbances of the Lock Profile as a Function of Disturbance Frequency β and Mach Number M for the Environment Temperature $\bar{T}_2 = 1$.

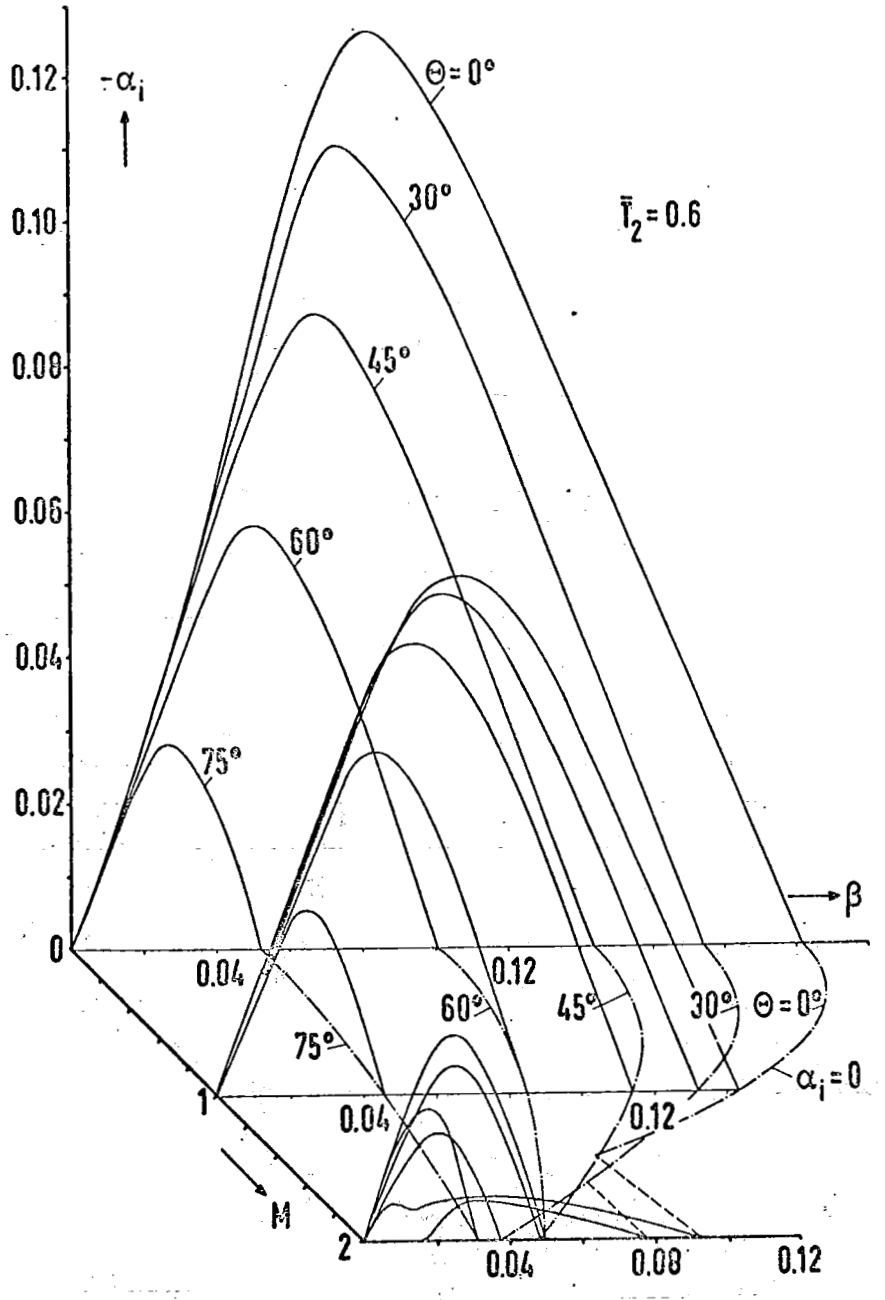

Figure 33. The Amplification Parameter $-\alpha_i$ for Three-Dimensional, Spacially Amplified Disturbances of the Lock Profile as a Function of Disturbance Frequency β and Mach Number M for the Environment Temperature $\bar{T}_2$ = 0.6.

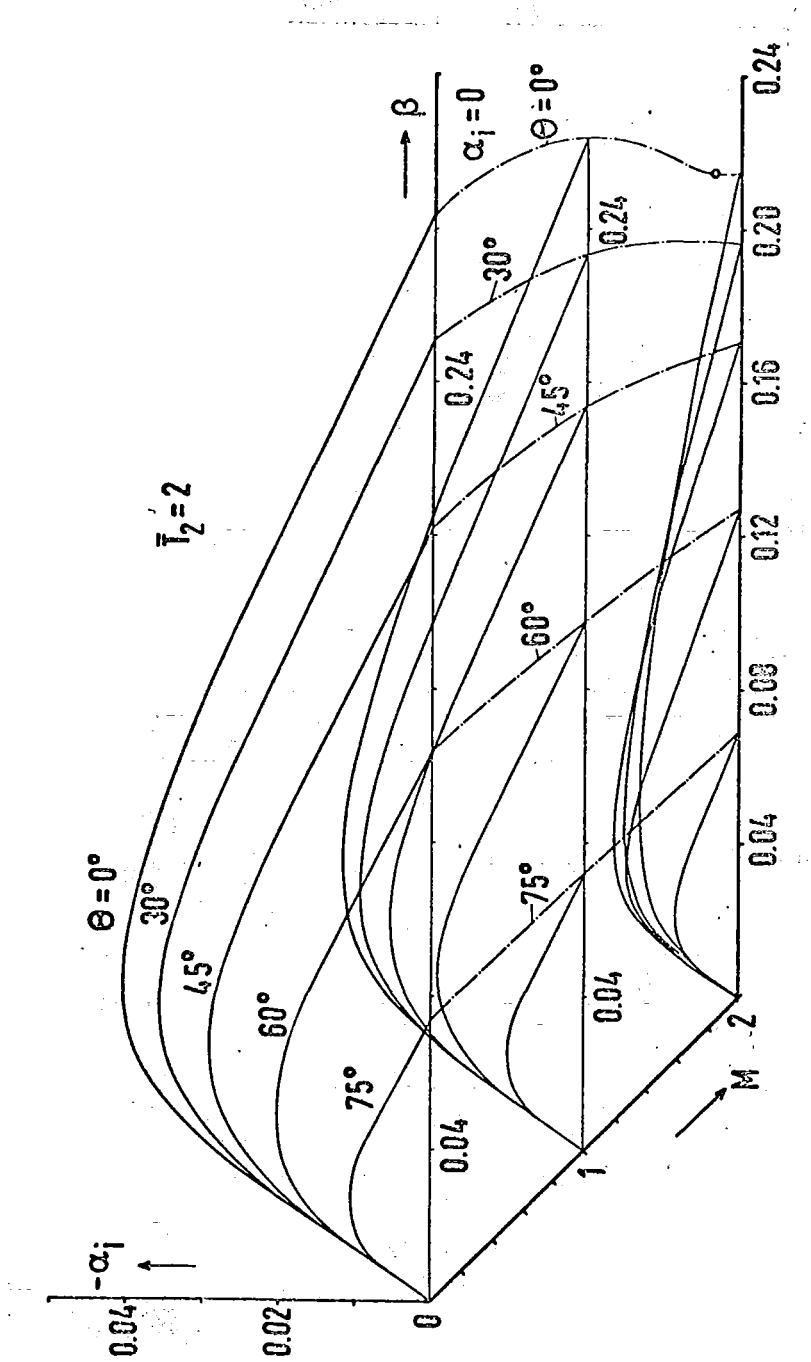

Figure 34. The Amplification Parameter $-\alpha_i$ for Three-Dimensional, Spacially Amplified Disturbances of the Lock Profile as a Function of Disturbance Frequency β and Mach Number M for the Environment Temperature $\bar{T}_2 = 2$.

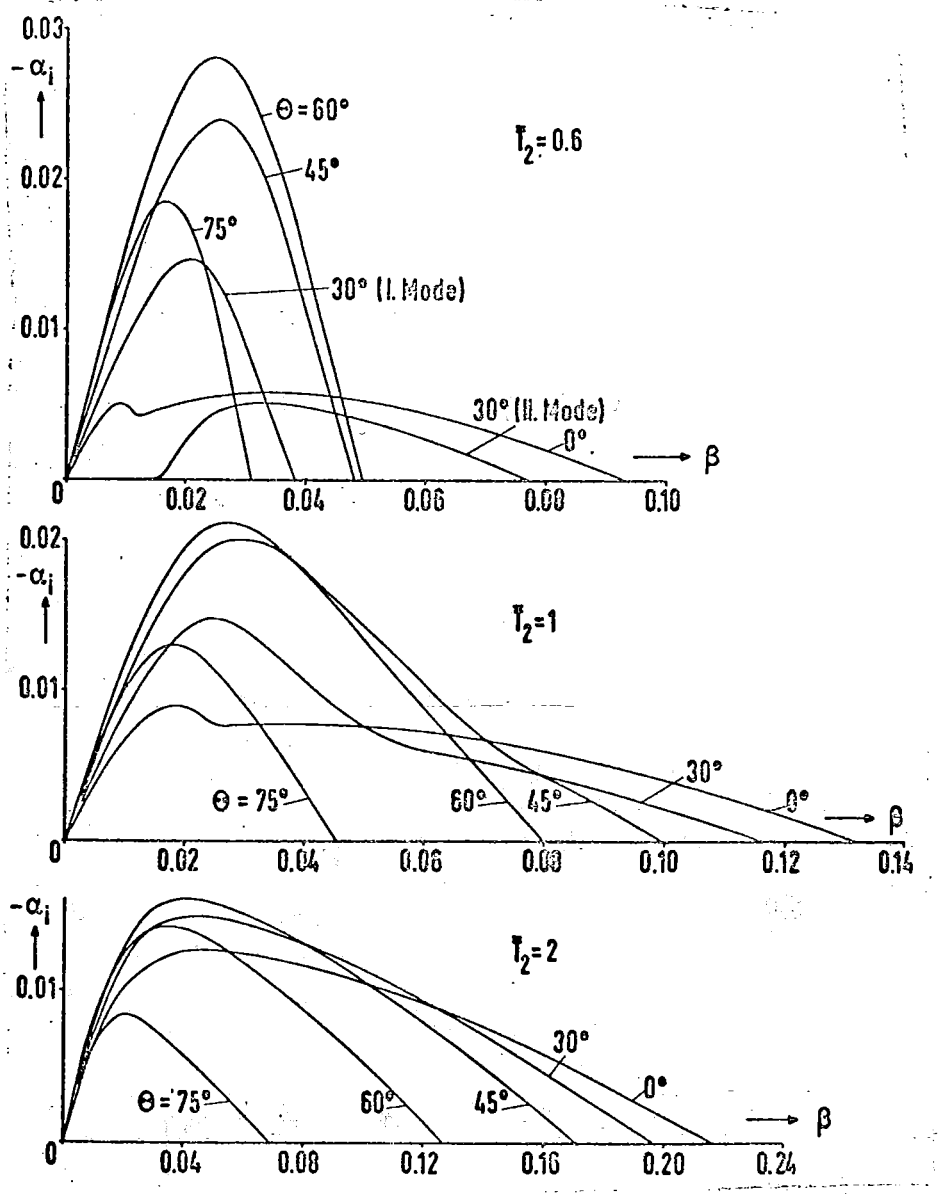

Figure 35. Amplification Parameter $-\alpha_i$ for Three-Dimensional, Spacially Amplified Disturbances of the Lock Profile as a Function of Disturbance Frequency β For the Mach Number M = 2 and Various Environment Temperatures $\bar{T}_2$. (Note the Different Scales for Disturbance Frequency β.)

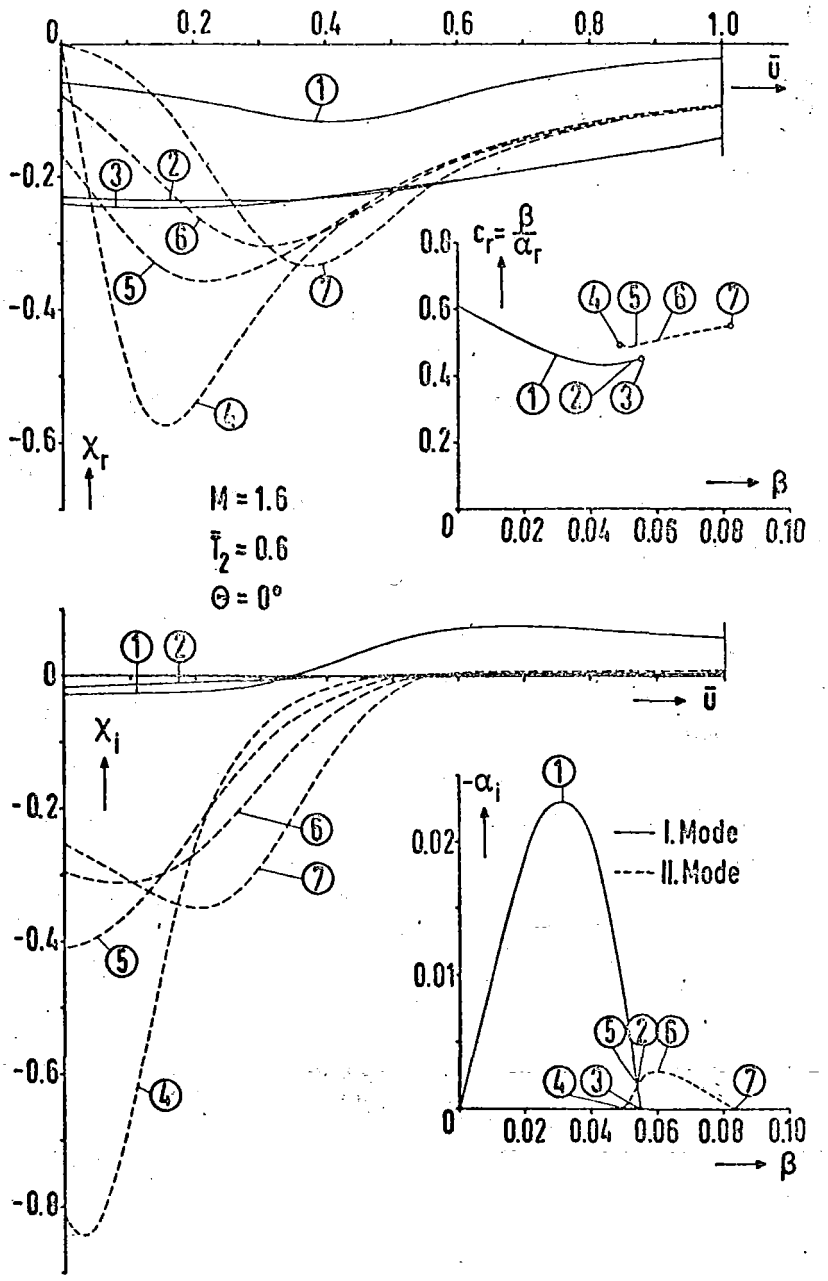

Figure 36. Curves of the Complex Function $\chi(\bar{u})$, First and Second Mode, of the Lock Profile for Various Disturbance Frequencies at M = 1.6, $\bar{T}_2$ = 0.6 and Θ = 0°.

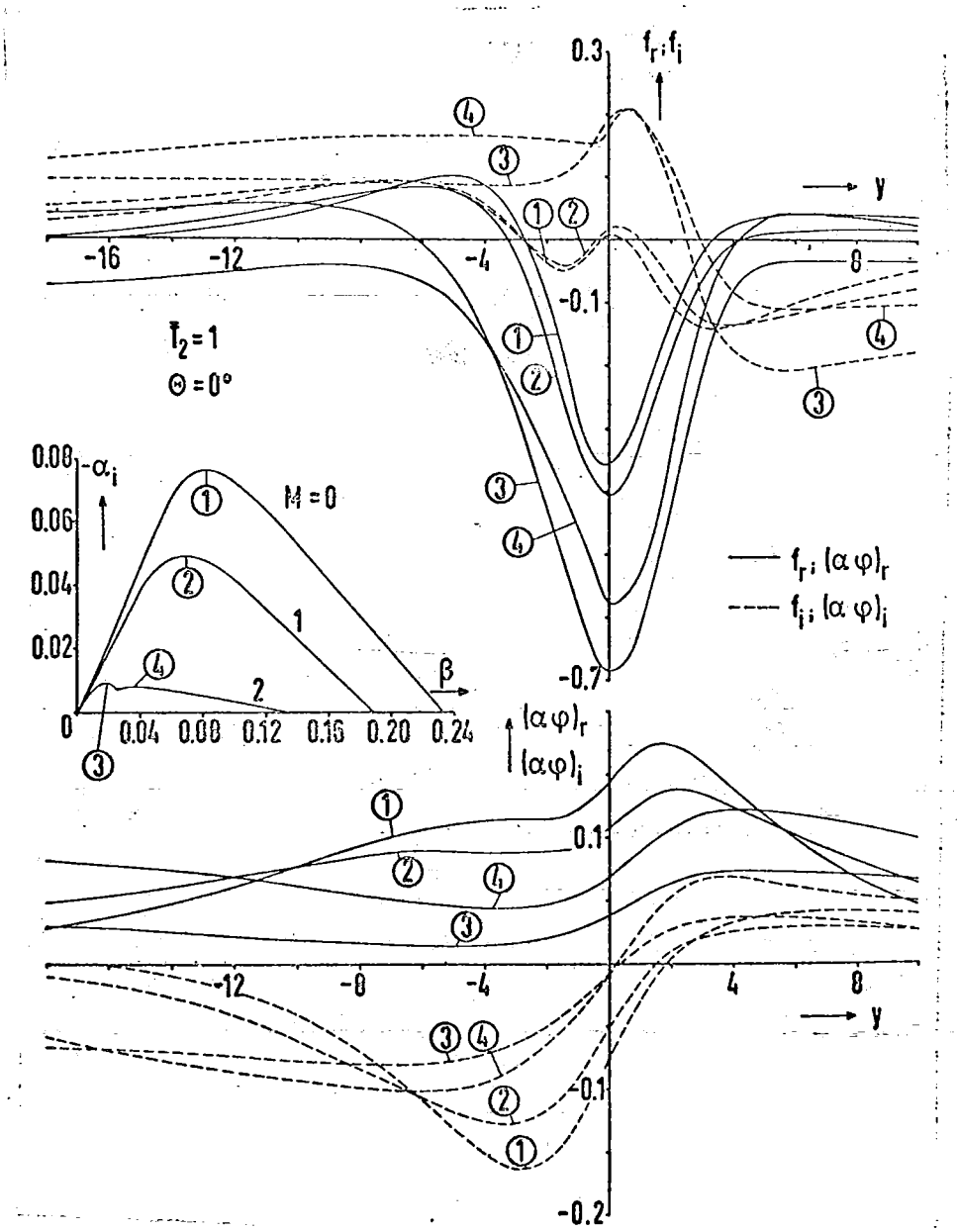

Figure 37. Curves of the Complex Eigenfunctions f(y) and $\alpha\phi(y)$ of the u' and v' Disturbances (Θ = 0°) at Maximum Amplification for Various Mach Numbers M and the Environment Temperature $\bar{T}_2$ = 1.

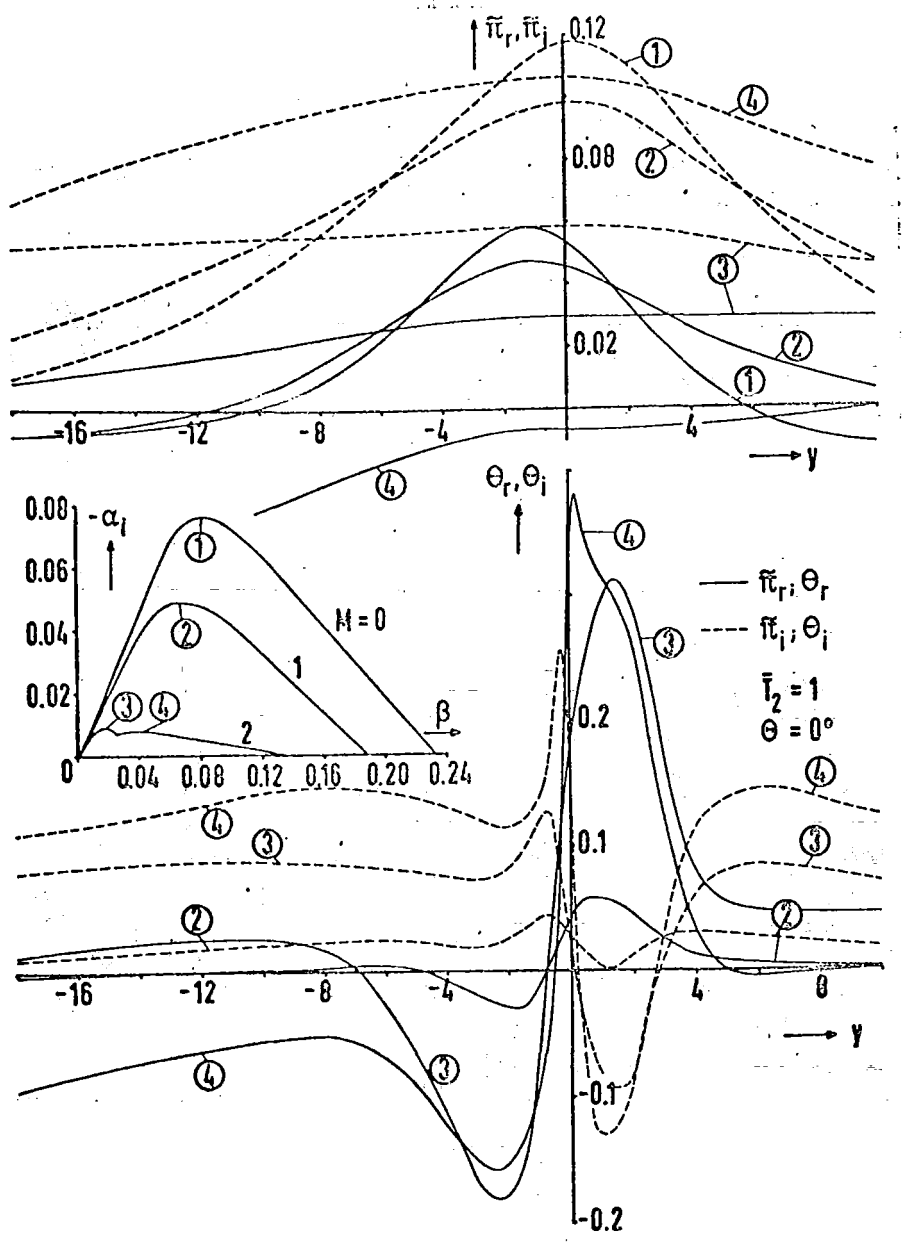

Figure 38. Curves of the Complex Eigenfunctions $\tilde{\pi}(y)$ and $\theta(y)$ of the p' and T' Disturbances at Maximum Amplification For Various Mach Numbers M and the Environment Temperature $\bar{T}_2 = 1$ ($\Theta = 0°$).

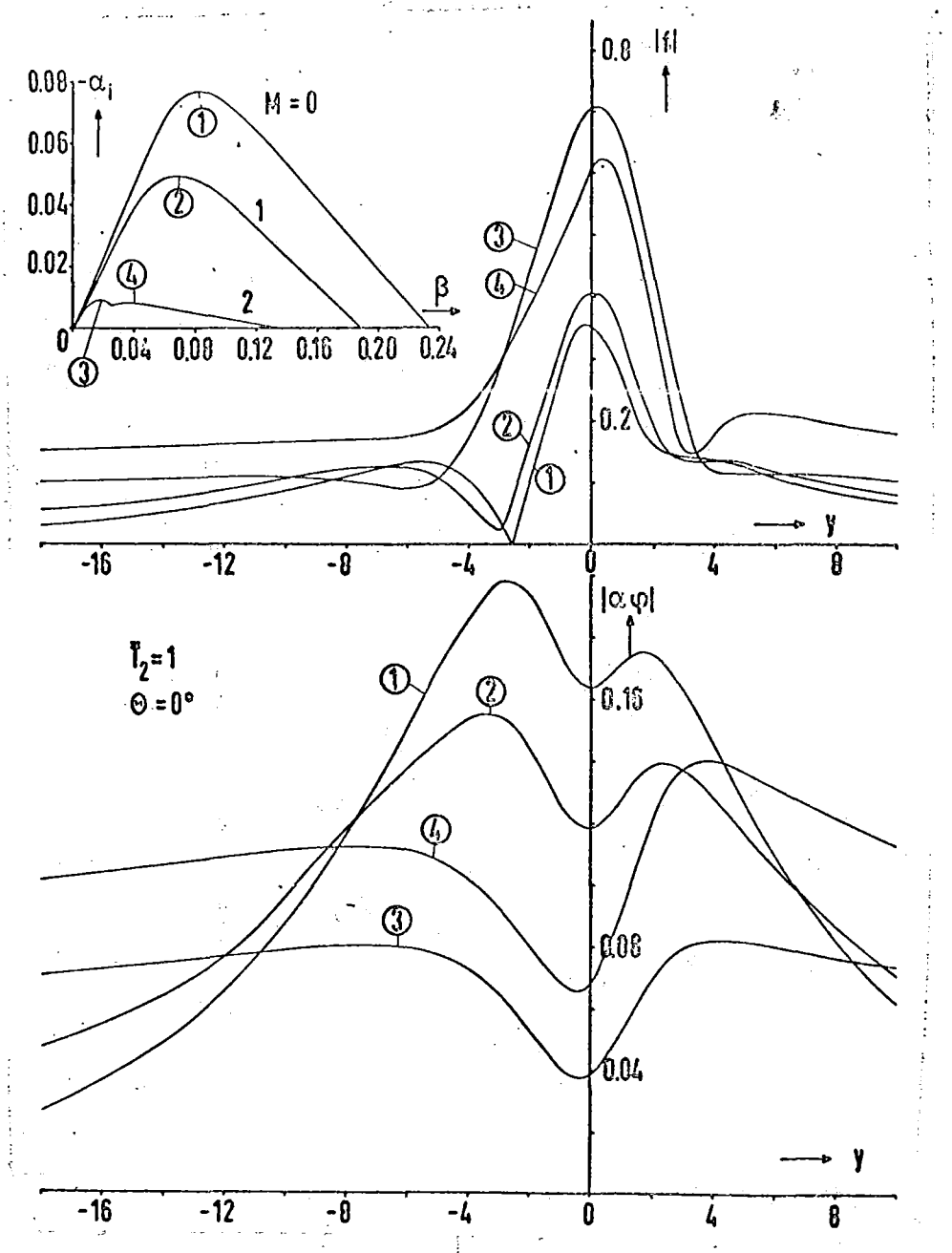

Figure 39. Amplitude Distribution $|f(y)|$ and $|\alpha\phi(y)|$ of The u' and v' Disturbances ($\Theta = 0°$) at Maximum Amplification for Various Mach Numbers M and the Environment Temperature $\overline{T}_2 = 1$.

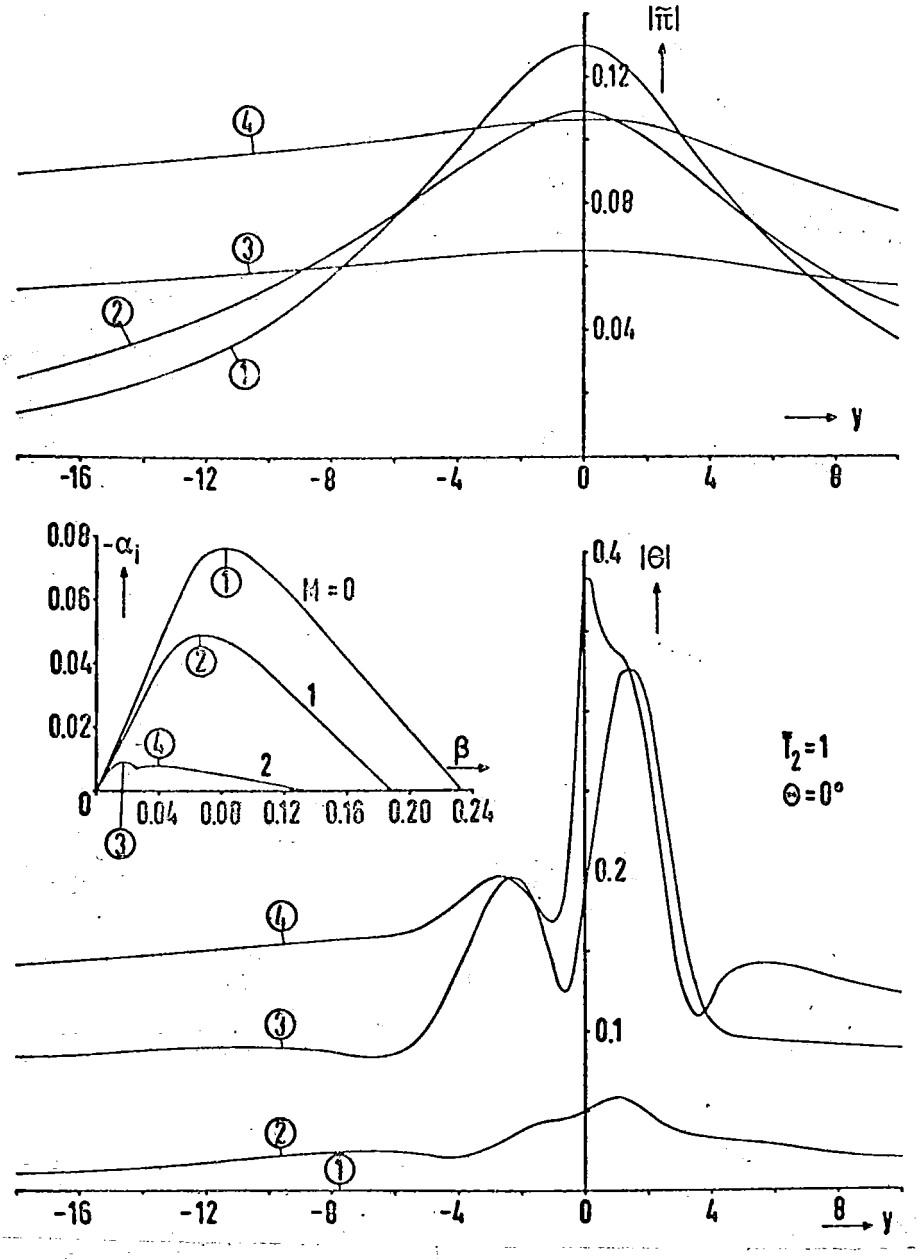

Figure 40. Amplitude Distribution $|\pi(y)|$ and $|\theta(y)|$ of The p' and T' Disturbances ($\Theta = 0°$) at Maximum Amplification For Various Mach Numbers M and the Environment Temperature $\bar{T}_2 = 1$.

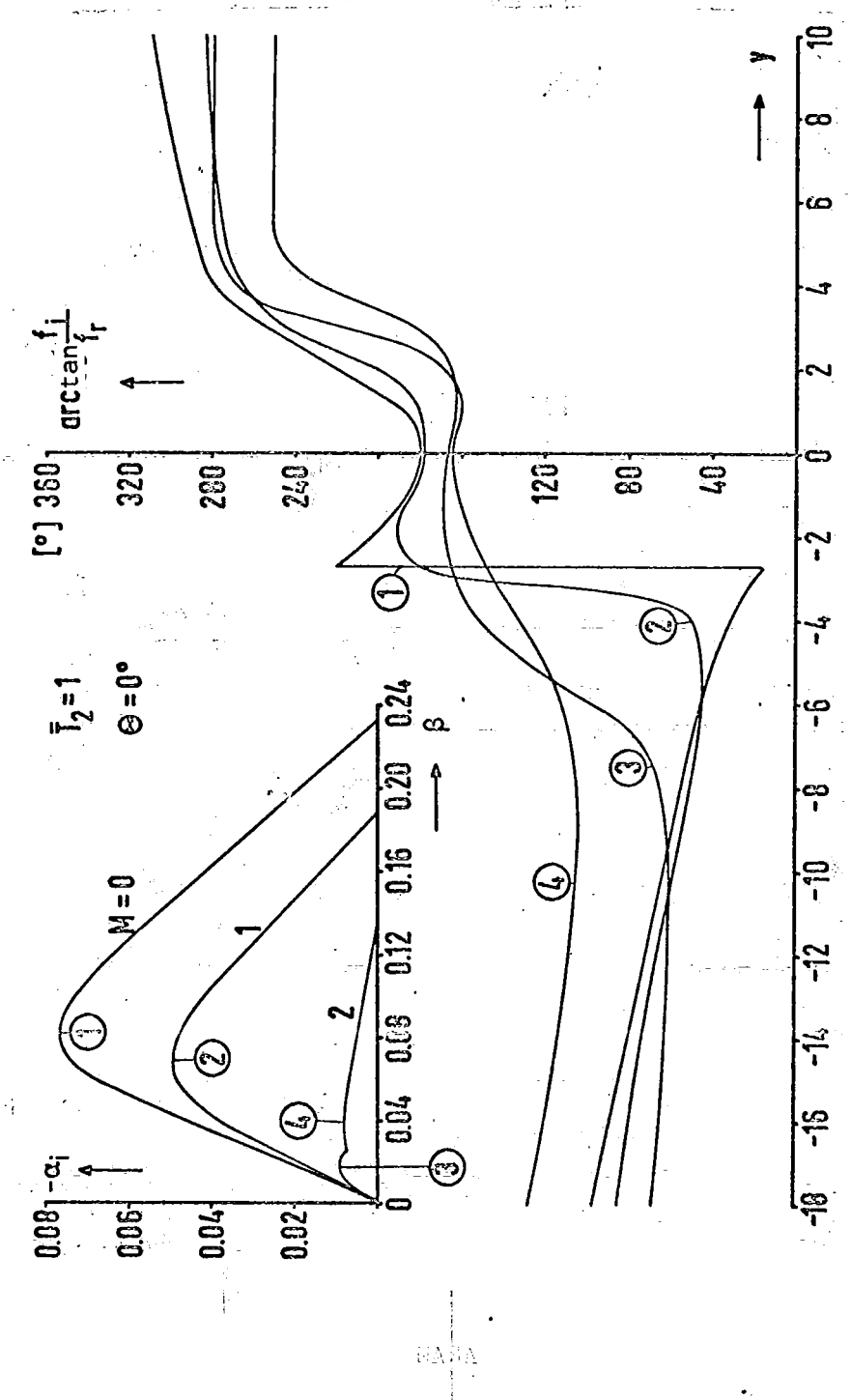

Figure 41. Phase Transition of the u' Disturbance ($\Theta = 0°$) at Maximum Amplification For Various Mach Numbers M and the Environment Temperature $\bar{T}_2 = 1$.

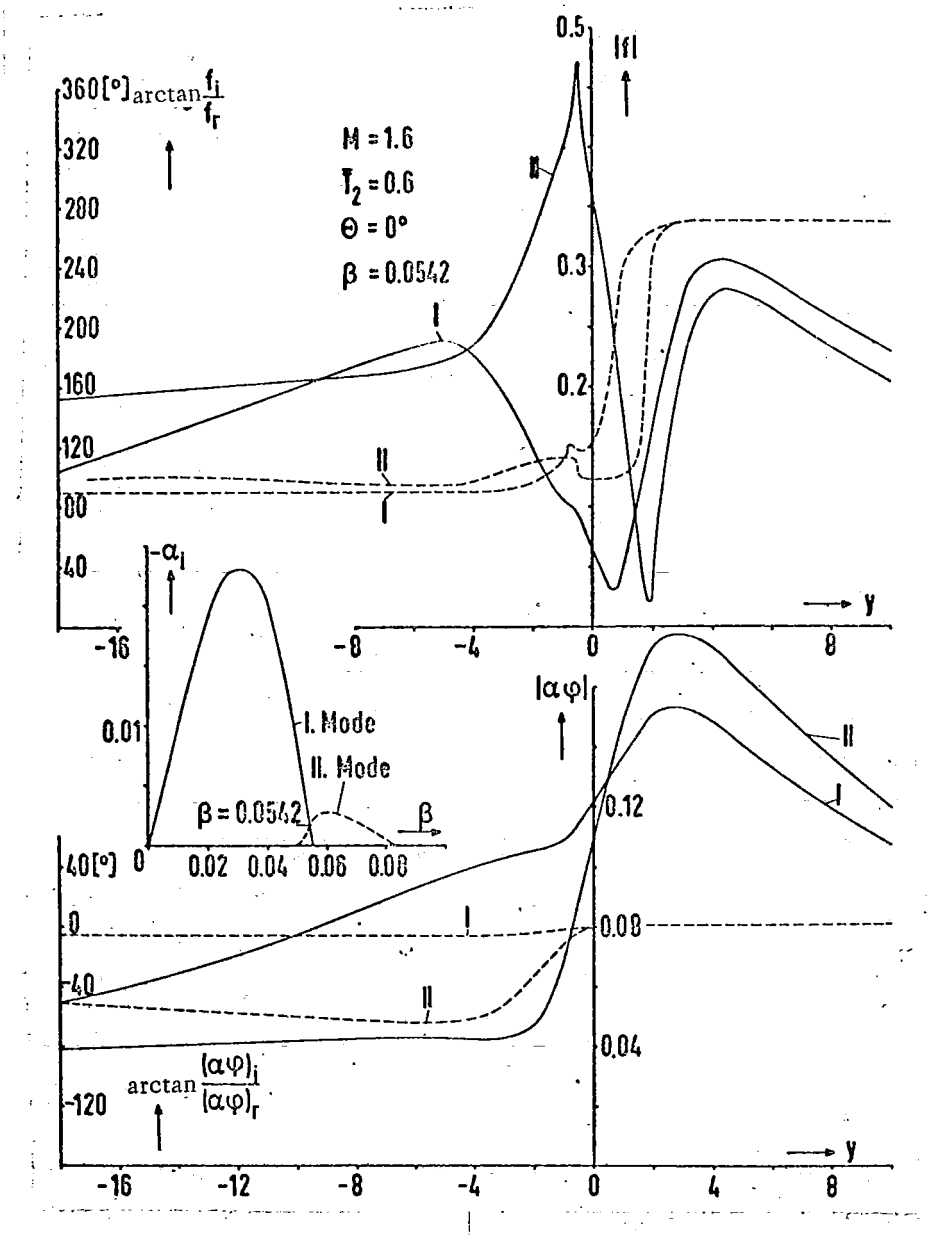

Figure 42. Amplitude Distribution (——) and Phase (---). Of the u' and v' Disturbances (Θ = 0°), First and Second Modes, of the Lock Profile for the Disturbance Frequency β = 0.0542 and the Mach Number M = 1.6, Environment Temperature $\bar{T}_2$ = 0.6.